UNIVERSITY OF CALGARY

Characterization of a novel interaction between the Ca^{2+}-binding protein S100A11 and the Ca^{2+}- and phospholipid - binding protein annexin A6 of smooth muscle

by

Ning Chang

A THESIS

SUBMITTED TO THE FACULTY OF GRADUATE STUDIES

IN PARTIAL FULFILMENT OF THE REQUIREMENTS FOR

THE DEGREE OF MASTER OF SCIENCE

DEPARTMENT OF BIOCHEMISTRY & MOLECULAR BIOLOGY

CALGARY, ALBERTA

MAY, 2006

UNIVERSITY OF CALGARY

FACULTY OF GRADUATE STUDIES

The undersigned certify that they have read, and recommend to the Faculty of Graduate Studies for acceptance, a thesis entitled "Characterization of a novel interaction between the Ca^{2+}-binding protein S100A11 and the Ca^{2+}- and phospholipid-binding protein annexin A6 of smooth muscle" submitted by Ning Chang in partial fulfilment of the requirements for the degree of Master of Science.

_____

Dr. Michael P. Walsh, Department of Biochemistry and Molecular Biology

_____

Dr. S. R. Wayne Chen, Department of Physiology and Biophysics

_____

Dr. Justin A. MacDonald, Department of Biochemistry and Molecular Biology

_____

Dr. Hans J. Vogel, Department of Biological Sciences

Date _____

Abstract

S100A11, an EF-hand-containing Ca^{2+}-binding protein, undergoes a conformational change upon binding Ca^{2+}, with exposure of a hydrophobic surface for interaction with a target protein(s). A novel Ca^{2+}-dependent interaction between S100A11 and the Ca^{2+}- and phospholipid-binding protein annexin A6 of smooth muscle was identified by affinity chromatography, gel overlay, co-sedimentation with liposomes and chemical cross-linking. The expression of S100A11 and annexin A6 in smooth muscle was confirmed by RT-PCR and Western blotting. S100A11-binding sites were identified in both *N*- and *C*-terminal domains of annexin A6 by deletion mutagenesis and partial tryptic digestion. The unique *N*-terminal head region of annexin A6 was not required for Ca^{2+}-dependent binding to S100A11. The S100A11-annexin A6 interaction, which was disrupted by phosphorylation of S100A11 at Thr9 by Ca^{2+}-dependent protein kinase C, may play a role in control of membrane-cytoskeleton connections, which are necessary for force development, and/or control of formation of signaling complexes at the sarcolemma.

Acknowledgements

I wish to extend sincere thanks to my supervisor, Dr. Michael P. Walsh for his invaluable guidance and encouragement, to my Supervisory Committee, Dr. Wayne Chen and Dr. Justin MacDonald for their critical advice and to Dr. Hans Vogel for his contributions as a member of my Thesis Examination Committee. Special thanks also to the members of the Walsh laboratory for all their friendship and help.

Finally, I would like to thank my wonderful family and friends for their constant and never-ending love and support.

TABLE OF CONTENTS

LIST OF FIGURES

LIST OF TABLES

LIST OF ABBREVIATIONS

A6	annexin A6
ACN	acetonitrile
AMBIC	ammonium bicarbonate
APS	ammonium persulfate
ATP	adenosine 5'-triphosphate
bp	base pair
CaM	calmodulin
CIP	calf-intestinal alkaline phosphatase
DFP	diisopropylfluorophosphate
DMS	dimethylsuberimidate
dNTP	deoxynucleoside triphosphates
DTT	dithiothreitol
EDTA	ethylenediamine tetraacetic acid
FPLC	fast protein liquid chromatography
g	gram
GST	glutathione *S*-transferase
His	histidine
IPTG	isopropyl-β-D-thiogalactopyranoside
kDa	kiloDalton
LB	Luria-Bertani medium
ng	nanogram
nm	nanometer
PB	DNA binding buffer for QIAquick PCR purification
PBS	phosphate-buffered saline
PCR	polymerase chain reaction
PMSF	phenylmethylsulfonyl fluoride
PVDF	polyvinylidene difluoride
QG	solubilization and binding buffer for QIAquick gel extract
SDS	sodium dodecyl sulfate

SOC	growth medium similar to LB-medium, but enhances bacterial growth due to the presence of glucose. Used as a cell growth medium to ensure maximum transformation efficiency.
STI	soybean trypsin inhibitor
TBS	Tris-buffered saline
TE	Tris-EDTA buffer
TEMED	N,N,N',N'-tetramethylethylenediamine
TFA	trifluoroacetic acid
µg	microgram
µl	microlitre

CHAPTER 1:

GENERAL INTRODUCTION

1.1 Ca^{2+} signaling via Ca^{2+}-binding proteins

Studies on Ca^{2+} signaling originated with investigations of the mechanisms of skeletal muscle contraction, but it is now accepted that Ca^{2+} ions serve as key intracellular messengers that mediate the effects of a variety of extracellular signals (hormones, neurotransmitters, growth factors, etc.) in eliciting diverse physiological responses such as muscle contraction, secretion, metabolism, cell growth, differentiation and mitogenesis (Niki *et al.*, 1996; Karaki *et al.*, 1997; Berridge *et al.*, 1998; *ibid*, 2000). The effects of Ca^{2+} ions are mediated by a host of Ca^{2+}-binding proteins that can be divided into 3 principal classes on the basis of the primary structures responsible for the actual binding of Ca^{2+}: EF-hand domain proteins (e.g. calmodulin), Ca^{2+}- and phospholipid-binding proteins (e.g. annexins and conventional and novel isoforms of protein kinase C) and Ca^{2+} storage proteins (e.g. calsequestrin) (Niki *et al.*, 1996; Haeseleer *et al.*, 2002).

1.2 EF-hand proteins and the S100 family

The EF-hand, a helix-loop-helix structure, was originally identified in the three-dimensional structure of carp parvalbumin and has since been detected in large numbers of Ca^{2+}-binding proteins (Marsden *et al.*, 1990; Kawasaki *et al.*, 1998). This structure most commonly consists of 40 amino acid residues: a 12-amino acid loop, which is directly responsible for Ca^{2+} binding, sandwiched between a pair of α-helices. EF-hand Ca^{2+}-binding proteins have been classified into 45 subfamilies, including the calmodulin and S100 protein subfamilies (Kawasaki *et al.*, 1998). Calmodulin, troponin C, neurocalcin and others are monomers containing 4 EF-hands and M_r ~20 kDa. S100 (soluble in 100% ammonium sulfate) proteins (Heizmann & Cox, 1998; Donato, 1999;

ibid, 2001; *ibid*, 2003), on the other hand, form dimers (M_r ~22 kDa) with 2 Ca^{2+}-binding sites per monomer. Structural information indicates that most S100 proteins exist in the form of antiparallel packed homodimers (in some cases heterodimers), capable of functionally cross-linking two homologous or heterologous targets. These proteins are characterized by a high degree of amino acid sequence conservation (Taylor & Geisow, 1987), 3-D structure (Wilder *et al.*, 2003) and genomic structure (Heizmann *et al.*, 2002; Zimmer *et al.*, 1996). Despite their similar amino acid sequences and 3-D structures, individual family members exhibit diverse biochemical and physical properties, including affinity for metal ions (Ca^{2+}, Zn^{2+} and Cu^{2+}) (Donato, 1999), oligomerization properties, heterodimerization, post-translational modifications and lipid binding. In addition, some S100 family members contain unique amino- and/or carboxyl-terminal extensions that are homologous to structural motifs found in other proteins. In some instances, these differences have been documented to have profound effects on target protein interactions.

There are 21 S100 subfamily members encoded by the human genome, many of which form a tight cluster on chromosome 1q21 (Schäfer & Heizmann, 1996; Wicki *et al*., 1996a, b; Eckert *et al.,* 2004). The sequences of the Sl00 proteins show the presence of two Ca^{2+}-binding domains of the EF-hand type, and heterologous target proteins bind in a Ca^{2+}-dependent (and, in some instances, Ca^{2+}-independent) manner. An increasing body of evidence indicates that members of the multigenic S100 protein family play regulatory roles within cells and exert regulatory effects on target cells once released into the extracellular space (Donato, 1999; *ibid*, 2001; Zimmer *et al.*, 1995). S100 proteins have been implicated in the Ca^{2+}-dependent regulation of diverse physiological processes, including cell cycle regulation, growth and metabolic control, protein phosphorylation,

the inflammatory response, cAMP signalling pathways, dynamics of cytoskeletal components, and cell proliferation and differentiation (Heizmann & Cox, 1998; Donato, 1999; *ibid*, 2001; *ibid*, 2003; Bianchi *et al.*, 2003). S100 proteins have also been associated with a variety of pathological events, including neoplastic transformation and neurodegenerative diseases such as Down's syndrome and Alzheimer's disease. Other diseases in which S100 proteins have been implicated include cancer, cardiomyopathy, psoriasis, cystic fibrosis, amyotrophic lateral sclerosis and epilepsy (Heizmann *et al.*, 2002), usually via overexpression of the protein (Odink *et al*., 1987; Van Eldik & Griffin,1994).

In response to a rise in cytosolic free [Ca^{2+}], EF-hand proteins bind Ca^{2+} and act either as activators of target enzymes or non-enzyme proteins (e.g. calmodulin, troponin C, S100 proteins, neurocalcin) or Ca^{2+} buffers (e.g. calbindin, parvalbumin) (Niki *et al.*, 1996; Smith & Shaw, 1998; Haeseleer *et al*., 2002). In the case of activators, Ca^{2+} binding induces a conformational change that exposes a hydrophobic surface for interaction with a target protein(s), a crucial step in the regulation of specific physiological events (Smith & Shaw, 1998). A well-known example is the interaction of calmodulin with myosin light chain kinase (MLCK) (e.g. Walsh *et al*., 1982; *ibid*, 1983; Ngai *et al.*, 1984; Wilson *et al*., 2002; Van Lierop *et al*., 2002); Ca^{2+}-dependent activation of MLCK is the key event in the activation of smooth muscle contraction and non-muscle motility (Kamm & Stull, 2001).

1.3 S100A11

Several years ago, our laboratory exploited the Ca^{2+}-induced exposure of a hydrophobic surface on EF-hand proteins to analyze this class of regulatory proteins in smooth muscle and was the first to describe a member of the S100 subfamily now referred to as S100A11 (De Vries *et al.*, 1989). The approach used was to prepare a cytosolic fraction from chicken gizzard smooth muscle in the absence of Ca^{2+} (presence of EGTA) to dissociate EF-hand proteins from their targets. Excess Ca^{2+} was then added to induce exposure of these hydrophobic surfaces and the extract applied to a hydrophobic matrix (a phenyl-Sepharose column) in the presence of Ca^{2+}, the rationale being that the exposed hydrophobic domain would bind tightly to the matrix. Most cellular proteins, on the other hand, would not be expected to bind to the column since they lack exposed hydrophobic regions and therefore would flow through the column. This was indeed found to be the case: >95% of cellular proteins did not bind to the phenyl-Sepharose column (De Vries *et al.*, 1989). Subsequently, several proteins that bound to the column in a Ca^{2+}-dependent manner were eluted by chelation of Ca^{2+} with EGTA (Fig. 1).

Another key feature of EF-hand proteins is their heat stability in the presence of bound Ca^{2+}, and this was exploited for their further purification. Finally, purification to electrophoretic homogeneity was achieved by anion-exchange chromatography of the supernatant obtained following heat treatment of the EGTA extract from Fig. 1 in the presence of Ca^{2+} (Fig. 2). The flow-through fractions contained S100A11. This protein was rediscovered by other groups and referred to as calgizzarin (Todoroki *et al.*, 1991), S100C (Ohta *et al.*, 1991) and more recently, according to the currently accepted systematic nomenclature (Schäfer *et al*., 1995), as S100A11 (Wicki *et al*., 1996a, b). Ca^{2+} binding to S100A11 was demonstrated by its Ca^{2+}-dependent interaction with phenyl-

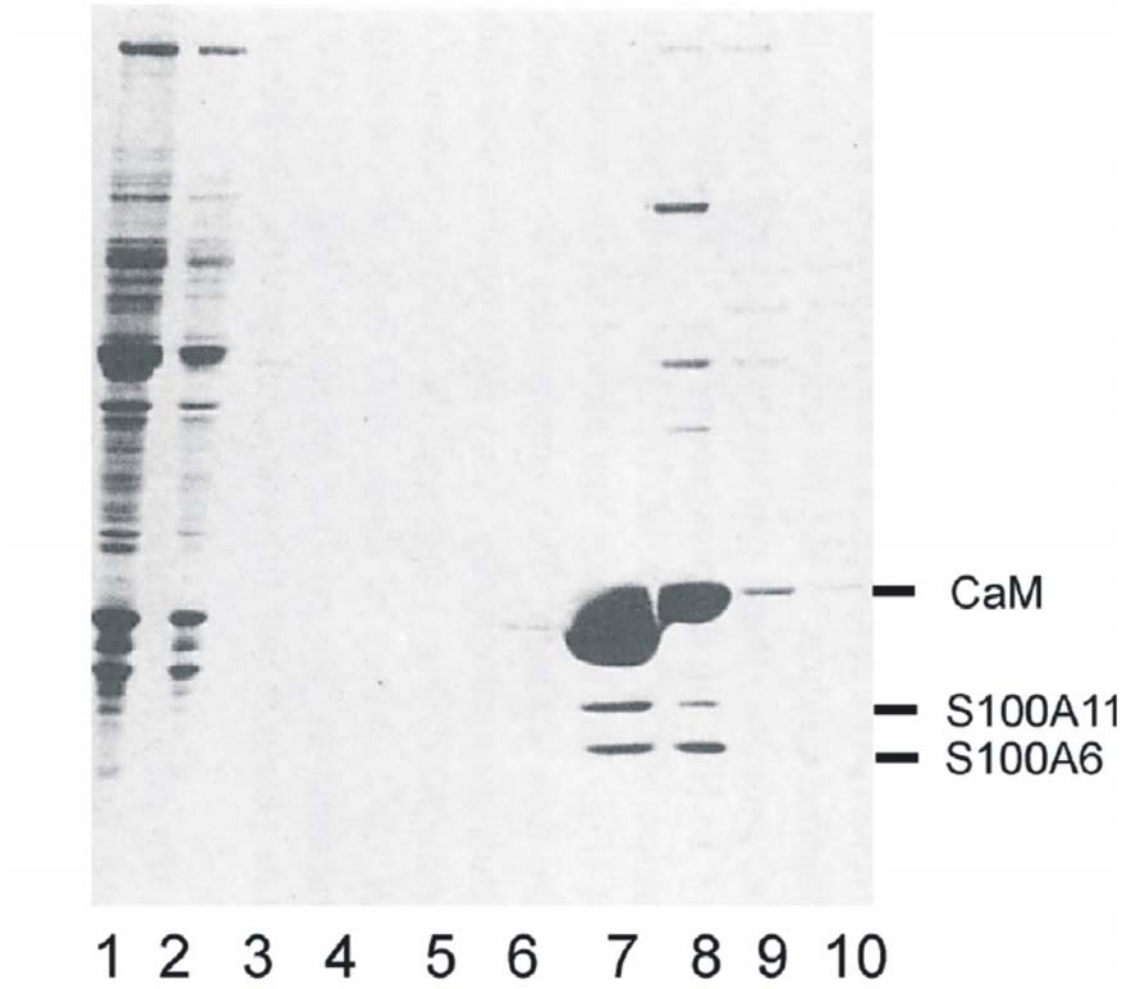

Fig. 1: Hydrophobic interaction chromatography to isolate smooth muscle Ca^{2+}-binding proteins. SDS-PAGE analysis with Coomassie Blue-staining of: 1 = phenyl-Sepharose column load; 2 = flow-through fractions; 3 = 1 M NaCl eluate; 4 - 10 = consecutive fractions eluted with EGTA. CaM = calmodulin, S100A11 = S100C or calgizzarin, S100A6 = calcyclin. (Taken from De Vries *et al.*, 1989 with permission).

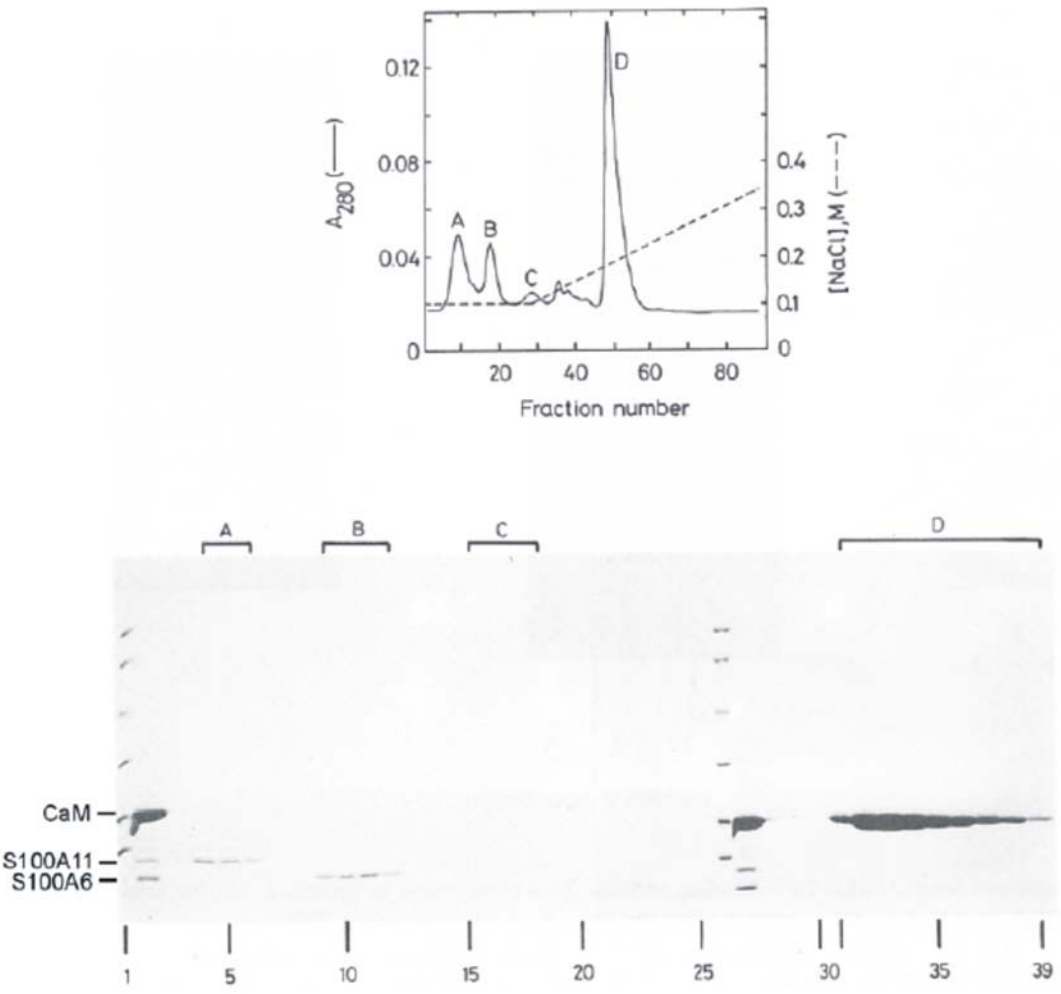

Fig. 2: Purification of S100A11 to electrophoretic homogeneity by anion-exchange chromatography. EGTA-eluted fractions from Fig. 1 were heat-treated in the presence of Ca^{2+}, centrifuged to remove denatured proteins and loaded onto a DEAE-Sephacel column. Bound proteins were eluted with a [NaCl] gradient as shown in the upper panel. Fractions corresponding to protein peaks A-D in the upper panel are shown in the lower panel above the Coomassie Brilliant Blue-stained gel profile. Key to lanes: 1, 26 = molecular weight markers; 2, 27 = column load; 3 - 25 and 28 - 39 = selected fractions. Peak A corresponds to S100A11, peaks B and C to two isoforms of S100A6 and peak D to calmodulin. (Taken from De Vries *et al*., 1989 with permission).

Sepharose, $^{45}Ca^{2+}$ overlay, gel filtration ± Ca^{2+}, fluorescence spectroscopy and flow dialysis (Allen *et al.*, 1996; Schönekess & Walsh, 1997). The monomeric molecular weight of S100A11 is ~11 kDa and the native structure is a dimer, as shown initially by gel filtration (Allen *et al.*, 1996) and recently confirmed by NMR spectroscopy (Dempsey *et al.*, 2003). These characteristics are common to S100 proteins. Flow dialysis confirmed that S100A11 binds 2 Ca^{2+} ions per monomer at physiological pH and ionic strength, as predicted from the amino acid sequence, with $[Ca^{2+}]_{0.5}$ = 0.3 mM and n_H (Hill coefficient) = 1.2 (Allen *et al.*, 1996). Our laboratory cloned chicken gizzard S100A11 by RT-PCR, 5′- and 3′-RACE and sequenced the cDNA (Schönekess & Walsh, 1997). The protein consists of 101 amino acids with a molecular weight of 11,282 Da and pI = 6.1. Electrospray mass spectrometry yielded a molecular weight of the tissue-purified protein of 11,281 Da. The amino acid sequence is consistent with 2 Ca^{2+}-binding sites per monomer, the first being an atypical EF-hand with 14 residues and the second a classical 12-residue EF-hand; the Ca^{2+}-coordinating residues are indicated with asterisks in Fig. 3. The 12-residue *C*-terminal EF-hand ligates Ca^{2+} in a similar manner to calmodulin, resulting in a higher calcium affinity site. The *N*-terminal or 'pseudo-canonical' EF-hand is formed by 14 residues and binds Ca^{2+} mostly through main-chain carbonyl groups, except for the bidentate side chain of glutamate at the last position of the loop. This results in a lower affinity for Ca^{2+} (Santamaria-Kisiel *et al.*, 2006). S100A11, like most S100 proteins, is structurally highly conserved: Fig. 3 shows a species comparison of S100A11 sequences. The chicken protein exhibits 72.4% sequence identity and 81% sequence similarity to the human protein (Schönekess & Walsh, 1997). It was also confirmed, using the hydrophobic fluorescent probe TNS (2-*p*-toluidinylnaphthalene-6-

sulfonate), that Ca^{2+} binding to S100A11 exposes a hydrophobic surface, and demonstrated that the affinity of S100A11 for Ca^{2+} is increased ~10-fold in the presence of TNS (to $[Ca^{2+}]_{0.5}$ = 35 μM) (Allen *et al.*, 1996). This latter observation suggests that the affinity of S100A11 for Ca^{2+} is likely to be markedly enhanced in the presence of a target protein, a very common phenomenon amongst EF-hand proteins (Niki *et al.*, 1996). In addition, our laboratory found that S100A11 binds Zn^{2+} (Allen *et al.*, 1996), another feature common to many S100 proteins and of potential physiological significance (Heizmann & Cox, 1998). Polyclonal antibodies to S100A11 were raised in the Walsh laboratory and its tissue distribution examined in the chicken: S100A11 was detected at highest levels in lung, followed by smooth muscles (esophagus, large intestine, trachea and gizzard), kidney, liver, brain and heart (Allen *et al.*, 1996). S100A11 was expressed in *E. coli* and the properties of the purified recombinant protein found to be indistinguishable from the tissue-purified protein (Schönekess & Walsh, 1997).

The three-dimensional structure of apo-S100A11 was determined by multi-dimensional NMR spectroscopy in collaboration with Dr. Gary Shaw (UWO) (Rintala *et al.*, 2002; Dempsey *et al.*, 2003). Fig. 4 shows the Ca^{2+}-induced conformational change in S100A11. Apo-S100A11 forms a tight globular structure in which helices III and IV that form part of Ca^{2+}-binding site II are nearly parallel. Helices I and IV, and I and I′ form a more closed arrangement than observed in other apo-Ca^{2+}-binding proteins. S100A11 undergoes a conformational change upon Ca^{2+} binding. The rearrangement of helix III exposes previously buried residues that are essential for target recognition. Fig. 5 shows the accessible surface area representations of apo-S100A11 and Ca^{2+}-bound S100A11 in

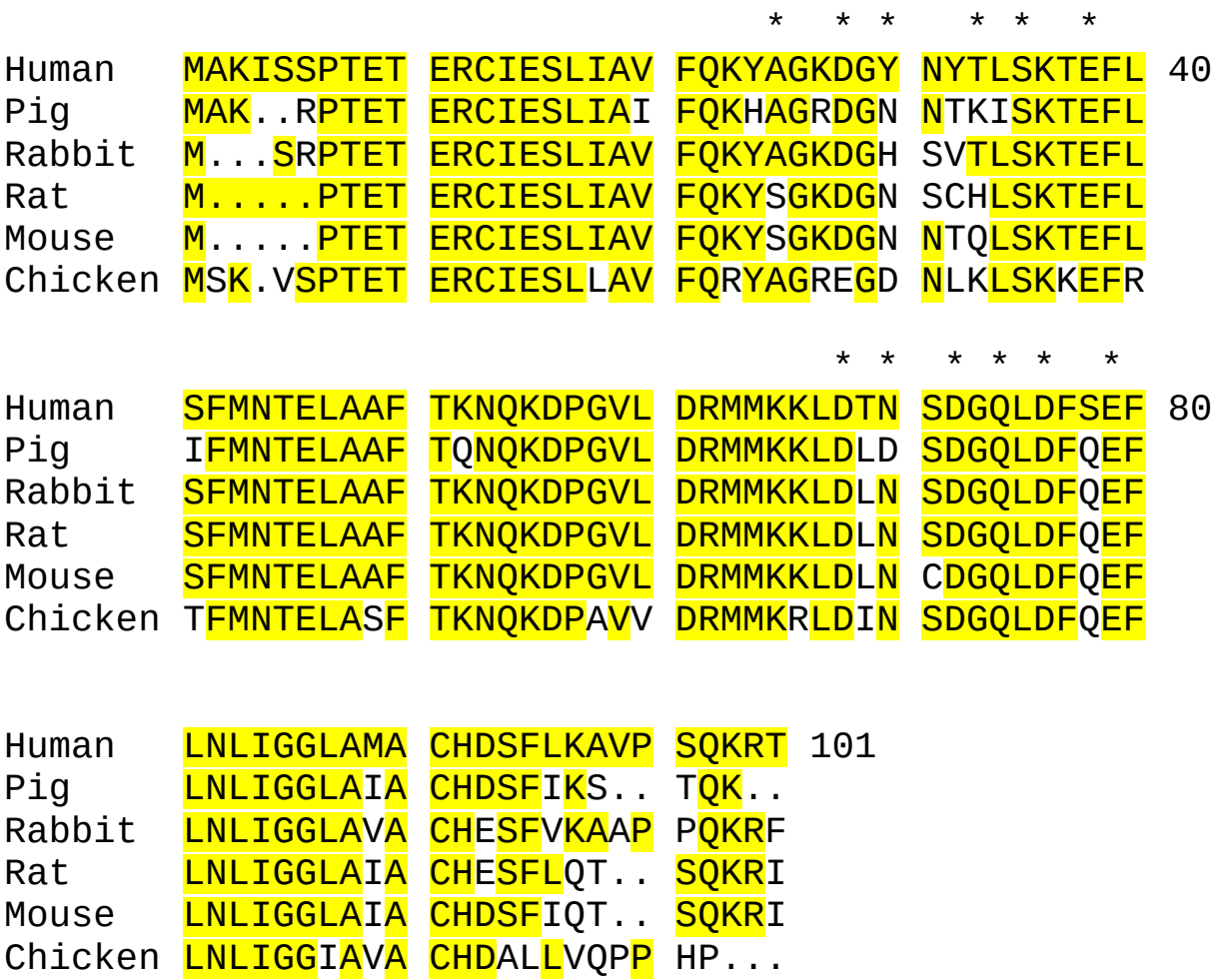

Fig. 3: Comparison of the amino acid sequences of S100A11 from different species. Yellow shaded residues are identical to human S100A11. Dots indicate deletions. Coordinating sites for Ca^{2+} binding are designated by *. NCBI accession numbers: human, NP_005611; pig, P31950; rabbit, P24480; rat, Q6B345; mouse, P50543; chicken, P24479. The rat and chicken sequences were determined in the Walsh laboratory (rat: Hesse, E. M. M., Wiehler, W. B., Pho, M. V. C. and Walsh, M.P.; chicken: Schönekess, B. O. and Walsh, M. P.).

complex with a target peptide (see section *1.4*). Residues in helices I (P3, E11, A14), III (V55, R58, M59), IV (A86, C87, S90) and the linker between the *N*- and *C*-terminal domains (A45, F46) are partially buried in apo-S100A11 and become exposed upon Ca^{2+} binding to form a continuous hydrophobic surface for interaction with a target protein.

The properties of S100A11 described above are consistent with a function as a "Ca^{2+} sensor", i.e., the protein detects the increase in cytosolic [Ca^{2+}] in response to an appropriate stimulus and undergoes a conformational change with exposure of a hydrophobic surface that interacts with a target protein(s) and thereby regulates its function. Consistent with this hypothesis, S100A11 was shown to interact with annexin A1 (annexin I) in a Ca^{2+}-dependent manner and plays a role in early endosomes (Mailliard *et al.*, 1996; Seemann *et al.*, 1996; Robinson & Eckert, 1998). Another report provided evidence for an interaction between S100A11 and actin (Zhao *et al.*, 2000), but we have been unable to confirm this observation in the Walsh laboratory. Evidence has also been presented for an interaction between S100A11 and S100B, most likely forming a heterodimer through subunit exchange (Deloulme *et al*., 2000).

Recently, more attention was paid to the potential physiological function of S100A11. The indisputable relationship between the deregulated expression of S100 proteins and cancer and Alzheimer's disease strongly suggests their profound involvement in these processes. However, despite the overwhelming correlation between S100 protein expression and different pathological processes, many questions remain unanswered. Hence, analysis of the cellular processes in which they are involved, and elucidation of their signaling pathways should lead eventually to understanding of their pathological

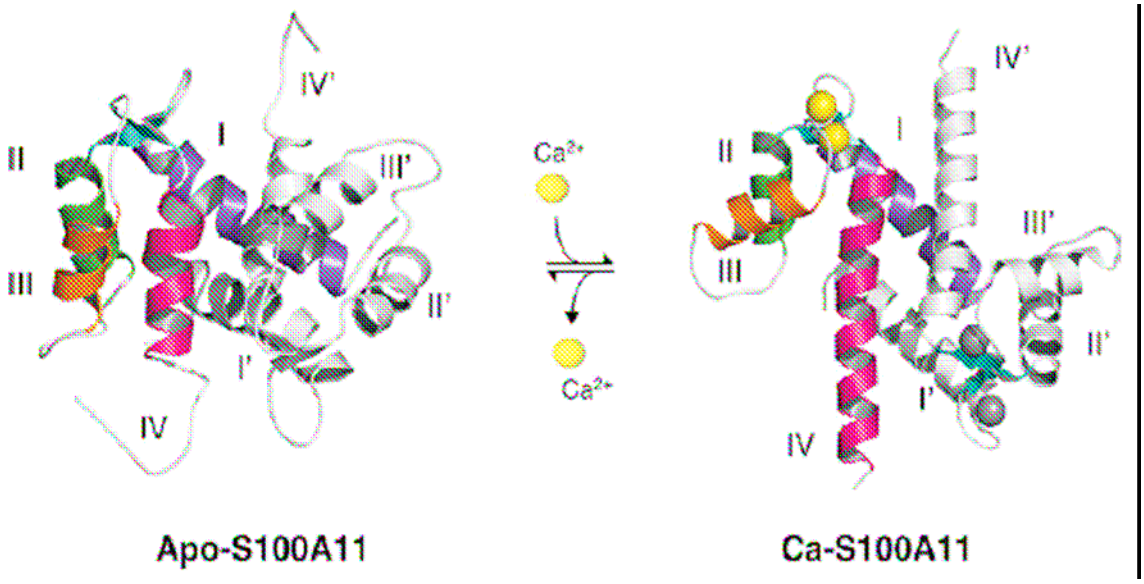

Fig. 4: Calcium-dependent conformational change in S100A11. The three-dimensional structures of calcium-free S100A11 and calcium-bound S100A11 are shown to demonstrate the Ca^{2+}-induced conformational change. In the symmetrical dimer, helices of one monomer (I–IV) are highlighted in different colours, while the other monomer (helices I'–IV') is coloured grey. As sensors, the S100 proteins experience a conformational change upon Ca^{2+} binding (four ions/dimer). The rearrangement of helix III (orange) exposes previously buried residues that are essential for target recognition. (Taken from Santamaria-Kisiel *et al*., 2006 with permission).

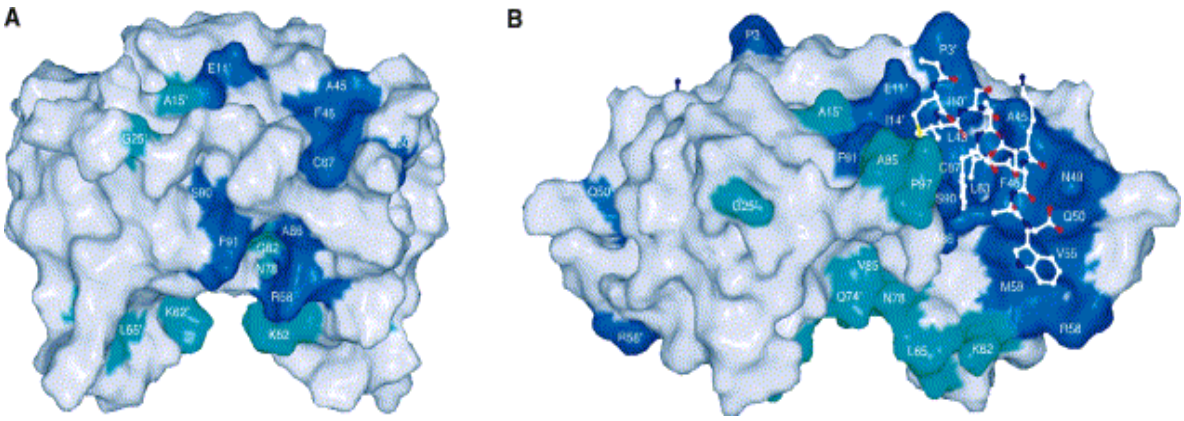

Fig. 5: Formation of the annexin A1-binding surface upon Ca^{2+} binding to apo-S100A11. Accessible surface area representation of apo-S100A11 (A) and Ca^{2+}-bound S100A11 in complex with annexin A1 peptide (B). Residues in S100A11 that directly interact with annexin A1 are coloured dark blue and those whose side chain exposure is increased by 20% upon Ca^{2+} binding are coloured cyan. (Taken from Dempsey *et al.*, 2003 with permission).

roles. Recently, it was reported that, upon exposure of human keratinocytes to a high concentration of Ca^{2+}, S100A11 was specifically phosphorylated at Thr10 by PKC and phosphorylation facilitated the binding of S100A11 to nucleolin, resulting in nuclear translocation of S100A11. In the nuclei, S100A11 liberated Sp1/3 from nucleolin. The resulting free Sp1/3 transcriptionally activated $p21^{CIP1/WAF1}$, a negative regulator of cell growth. S100A11, therefore, plays a role as a key mediator of Ca^{2+}-induced growth inhibition of human epidermal keratinocytes (Sakaguchi *et al.*, 2003; *ibid*, 2004). Interestingly, introduction of an *N*-terminal peptide of S100A11 into human cells induced apoptotic cell death (Makino *et al.*, 2004). It was also reported that loss of nuclear localization of S100A11 is related to DNA synthesis, which is thought to be one of the mechanisms of immortalization, one of the multistep processes of cancer development (Sakaguchi *et al.*, 2000; *ibid*, 2001). S100A11 is found to be abnormally expressed in different cancers (Tanaka *et al.*, 1995). For example, it is down-regulated in bladder cancer (Memon *et al.*, 2005) but overexpressed in human uterine smooth muscle tumours (Kanamori *et al.*, 2004).

1.4 Ca^{2+}/phospholipid-binding proteins and annexins

There also exist Ca^{2+}-binding proteins which bind phospholipids in a Ca^{2+}-dependent manner, including the annexins, and conventional and novel isozymes of protein kinase C (PKC), which increases their affinity for Ca^{2+} and/or enzymatic activity. These properties allow such proteins to translocate to cell membranes and to become active in the vicinity of the membranes in response to an increase in $[Ca^{2+}]$. Such proteins are classified into 2 groups: the annexins and the C2 region proteins (Niki *et al.*, 1996). Annexins bind

negatively-charged phospholipids and membranes in a Ca^{2+}-dependent and reversible manner (Creutz, 1992; Raynal & Pollard, 1994; Gerke & Moss, 1997; Seaton & Dedman, 1998; Gerke & Moss, 2002). They contain a highly-conserved structural element, the annexin repeat, which consists of ~70 amino acids. Most annexins contain 4 such repeat motifs packed into a highly α-helical disk, which forms the membrane-binding module. Fig. 6 shows crystal structures of annexin A1 and annexin A6 (Gerke & Moss, 2005). Annexins differ primarily in the *N*-terminal head region, which varies in length. For example, annexin A1 has an *N*-terminal head region composed of 40 amino acids, the first 10-14 residues of which constitute the S100A11-binding site (Mailliard *et al.*, 1996; Seemann *et al.*, 1996). The crystal structure of Ca^{2+}-bound S100A11 in complex with a synthetic peptide corresponding to the *N*-terminal 14 residues of annexin A1 shows that the annexin interface occurs through interactions with the linker and helices III and IV of one monomer and helix I of the other monomer in S100A11 (Rety *et al.*, 2000), there being two bound peptide molecules per S100A11 dimer. The annexin molecule thereby bridges the two S100A11 monomers, which are also cross-linked by a disulfide bridge between Cys11 of each subunit. Other S100-annexin partnerships have also been identified. Annexin A2 forms a tetramer, commonly referred to as the annexin II tetramer, composed of two subunits of annexin A2 and two of S100A10 (Glenney, 1986). Formation of this complex is actually Ca^{2+} independent. Annexin A11 interacts in a Ca^{2+}-dependent manner with S100A6 (calcyclin) (Sudo & Hidaka, 1999). S100A6 has also been shown to interact with annexin A2 (Filipek *et al.*, 1995). S100B binds to annexins A2 (Bianchi *et al.*, 1992), A5 and A6 (Garbuglia *et al.*, 1998). Finally, S100A1 interacts with annexins A5 and A6 (Garbuglia *et al.*, 1998). Annexins have been implicated in

diverse physiological functions, including regulation of membrane organization, membrane trafficking, membrane-cytoskeleton linkage, ion conductance across membranes, anti-inflammatory and anti-coagulant effects, Ca^{2+} handling in the heart, and as mediators or regulators of certain cell-cell and cell-matrix interactions (Creutz, 1992; Raynal & Pollard, 1994; Gerke & Moss, 1997; Seaton & Dedman, 1998; Gerke & Moss, 2002; Camors *et al*., 2005). The formation of tetramers composed of two annexin subunits and two S100 subunits could link two distinct membranes in a Ca^{2+}-dependent manner (Gerke & Moss, 2002). Annexins have also been shown to bind to actin-based cytoskeletal elements (Gerke & Weber, 1984; Glenney, 1986; Glenney *et al*., 1987; Ikebuchi & Waisman, 1990; Hosoya *et al*., 1992; Diakonova *et al*., 1997; Raynal *et al*., 1997), which could explain their possible involvement in Ca^{2+}-dependent regulation of membrane-cytoskeleton dynamics.

1.5 Identification of a novel S100A11-binding protein

Our laboratory addressed the broader issue of S100A11 target proteins using S100A11-Sepharose affinity chromatography. An extract of chicken gizzard smooth muscle, prepared in the absence of Ca^{2+}, was applied to the affinity column in the presence of Ca^{2+}. Unbound proteins were washed through the column and non-specifically-bound proteins were eluted with NaCl. Proteins bound in a Ca^{2+}-dependent manner were then eluted by chelation of Ca^{2+} with EGTA. Fig. 8 (page 58) shows a Coomassie Blue-stained SDS gel of the EGTA-eluted fractions. Three prominent protein bands were detected with M_r = 70, 44 and 37 kDa. Control experiments demonstrated that the 70 kDa band did not bind to a blank Sepharose column (without S100A11) or if loaded on an S100A11

affinity column in the presence of EGTA. On the other hand, the 44 and 37 kDa bands bound to both control columns (Fig. 9, page 59). We concluded that the 70 kDa protein interacts specifically with S100A11 in a Ca^{2+}-dependent manner. This protein was cut out of the gel, digested with trypsin and the digest subjected to matrix-assisted laser desorption ionization/time-of-flight (MALDI-TOF) mass spectrometry (Mann *et al*., 2001) in the Southern Alberta Mass Spectrometry Centre. The profile of tryptic peptide masses was compared with the predicted tryptic peptide mass profiles in the protein sequence data banks and the protein identified as annexin A6 with an expectation value of 2.3×10^{-7} and 24 matched peptides covering 39% of the sequence (Fig. 10, page 60). ***This is the first demonstration of an interaction between S100A11 and annexin A6.*** Furthermore, this interaction is Ca^{2+} dependent.

1.6 Annexin A6

Annexin A6 is approximately twice the size of other annexins and contains 8 annexin repeats rather than the usual 4. In the crystal structure, these are arranged as two four-repeat lobes oriented perpendicular to one another and separated by a linker between repeats 4 and 5 as shown in Fig. 6B (Benz *et al*., 1996; Kawasaki *et al*., 1996; Avila-Sakar *et al*., 1998; *ibid,* 2000; Freye-Minks *et al*., 2003). Each lobe has a disk-like shape. Once membrane binding takes place, a conformational change occurs allowing the two planes of the cores to face a single membrane in a "parallel" manner. Alternatively, one of the cores may twist 180^{o} about the flexible linker so that, in the resulting "antiparallel" orientation, the protein could bind two closely-apposed membranes simultaneously.

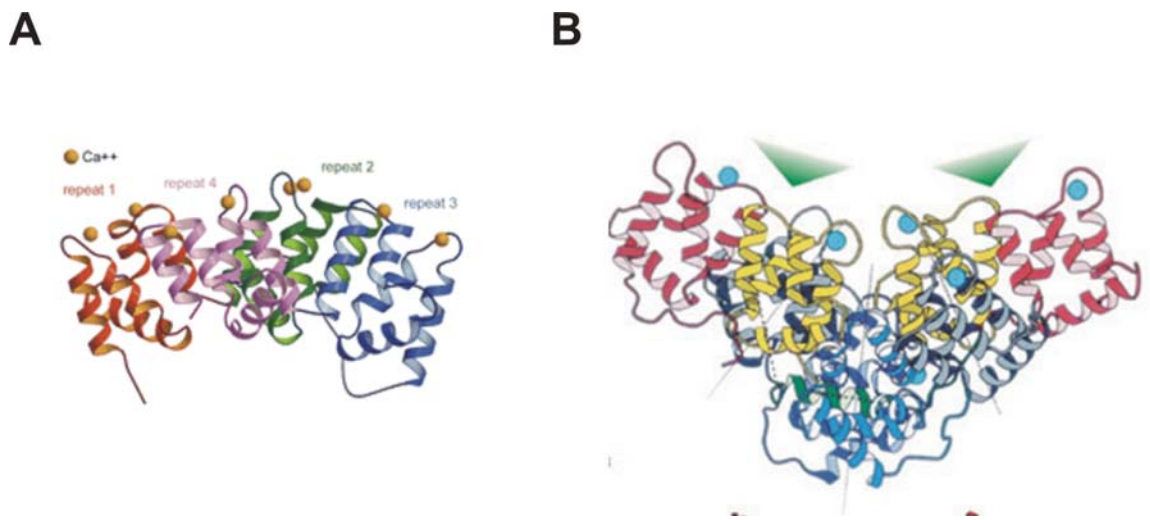

Fig. 6: Structures of annexin A1 and annexin A6. ***A.*** Molecular structure of annexin A1. Ribbon representation shows the three-dimensional fold of the backbone of annexin A1 in the presence of Ca^{2+}. In the Ca^{2+}-bound conformation, the annexin can attach to membranes through its convex (upper) side, with the Ca^{2+} ions serving a bridging function. (Taken from Rescher & Gerke, 2004 with permission). ***B.*** Ribbon representation of the annexin A6 crystal structure. Annexin A6 contains eight repeat segments, and the two halves of the protein, which each consist of a four-annexin-repeat unit (core), are connected by a linker (depicted in dark green). The flexibility of the linker enables the two halves to adopt different orientations with respect to one another. Bound Ca^{2+} is shown as blue spheres. The membrane attachment sites of the annexin core units are indicated by green triangles. (Taken from Gerke & Moss, 2005 with permission).

1.7 Potential physiological function of the S100A11-annexin A6 interaction

The sarcolemma of smooth muscle cells is segregated into force-transmitting regions (adherens junctions), which are directly linked to the cytoskeleton, and flexible vesicular domains containing numerous caveolae, sites of localization of signaling complexes (Small & Gimona, 1998). Since smooth muscle cells must adapt rapidly and continuously to changes in length, sarcolemmal and cytoskeletal protein reorganization must be precise and flexible. Members of the annexin protein family, including annexin A6, have been implicated in smooth muscle membrane organization, constituting a reversible, Ca^{2+}-dependent link between the sarcolemma and the cytoskeleton (Babiychuk *et al*., 1999). Effective regulatory mechanisms for coordinated cytoskeletal and sarcolemmal rearrangement are required to protect smooth muscle cells from mechanical damage during contraction-relaxation cycles. Work by Draeger's group has implicated annexin A6 in the formation of a Ca^{2+}-dependent and reversible membrane-cytoskeleton complex in smooth muscle cells, which they propose is involved in sarcolemmal organization during smooth muscle contraction (Babiychuk *et al.*, 1999). Since we have shown that S100A11 interacts with annexin A6 in a Ca^{2+}-dependent manner, the possibility arises that this Ca^{2+}-dependent linkage of the plasma membrane to the cytoskeleton also requires S100A11, which would not have been detected in the experiments of Babiychuk *et al* (1999). S100A11 may confer the high sensitivity to Ca^{2+} that is observed for association of annexin A6 with the sarcolemma (Babiychuk & Draeger, 2000). Most interestingly, Draeger and coworkers provided evidence that annexin A6 translocates to the caveolar domain, not the adherens junctions. Evidence from other cell types has implicated annexin A6 in Ca^{2+}-dependent formation of signaling complexes. For example,

annexin A6 has been shown to associate in a Ca^{2+}-dependent manner with lipid rafts along with PKCα and neurocalcin-α (Orito *et al*., 2001) and direct interaction between annexin A6 and skeletal muscle PKCα has been demonstrated (Schmitz-Peiffer *et al*., 1998). Annexin A6 has also been identified in a complex with the GTPase activating protein p120 Ras-GAP and the tyrosine kinases Fyn and Pyk2, annexin A6 interacting directly with p120 Ras-GAP and Fyn, but not Pyk2 (Chow *et al*., 2000). Annexin A6 is also thought to play a role in the regulation of cardiac function (Kaetzel & Dedman, 2004) and oxidation-induced Ca^{2+} mobilization (Cuschieri *et al*., 2005).

1.8 Hypothesis

That annexin A6 and S100A11 interact with each other in a Ca^{2+}-dependent manner.

The specific questions addressed were:

1. Are S100A11 and annexin A6 co-expressed in vascular smooth muscle cells?

2. Can the interaction between S100A11 and annexin A6 be verified independently?

3. Where is the site on annexin A6 that binds to S100A11?

4. Is the Ca^{2+}-dependent interaction between S100A11 and annexin A6 affected by phosphorylation of S100A11 by PKC?

CHAPTER 2:

MATERIALS AND METHODS

2.1 DNA methods

2.1.1 Design of PCR primers

Chicken S100A11 cDNA (NCBI accession number P24479) was amplified and subcloned into pGEX-6P-1 (Pharmacia Biotech.), via BamH I and Sma I sites, from a first strand cDNA prepared from chicken gizzard total RNA. The forward primer introduced a BamH I cleavage site (underlined) upstream of the ATG start codon (5'-CGGGATCCatgTCCAAGGTTTCCCCCACT-3') and the reverse primer introduced a Sma I cleavage site (underlined) downstream of the stop codon (5'-TCCCCCGGGctaAGGATGAGGAGGCTGAAC-3'). T9A and T9D substitutions were made in that clone as follows: a pair of T9A oligonucleotides (upper, 5'-GATCCATGTCCAAGGTTTCCCCCACTGAGgccGAAC-3' and lower, 5'-GTTCggcCTCAGTGGGGGAAACCTTGGACATG-3' (where substituted amino acids are indicated in lower case)) and a pair of T9D oligonucleotides (upper, 5'-GATCCATGTCCAAGGTTTCCCCCACTGAGgacGAAC-3' and lower, 5'-GTTCgtcCTCAGTGGGGGAAACCTTGGACATG-3') were annealed in 10 mM Tris-HCl, pH 7.5, 100 mM NaCl and 10 mM $MgCl_2$ by first heating to 95 °C for 2 min followed by slow cooling to room temperature over a period of 1 h, resulting in annealed, double stranded "adaptors". pGEX-6P-1/chicken S100A11 was digested with BamH I and Eco47 III and the released fragment was replaced with either the T9A or T9D annealed adaptor.

Rat S100A11 (NCBI accession number AY688465) was amplified from a rat cerebral vessel first strand cDNA using oligonucleotides designed against the mouse S100A11 cDNA (NCBI accession number BC021916) using a Kpn I containing forward primer 5'-

GGGGTACCatgCCTACAGAGACTGAGAG-3' and a Xba I containing reverse primer 5'-GCTCTAGAttaGATTCGCTTCTGGGAAGT-3' followed by cloning into the same sites of pcDNA3.0. For protein expression in bacteria, that coding region was amplified using the forward Nde I containing primer: 5'-CACACATatgCCTACAGAGACTGAGAGATG-3' and reverse EcoR I primer: 5'-GTGTGAATTCttaGATACGCTTCTGGGAAG-3' and cloned into those same sites in the expression vector pAED4.

Chicken annexin A6 (NCBI accession number Q6B344) was amplified from a first strand cDNA prepared from chicken gizzard total RNA, and subcloned into pGEX-6P-1 (Amersham Biosciences) via the EcoR I and Xho I sites. The forward primer introduced an EcoR I cleavage site (5'-CGGAATTCatgGCACCCAAAGGAAAGGTT-3') and the reverse primer introduced an Xho I cleavage site (5'-CCGCTCGAGctaGTCGTCCCCCCCGCACAG-3'). The pGEX-6P-1/Δ(1-20)annexin A6 was prepared by amplifying the above clone using the forward EcoR I containing primer 5'-CGGAATTCAGCCAGGATGCAGACGCCTTG-3' and the same reverse primer listed above for the full length chicken annexin A6. pGEX-6P-1/*N*-terminal half annexin A6 (G5-R339) was amplified using the forward EcoR I containing primer 5'-GAGAGAATTCGGAAAGGTTTACAGGGGCTCGGTGAAGGAC-3' and the reverse Xho I containing primer 5'-TCTCTCTCGAGtcaCCGATAGGCCACCTGCGCTGCCTCG-3'. pGEX-6P-1/*C*-terminal half annexin A6 (M340-D672) construct was generated from the pGEX-6P-1/annexin A6 clone by digestion with EcoR I and Blp I and replacement of the *N*-

terminal half fragment released with the annealed oligonucleotides (upper, 5'-AATTCATGTGGGAGC-3' and lower, 5'-TAAGCTCCCACATG-3').

2.1.2 PCR

PCR was carried out by adding 2 µL of cDNA into 48 µL of PCR mixture. The PCR mixture contains 1X PCR buffer (50 mM KCl, 10 mM Tris-HCl, pH 8.3, 1.5 mM $MgCl_2$), 0.2 mM dNTP mixture (Promega, WI), 0.1 µg of each primer, and 2 units of Taq DNA polymerase (Promega, WI).

2.1.3 Electrophoresis of DNA on agarose gels

Agarose was added to 1 x TAE to obtain a final concentration between 0.7 - 2% and the suspension was boiled until the agarose was completely solubilized. When the solution was cooled to ~ 50 °C, ethidium bromide was added (1 µL/mL). DNA samples were mixed with gel loading buffer and applied to the gel. Electrophoresis was carried out in 1 x TAE buffer at 100 V. The DNA was visualized under UV light.

2.1.4 Isolation of DNA from agarose gels

The desired DNA bands were excised from the agarose gel. The gel slice was weighed and 3 volumes of Buffer QG were added to 1 volume of gel. To solubilize the agarose and bind the DNA, the solution was incubated at 50 °C for 10 min. Every 2 min, the sample was mixed by vortexing. The solution was then applied to a QIAquick spin column. After centrifuging the sample for 30 s, the supernatant was carefully removed with a pipette. The pellet was washed with 500 µL of buffer QG and then twice with

buffer PE. DNA was eluted with 10 mM Tris-HCl, pH 7.5 or H_2O. All non-nucleic acid impurities such as agarose, proteins, salts and ethidium bromide were removed during the washing steps.

2.1.5 Purification of DNA from the PCR mixture

5 volumes of buffer PB were added to 1 volume of the PCR mixture. A QIAquick spin column was placed in a 2 mL collection tube. The mixed sample was applied to the QIAquick column and centrifuged for 30 - 60 s. The flow-through was discarded and the QIAquick column was washed with 0.75 mL buffer PE. The flow-through was discarded again prior to centrifugation for an additional 1 min at maximum speed. Finally, the QIAquick column was placed in a clean 1.5 mL microfuge tube, 50 µL elution buffer EB or H_2O was added to the centre of the QIAquick column and centrifuged for 1 min.

2.1.6 Dephosphorylation of DNA by calf intestinal phosphatase (CIP)

For blunt-end ligation and to prevent the re-ligation of vectors, the 5' phosphate group of the vector must be removed. DNA fragments (2.5 µg) were dephosphorylated at 37 °C for 30 min in 100 µL of reaction mixture consisting of 1x CIP buffer and 1 µL of calf intestinal phosphatase (CIP) (Fermentas Life Science). EDTA (5 mM) was then added to the reaction and incubated at 65 °C for 15 min to inactivate the enzyme. The DNA fragments were purified by phenol and ethanol precipitation before ligation.

2.1.7 Cohesive-end ligation

The plasmid DNA or DNA fragment was prepared by cutting with suitable restriction enzymes, followed by purification. 1:3 molar ratio of vector: insert DNA fragments together with 1 µL of T4 ligase were incubated in 1x ligation buffer in a total volume of 20 µL for 4 h at RT or overnight at 16 °C.

2.1.8 Mini-preparation of plasmid DNA

Three mL overnight cultures were grown in LB media with 100 µg/mL ampicillin at 37 °C overnight. Cells were pelleted at 3000 × g for 15 min. The supernatant was removed and pellets were resuspended in 250 µL Buffer P1. 250 µL Buffer P2 (Lysis Buffer) was added and incubated at RT for 5 min. 350 µL ice-cold 3 M acidic KOAc (Neutralisation Buffer) was added and mixed by inverting the tubes 6 - 7 times and incubated on ice for 5 min. After centrifugation (10,000 × g for 10 min), the supernatant was transferred to a fresh Qiagen mini-prep column. PE buffer (750 µL) was added and the column spun at 10,000 × g for 1 min. The column was spun again at 10,000 × g for 1 min to remove the remaining PE buffer. The column was put into an autoclaved Eppendorf tube and 50 µL of TE buffer or autoclaved dd H_2O added to the column, prior to centrifugation at 13,000 × g for 1 min to obtain purified DNA.

2.1.9 Bacterial colony PCR

Bacterial colony PCR allows rapid detection of transformation success when primers are available to allow determination of correct ligation products by size or hybridization. The strain of interest was streaked to obtain single colonies ~ 15 h before use and an average colony was selected for amplification. The 40 µL reaction cocktail [1 µL of colony

suspension, 4 μL 10 × PCR Buffer (without Mg^{2+}), 4 μL 25 mM $MgCl_2$ (final conc. = 2.5 mM), 1 μL dNTP (2.5 mM each, final conc. = 62.5 μM), 0.4 μL forward primer (10 mM stock, final conc. = 100 nM), 0.4 μL reverse primer (10 mM stock, final conc. = 100 nM), 28.7 μL ddH_2O, 0.5 μL Taq polymerase] was prepared. The PCR was performed as follows: 96 °C for 2 min, 94 °C for 40 s, 55 °C for 40 s, 72 °C for 1 min/kb expected product, 29 more cycles (30 total), 72 °C for 10 min, and 4 °C on hold.

2.1.10 Measurement of DNA concentration

The identity, integrity and purity of the DNA were subsequently analyzed by agarose gel electrophoreses. The DNA concentration was determined using a UV spectrophotometer at a wavelength of 260 nm. An absorption of 1.0 at 260 nm corresponds to a concentration of 50 μg/μL double-stranded DNA.

2.1.11 DNA sequencing

After subcloning and PCR-based mutagenesis, all products were subjected to DNA sequencing in the University of Calgary DNA Sequencing Facility. Basically, DNA was sequenced by generating fragments through the controlled interruption of enzymatic replication. DNA polymerase I was used to copy a particular sequence of single-strand DNA. The synthesis was primed by the complementary fragment. In addition to the four deoxyribonucleoside triphosphates (dNTP), the incubation mixture contained a 2', 3'-dideoxy analogue of one of them. The incorporation of this analogue blocked further growth of the new chain because it lacked the 3'-hydroxyl terminus needed to form the next phosphodiester bond. A fluorescent tag was attached to the oligonucleotide primer, a

differently colored one in each of the four chain-terminating reaction mixtures. The reaction mixtures were combined and electrophoresed together. The separated bands of DNA were then detected by their fluorescence, and the sequence of their colors directly yielded the base sequence.

2.1.12 RT-PCR

RT-PCR (*reverse transcriptase-polymerase chain reaction)* is a technique in which an RNA strand is transcribed into a DNA complement for amplification by PCR. Transcribing an RNA strand into a DNA complement is termed reverse transcription (RT) and is catalysed by the enzyme reverse transcriptase. The complementary DNA is then amplified by PCR. mRNA (~ 300 ng) was mixed with 1 µL oligo dT and 1 µL 10 mM dNTP and incubated at 65 °C for 5 min for denaturation and held at 4 °C. Then 4 µL 5 X PCR Buffer, 1 µL DTT, 1 µL RNAase out, 1 µL RT-superscript III were added and incubated at 25 °C for 5 min to anneal, 50 °C for 1 h to extend and stopped by heating at 70 °C for 15 min. Then a regular PCR was performed using specific primers to amplify the specific cDNA product.

2.1.13 Transformation of competent bacteria and bacterial manipulation

After thawing competent bacteria (BL21) on ice, a maximum of 20 ng ligated DNA or purified plasmid DNA was added to 15 µL competent cells in a cold 0.5 mL tube. Then the DNA and competent bacteria were mixed gently and kept on ice for 20 min or longer. The bacteria were then heat-shocked at 37 °C for 20 s, 250 µL antibiotic-free SOC medium were added, and aerated at 37 °C for 60 min. Selection of transformed bacteria

was done by plating 125 µL of the bacterial suspension on antibiotic-containing agar plates for 16 - 20 h. Only bacteria that have taken up the desired plasmids can grow on the agar plates. A single colony was then expanded in LB medium and used for DNA preparation.

For overnight mini cultures, single colonies were picked and inoculated in LB medium with antibiotic and shaken overnight at 37 °C. This pre-culture was then used for preparing frozen glycerol cultures, plasmid DNA or protein purification. For storage of bacteria, a glycerol stock culture was prepared by growing bacteria to an OD of 0.8 at a wavelength of 600 nm in culture medium. Bacterial culture (500 µL) was taken, added to 500 µL glycerol and mixed thoroughly in a small 1.5 mL tube. This stock solution was subsequently frozen at –80 °C.

2.2 Protein methods

2.2.1 Protein purification

2.2.1.1 Purification of S100A11 from chicken gizzard

Chicken gizzards (350 g, purchased from Lilydale Foods Ltd.) were minced and homogenized (2 × 30 s) using a Waring blender in 3.5 volumes of 40 mM Tris-HCl (pH 7.5), 80 mM NaCl, 10 mM EGTA, 5 mM EDTA, 1 mM PMSF and 1 mg/mL aprotinin. The homogenate was centrifuged at 30,000 × g for 60 min. The supernatant was filtered through cheesecloth and adjusted to 90% saturation with solid $(NH_4)_2SO_4$ over a period of 15 min. The mixture was stirred for an additional 30 min and centrifuged at 30,000 × g for 30 min. Pellets were suspended in a minimal volume (200 mL) of 40 mM Tris-HCl (pH 7.5), 80 mM NaCl and 1 mM EDTA (buffer A) and dialyzed against buffer A. The

dialysate was clarified by centrifugation at 30,000 × g for 60 min, adjusted to 0.2 mM with solid $CaCl_2$ and applied to a phenyl-Sepharose column (1.6 × 20 cm) equilibrated with 40 mM Tris-HCl (pH 7.5), 80 mM NaCl and 2 mM $CaCl_2$ (buffer B). The column was washed with buffer B until A_{280} returned to baseline and bound proteins were eluted using buffer B with 4 mM EGTA in place of 2 mM $CaCl_2$ at a flow rate of 20 mL/h. Fractions of 10 mL were collected and analyzed by SDS-PAGE, pooled and dialyzed against 20 mM imidazole-HCl (pH 6.2) and 1 mM EDTA (buffer C), and loaded onto a column (2.6 × 10 cm) of DEAE-Sephacel equilibrated with buffer C. The column was washed with buffer C until A_{280} returned to baseline. S100A11 was recovered in the flow-through fractions. After dialysis against three changes of buffer B, this fraction was applied to a column (1 × 10 cm) of phenyl-Sepharose equilibrated with buffer B. The column was washed with buffer B until A_{280} returned to baseline and bound proteins were eluted with 40 mM Tris-HCl (pH 7.5), 80 mM NaCl and 4 mM EGTA. Fractions of 1 mL were collected and the protein content was determined by SDS-PAGE. S100A11-containing fractions were pooled and stored frozen at -80 °C.

2.2.1.2 Purification of GST fusion protein

2.2.1.2.1 S100A11 and site-directed mutants

Four hundred mL of 2 × YT medium were inoculated with a single colony of *E.coli* BL21 (DE3) transformed with the expression vector (pGEX-6P-1/S100A11 construct), and grown at 37 °C with shaking for aeration (OD_{600} = 0.6 - 0.8). S100A11 expression was induced by the addition of isopropyl-β-D-thiogalactopyranoside to a final concentration of 0.1 mM. After 4 h of incubation, the culture was harvested by centrifugation at 8,000 ×

g. The pellet was resuspended in 25 mL of 1 × PBS and frozen at -80 °C. The cell pellet was thawed and sonicated (6 × 30 s) on ice. Triton X-100 was added to a final concentration of 1% and mixed gently for 30 min at room temperature. The sample was centrifuged for 20 min at 15,000 × g at 4 °C. The supernatant was collected, glutathione-Sepharose 4 beads (Pharmacia Biotech.) were added and gently rotated at room temperature for 30 min prior to centrifugation for 1 min at 3,000 × g and 4 °C. The supernatant was discarded. The beads were washed 3 times with 1 × PBS and packed into a column (1.6 × 10 cm). The bound GST-S100A11 was eluted with 10 mM reduced glutathione in 50 mM Tris-HCl (pH 8.0). The eluates containing GST-S100A11 were collected and dialyzed against 50 mM Tris-HCl (pH 7.0), 150 mM NaCl, 1 mM EDTA and 1 mM DTT (PreScission Cleavage Buffer). To cleave the GST from S100A11, the PreScission protease (Pharmacia Biotech.) was added to the dialysate and the cleavage reaction proceeded at 4 °C for 16 h.

Typically, glutathione-Sepharose 4B is used to remove the GST following the cleavage reaction. We found that a few proteins "co-purified" with the cleaved S100A11 which required a second purification step to be removed. A phenyl-Sepharose CL-4B (Pharmacia Biotech.) column purification step was employed as follows: Phenyl-Sepharose was washed and equilibrated with 1 × PBS containing 2 mM $MgCl_2$ and $CaCl_2$. $MgCl_2$ and $CaCl_2$ were added to a final concentration of 2 mM. Phenyl-Sepharose (50% slurry) was added, rotated for 10 min at room temperature, and poured into a column (1.6 × 10 cm). The flow-through fractions were discarded. Non-specifically bound proteins were washed off the column using high salt buffer containing 20 mM

Tris-HCl (pH 7.5), 1 M NaCl and 0.2 mM DTT. Purified S100A11 was eluted with 20 mM Tris-HCl (pH 7.5), 4 mM EGTA and 0.2 mM DTT.

The site-directed mutants, T9A and T9D of S100A11 were purified following the same process as the purification of WT S100A11.

2.2.1.2.2 Annexin A6, GST-annexin A6, Δ(1-20)annexin A6, *C*-terminal half annexin A6 (M340-D672), Δ(1-4)*N*-terminal half annexin A6 (G5-R339)

2 × YT medium (400 mL) was inoculated with a single colony of *E. coli* BL21 (DE3) transformed with the expression vector, and grown at 37 °C with shaking for aeration (OD_{600} = 0.8). Protein expression was induced by the addition of IPTG to a final concentration of 0.1 mM. After 3 h of incubation, the culture was harvested by centrifugation at 8,000 × g. The pellet was resuspended in 25 mL of 1 × PBS and frozen at -80 °C. The cell pellet was thawed and sonicated (6 × 30 s) on ice. Triton X-100 was added to a final concentration of 1%, mixed gently for 30 min and centrifuged for 20 min at 17,000 × g and 4 °C. The supernatant was collected, glutathione-Sepharose 4B (Pharmacia Biotech.) added and gently rotated at room temperature for 30 min prior to centrifugation for 1 min at 3,000 × g and 4 °C. The supernatant was discarded. The beads were washed 3 times with 1 × PBS and packed into a column (1.6 × 10 cm). The bound GST-fusion protein was eluted with 10 mM reduced glutathione in 50 mM Tris-HCl (pH 8.0). The eluted fractions containing GST-fusion protein were pooled and dialyzed against 50 mM Tris-HCl (pH 7.0), 150 mM NaCl, 1 mM EDTA and 1 mM DTT (PreScission Cleavage Buffer). To cleave the GST from the target protein, the

PreScission protease (Pharmacia Biotech.) was added to the dialysate and incubated at 4 °C for 16 h.

A Mono Q HR 16/10 anion exchange column for FPLC (Fast Protein Liquid Chromatography) System (Pharmacia Biotech.) was employed to remove the co-purified proteins as follows:

Purification of annexin A6: The cleaved protein was dialyzed against buffer A (20 mM Tris-HCl, pH 7.5) and applied to a Mono Q column previously equilibrated with buffer A. The column was washed with buffer A until A_{280} returned to baseline and bound proteins were eluted with a linear gradient of 0 – 0.5 M NaCl. Fractions were collected at a flow rate of 0.5 mL/min.

Purification of C-terminal half annexin A6 (M340-D672): The cleaved protein was dialyzed against buffer A (20 mM Tris-HCl, pH 7.5) and applied to a Mono Q column previously equilibrated with buffer A. The column was washed with buffer A until A_{280} returned to baseline. The target protein eluted with 180 mM NaCl and the contaminating proteins with 1 M NaCl.

Purification of Δ(1-20)annexin A6: The cleaved protein was dialyzed against buffer A (20 mM Tris-HCl, pH 7.5) and applied to a Mono Q column previously equilibrated with buffer A. The column was washed with buffer A until A_{280} returned to baseline and bound proteins were eluted with a linear gradient of 0 – 0.5 M NaCl. Fractions were collected at a flow rate of 0.5 mL/min.

Purification of Δ(1-4)N-terminal half annexin A6 (G5-R339): The cleaved protein was dialyzed against buffer A (20 mM Tris-HCl, pH 7.5) and applied to a column (1.2 × 5 cm) of DEAE-Sephacel equilibrated with buffer A. The column was washed with

buffer A until A_{280} returned to baseline. The column was washed with 100 mM NaCl and bound proteins were eluted with a linear 0.1 - 0.3 M NaCl gradient. Fractions were collected at a flow rate of 15 mL/h.

As shown in Fig. 11 (page 61), S100A11, annexin A6, *C*-terminal half annexin A6 (M340-D672) and their GST-fusion counterparts were purified to electrophoretic homogeneity. The Δ(1-20)*N*-terminal annexin A6 and Δ(1-4)*N*-terminal half annexin A6 (G5-R339) were to some extent contaminated with GST.

2.2.2 S100A11 affinity chromatography

2.2.2.1 Generation of S100A11-Sepharose and control columns

CNBr-activated Sepharose 4 Fast flow beads (Pharmacia Biotech.) were swollen in 1 mM HCl for 30 min. Beads were washed with 15 gel volumes of cold 1 mM HCl and then with coupling buffer (0.1 M $NaHCO_3$, pH 8.3, 0.5 M NaCl). S100A11 (7 mg) was coupled to the resin in the same buffer overnight at 4 °C. For the control column, no S100A11 was included. The supernatant was collected and the protein concentration determined by the BCA assay. After washing the resin with coupling buffer again, any remaining reactive groups were blocked with 1 M ethanolamine (pH 9) for 2 h at room temperature. The resin was washed with alternating pH buffers of 0.1 M NaOAC (pH 4), 0.5 M NaCl and 0.1 M $NaHCO_3$ (pH 10), 0.5 M NaCl for 5 cycles. The resin was equilibrated with the appropriate buffer.

2.2.2.2 Affinity chromatography of chicken gizzard extract

Buffer A: 30 mM Tris-HCl (pH 7.5), 150 mM NaCl, 2 mM EGTA, 0.3% Triton X-100, 1 mM DTT, 0.1 mg/mL leupeptin and 0.01 mg/mL pepstatin A.

Buffer B: 30 mM Tris-HCl (pH 7.5), 150 mM NaCl, 2.4 mM $CaCl_2$, 0.3% Triton X-100, 1 mM DTT, 0.1 mg/mL leupeptin and 0.01 mg/mL pepstatin A.

Buffer C: 30 mM Tris-HCl (pH 7.5), 150 mM NaCl, 0.2 mM $CaCl_2$, 1 mM DTT.

Buffer D: 30 mM Tris-HCl (pH 7.5), 150 mM NaCl, 4 mM EGTA, 1 mM DTT.

All procedures were carried out at 4 °C. Frozen chicken gizzards were chopped and minced to yield 1 g of muscle mince and homogenized in a Waring blender for 2 × 30 s in 4 volumes of buffer A. The homogenate was centrifuged at 10,000 × g for 15 min. The supernatant was diluted with the same volume of buffer B to reach a final concentration of 0.2 mM $CaCl_2$ (buffer C) and loaded on the S100A11 affinity column (1.6 × 10 cm) overnight (10 mL/h). The column was washed with buffer C until A_{280} returned to baseline (10 mL/h). The bound proteins were eluted with buffer D and fractions (3 mL) were collected at a flow rate of 10 mL/h.

Two control experiments were performed:

(i) To the control column (no S100A11 coupled), the same procedures as described above were performed.

(ii) The homogenate supernatant was loaded on the S100A11 affinity column in buffer D (4 mM EGTA) and bound proteins eluted with buffer D.

2.2.2.3 Affinity chromatography with purified annexin A6, Δ(1-20)annexin A6, C-terminal half annexin A6 (M340-D672), Δ(1-4)N-terminal half annexin A6 (G5-R339)

Purified annexin A6, Δ(1-20)annexin A6, *C*-terminal half annexin A6 (M340-D672), and *N*-terminal half annexin A6 (G5-R339) were dialyzed against buffer C and loaded on the S100A11 affinity column. The column was washed with buffer C until A_{280} returned to baseline (10 mL/h). Bound proteins were eluted with buffer D and fractions (1 mL) collected at a flow rate of 10 mL/h.

2.2.3 Annexin A6 affinity chromatography

2.2.3.1 Generation of annexin A6-Sepharose and control column

CNBr-activated Sepharose 4 Fast flow beads (Pharmacia Biotech.) were swollen in 1 mM HCl for 30 min. Beads were washed with 15 gel volumes of cold 1 mM HCl and then with coupling buffer (0.1 M $NaHCO_3$, pH 8.3, 0.5 M NaCl). Purified recombinant annexin A6 (2.7 mg) in coupling buffer was coupled to 0.5 mL of the resin (with 6 mg protein/mL coupling capacity) overnight at 4 °C. For the control column, no annexin A6 was included. The supernatant was collected and the protein concentration determined by the BCA assay to calculate the coupling efficiency (2.1 mg annexin A6 were coupled, i.e. 77.8% coupling efficiency). After washing the resin with coupling buffer again, any remaining reactive groups were blocked with 1 M ethanolamine (pH 9) for 2 h at room temperature. The resin was washed with alternating pH buffers of 0.1 M NaOAc (pH 4), 0.5 M NaCl and 0.1 M $NaHCO_3$ (pH 10), 0.5 M NaCl for 5 cycles. The resin was equilibrated with the appropriate buffer.

2.2.3.2 Affinity chromatography of purified chicken S100A11

Purified S100A11 (200 μg) was dialyzed against buffer C and loaded on the annexin A6 affinity column. The column was washed with buffer C until A_{280} returned to baseline. Bound proteins were eluted with buffer D and fractions (0.5 mL) were collected at a flow rate of 15 mL/h.

Control experiments were performed: The same procedures as described above were performed with the control column (no annexin A6 coupled).

2.2.4 In vitro phosphorylation of purified recombinant chicken S100A11

2.2.4.1 S100A11 phosphorylation by cPKC

Final concentrations (250 μl reaction mixture in a 1.5 mL tube): 0.1 mg/mL S100A11, 20 mM Tris-HCl (pH 7.5), 10 mM $MgCl_2$, 0.2 mM $CaCl_2$, fresh lipids (mixed micelles, 1/10 volume), cPKC (2.5 μg/mL), microcystin-LR (phosphatase inhibitor; 10 μM), 0.2 mM [γ-^{32}P]ATP.

61.8 μL phosphatidylserine from porcine brain (Avanti Polar Lipids, Inc.) and 15.4 μL 1, 2-diolein (Doosan Serdary Research Lab) were mixed and dried in a N_2 stream. 0.5 mL 0.3% Triton X-100/Na-HEPES, pH 7 was added and incubated at 30 °C for 30 min. The mixture was sonicated (2 × 10 s) and 25 uL were added to the reaction tube as mixed micelles. The mixture was preincubated for 2 min at 30 °C and reaction started by addition of [γ-^{32}P]ATP. A 20 μL aliquot was spotted onto P-81 phosphocellulose paper squares (Whatman). Following extensive washes for 5 min in 3 × 500 mL of 0.5% (v/v) phosphoric acid to remove residual radiolabeled ATP, the P-81 paper squares were briefly rinsed in acetone and dried. Radioactivity bound to the paper was quantified by Čerenkov counting in a Beckman model LS6000SC liquid scintillation counter. A 10 μL

aliquot (1 µg protein) was added to SDS gel sample buffer after 1 h, boiled for 5 min and subjected to SDS-PAGE. The gel was exposed to Kodak BioMax XAR film for 16 h.

2.2.4.2 Affinity chromatography of phosphorylated chicken S100A11

S100A11 (100 µg) was phosphorylated for 1 h in 1 mL of solution and applied to the annexin A6 affinity column. The column was washed with buffer C until A_{280} returned to baseline. Bound protein was eluted with buffer D and fractions (0.5 mL) were collected at a flow rate of 16 mL/h. All fractions were subjected to SDS-PAGE and exposed for 16 h to Kodak BioMax XAR film. Non-phosphorylated S100A11 was also applied to the affinity column in the presence of liposomes as control and subjected to the same procedure.

2.2.5 Antibody generation, purification and characterization

2.2.5.1 Generation and purification of rabbit anti-(rat annexin A6)

Polyclonal antibodies to rat annexin A6 were generated against the *N*-terminal peptide of 12 amino acids (AKIAQGAMYRGS) by Global Peptide Services (Fort Collins, CO, USA). The IgG fraction was purified using a High Trap-protein A column (5 mL, Sigma) as follows:

5 mL serum were diluted with 40 mL buffer A (20 mM sodium phosphate, pH 7) and centrifuged at 4,000 × g for 1 min. The pellet was removed. The column was washed with 20 mL water (2 - 5 mL/min) and then with 40 mL buffer A (2 - 5 mL/min). 50 mL diluted serum were loaded on the High Trap-protein A column (2 - 5 mL/min), keeping an aliquot (50 µL), and the column was washed with 25 mL buffer A (2 - 5 mL/min).

Bound protein was eluted with 100 mM citric acid (2 - 5 mL/min), and collected in tubes containing 1.5 mL Tris-HCl (2 M, pH 7.5). Protein eluted between 4 and 10 mL. The pH of the eluate was adjusted with Tris-HCl (2 M, pH 7.5) as needed. The column was washed with 20 mL buffer A (2 - 5 mL/min), then with water and finally with 20% ethanol for storage.

2.2.5.2 Characterization of polyclonal rabbit anti-(rat annexin A6) and monoclonal anti-(rat S100A11)

Proteins were extracted from 10 freeze-dried rat tail arteries by addition of 500 µL of 50 mM Tris/HCl, pH 6.8, containing 1% SDS and 100 µM diisopropylfluorophosphate. Samples were heated to 95 °C for 5 min, and mixed for 60 min before the addition of 100 µL of 2 × sample buffer prior to 7.5-20% acrylamide SDS-PAGE at 35 mA for 3.5 h. The proteins were transferred to 0.2 µm nitrocellulose membranes (Bio-Rad) for 3 h at 80 V and 4 °C in 25 mM Tris, 192 mM glycine, 20% (v/v) methanol using a Bio-Rad Trans Blot Cell. The blots were blocked with 5% non-fat dried milk in TBST for 1 h, and incubated with 1% non-fat dried milk/TBST containing anti-annexin A6 (1:10,000 dilution) for 1 h. Membranes were washed and incubated with anti-rabbit IgG–horseradish peroxidase-conjugated secondary antibodies (1:10,000 dilution, Chemicon). Immunoreactive bands were visualized using SuperSignal® West Pico Enhanced Chemiluminescent Substrate (Pierce). In control experiments to demonstrate antibody specificity, the annexin A6 antigenic peptide (AKIAQGAMYRGS) was added to 1% non-fat dried milk/TBST containing anti-annexin A6 (1:10,000 dilution) and incubated

for 1 h to block the antibody before addition to the blot. The ratio between annexin A6 antigenic peptide and anti-annexin A6 is 2/1 (w/w).

For rat S100A11 detection, proteins were transferred to 0.2 μm nitrocellulose membranes (Bio-Rad) for 3 h at 40 V and 4 °C in 25 mM potassium phosphate buffer (pH 7.0) using a Bio-Rad Trans Blot Cell. The blots were blocked with 5% non-fat dried milk in TBST for 1 h, and incubated with 1% non-fat dried milk/TBST containing monoclonal mouse anti-(rat S100A11) for 1 h. Membranes were washed and incubated with anti-rabbit IgG–horseradish peroxidase-conjugated secondary antibodies (1:10,000 dilution; Chemicon). Immunoreactive bands were visualized using SuperSignal® West Pico Enhanced Chemiluminescent Substrate (Pierce).

2.2.5.3 Characterization of polyclonal rabbit anti-(chicken S100A11)

Polyclonal rabbit anti-(chicken S100A11) was generated by our laboratory (Allen *et al.*, 1996). Serial dilutions of purified recombinant chicken S100A11 were subjected to 17.5% acrylamide SDS-PAGE at 200 V for 45 min. The proteins were transferred to 0.2 μm nitrocellulose membranes (Bio-Rad) for 3 h at 40 V and 4 °C in 25 mM potassium phosphate buffer (pH 7.0) using a Bio-Rad Trans Blot Cell. Potassium phosphate buffer was used instead of the usual Tris-glycine-methanol buffer to prevent small proteins like S100A11 from going through the membrane. The blots were blocked by treatment with 0.5% (w/v) I-BLOCK™ (Tropix) in TBS (20 mM Tris-HCl, pH 7.5, 0.5 M NaCl) for 1 h at room temperature, washed 4 times (5 min each) with TBS, and then incubated with primary antibody (polyclonal rabbit anti-(chicken S100A11)) at 1:10,000 dilution in TBS containing 0.1% I-BLOCK. The membranes were washed 4 times (5 min each) with TBS

and incubated for 1 h with goat anti-(rabbit IgG)-horseradish peroxidase (HRP) conjugate (Chemicon). The membranes were washed 4 times (5 min each) with TBS and immunoreactive bands were visualized using SuperSignal® West Femto Maximum Sensitivity Enhanced Chemiluminescent Substrate (Pierce).

2.2.6 Gel overlay

One μg of purified S100A11 (positive control) and 1 μg of purified annexin A6, Δ(1-20)*N*-terminal annexin A6, *C*-terminal half annexin A6 (M340-D672), or Δ(1-4)*N*-terminal half annexin A6 (G5-R339) were subjected to SDS-PAGE (7.5 - 20% acrylamide gradient gel). The proteins were transferred to 0.2 μm nitrocellulose membranes (Bio-Rad) for 3 h at 80 V and 4 °C in 25 mM Tris, 192 mM glycine, 20% (v/v) methanol using a Bio-Rad Trans Blot Cell and the membranes were dried overnight. Membranes were wet with TBS in the presence of 0.2 mM $CaCl_2$ or 4 mM EGTA and blocked by treatment with 0.5% (w/v) I-BLOCK™ in TBS for 1 h at room temperature in the presence of 0.2 mM $CaCl_2$ or 4 mM EGTA. Membranes were then incubated with purified S100A11 (100 μg/mL in 30 mM Tris-HCl, pH 7.5, 150 mM NaCl, 0.2 mM $CaCl_2$, 1 mM DTT or 30 mM Tris-HCl, pH 7.5, 150 mM NaCl, 4 mM EGTA, 1 mM DTT) for 4 h at room temperature and washed 4 times (5 min each) with TBS containing 0.2 mM $CaCl_2$ or 4 mM EGTA prior to incubation with primary antibody (polyclonal rabbit anti-(chicken S100A11)) at 1:10,000 dilution in TBS containing 0.1% I-BLOCK and either 0.2 mM $CaCl_2$ or 4 mM EGTA. Membranes were washed 4 times (5 min each) with TBS containing 0.2 mM $CaCl_2$ or 4 mM EGTA and incubated for 1 h with goat anti-(rabbit IgG)-horseradish peroxidase (HRP) conjugate. Membranes were then washed 4

times (5 min each) with TBS containing 0.2 mM $CaCl_2$ or 4 mM EGTA and immunoreactive bands were visualized using SuperSignal® West Femto Maximum Sensitivity Substrate. The protein molecular weight standards used in gel overlay procedures were PageRuler™ Prestained Protein Ladder (Fermentas).

2.2.7 Ca^{2+}-dependent binding of tryptic fragments of annexin A6 to immobilized S100A11

Purified recombinant annexin A6 was dialyzed against and diluted by 25 mM Tris (pH 7.5) to a final concentration of 0.2 mg/mL (10 mL total volume) prior to partial digestion by 40 µg [1/50 (w/w) ratio of trypsin/annexin A6] of Sequencing Grade Modified TPCK-Trypsin (Promega) at 30 °C for 15 min. Digestion was stopped by addition of soybean trypsin inhibitor (STI, United States Biochemical Corporation) to 0.1 mg/mL. Concentrated Tris-HCl (pH 7.5), NaCl, $CaCl_2$ and solid DTT were added to obtain a final buffer of 30 mM Tris-HCl (pH 7.5), 150 mM NaCl, 0.2 mM $CaCl_2$, 1 mM DTT and loaded onto the S100A11 affinity column. The column was washed with buffer (30 mM Tris-HCl pH 7.5, 150 mM NaCl, 0.2 mM $CaCl_2$, 1 mM DTT and 0.1 mg/mL STI) until A_{280} returned to baseline (10 mL/h). Bound peptides were eluted with 30 mM Tris-HCl (pH 7.5), 150 mM NaCl, 4 mM EGTA, 1 mM DTT and 0.1 mg/mL STI and fractions (1 mL) were collected at a flow rate of 10 mL/h.

2.2.8 Chemical cross-linking

Purified recombinant chicken annexin A6 (0.2 mg/mL) and purified recombinant chicken S100A11 (0.2 mg/mL) were incubated together in 0.2 M triethanolamine (pH 8.0) in the

presence of 4 mM EGTA or 1 mM $CaCl_2$ for 10 min at room temperature. A 50-fold molar excess (relative to annexin A6) of dimethylsuberimidate (DMS, Pierce) was added to start the cross-linking reaction and samples of reaction mixtures were withdrawn at selected times from 0 to 5 h. Cross-linking reactions were stopped by adding Tris to a final concentration of 50 mM. S100A11 or annexin A6 alone were treated simultaneously as controls. Then 10 µg S100A11 and 10 µg annexin A6 were subjected to SDS-PAGE (7.5 - 20 % acrylamide gradient gel).

The proteins on an identical gel run in parallel were transferred to 0.2 µm nitrocellulose membranes for 3 h at 80 V and 4 °C in 25 mM Tris, 192 mM glycine, 20% (v/v) methanol using a Bio-Rad Trans Blot Cell and the membranes were dried overnight. Membranes were wet with TBST, blocked by treatment with 0.5% (w/v) I-BLOCK™ in TBST (20 mM Tris-HCl pH 7.5, 0.5 M NaCl, 0.05% Tween) for 1 h at room temperature, and incubated with primary antibody (polyclonal rabbit anti-(chicken S100A11)) at 1:10,000 dilution in TBST containing 0.1% I-BLOCK. The membranes were washed 4 times (5 min each) with TBST, incubated for 1 h with goat anti-(rabbit IgG)-horseradish peroxidase (HRP) conjugate, washed 4 times (5 min each) with TBST and visualized using SuperSignal® West Femto Maximum Sensitivity Substrate.

2.2.9 Liposome co-pelleting assay

2.2.9.1 Ca^{2+}-dependent binding of S100A11 to phosphatidylserine liposomes

Four mg of phosphatidylserine from porcine brain (Avanti Polar Lipids, Inc.) were dried in a N_2 stream. 1.5 mL of buffer A (50 mM imidazole-HCl, pH 7.4, 150 mM NaCl) were added and incubated at 30 °C for 30 min. After vortexing, the suspension was sonicated

on ice for 10 × 30 s. The binding assay was carried out in a total volume of 200 µL of buffer A containing 0.2 mM $CaCl_2$ or 4 mM EGTA, 100 µg liposomes, with 0.5, 1, 2.5, 5 or 10 µg of purified recombinant chicken S100A11 at room temperature for 20 min. Liposomes were sedimented by centrifugation using a Beckman TL 100 tabletop ultracentrifuge at 100,000 × g for 30 min. The pellet was resuspended in 50 µL EGTA or Ca^{2+} buffer, 50 µL 2 × sample buffer was added and boiled for 5 min prior to SDS-PAGE of both the supernatants and pellets.

2.2.9.2 Liposome preparation from rat tail artery and co-pelleting assay

Rat tail arterial smooth muscle was ground in 15 volumes of buffer A (50 mM Tris-HCl, pH 7.5, 150 mM NaCl, 1 mM DTT, 1 mM $CaCl_2$, 1 µg/mL leupeptin, 1 µg/mL pepstatin, 1 mM PMSF) and shaken for 30 min. The extract was centrifuged at 100,000 × g for 30 min and the supernatant (S1) withdrawn. The pellet was resuspended in 15 volumes of buffer B (50 mM Tris-HCl, pH 7.5, 150 mM NaCl, 1 mM DTT, 4 mM EGTA, 1 µg/mL leupeptin, 1 µg/mL pepstatin, 1 mM PMSF), homogenized, shaken for 15 min and centrifuged at 100,000 × g for 30 min. The supernatant (S2) was withdrawn, the pellet resuspended in 15 volumes of buffer B and homogenized. After shaking for 15 min, the sample was centrifuged at 100,000 × g for 30 min. The supernatant (S3) was withdrawn, the pellet resuspended in 15 volumes of buffer B and homogenized. After shaking for 30 min, 1 mL of $CHCl_3$/methanol (50%/50%) was added and mixed end-over-end for 5 min. After low-speed centrifugation (3,000 × g), the $CHCl_3$ (lower) layer was extracted and dried in a N_2 stream. One mL of buffer C (50 mM imidazole-HCl, pH 7.4, 150 mM NaCl) was added and incubated at 30 °C for 30 min. After vortexing, the liposomes were

sonicated on ice for 10 × 30 s. Binding assays were carried out in a total volume of 200 µL of buffer C containing 0.2 mM $CaCl_2$ or 4 mM EGTA, 40 µL liposomes, 5 µg of purified recombinant chicken S100A11 and/or annexin A6 at room temperature for 20 min. Samples were centrifuged at 100,000 × g for 30 min. Pellets were resuspended in 50 µL EGTA or Ca^{2+} buffer, 2 × sample buffer was added and boiled for 5 min prior to SDS-PAGE of both the supernatants and pellets.

2.2.10 In-gel destaining and digestion of proteins separated by SDS-PAGE for analysis by MALDI-TOF/MS

Gloves were worn throughout to avoid contamination and to avoid contact with hazardous materials. All sample handling was conducted in the flow hood. All wash steps were performed on an orbital shaking platform to improve and standardize efficiency. All microfuge tubes used were pre-washed with freshly prepared 50% ACN/0.1% TFA to prevent contamination and dried thoroughly.

2.2.10.1 Destaining

A water bath was set to a stable temperature of 56 °C. The gel slices were cut into roughly 1 × 1 × 1 mm pieces with a clean scalpel blade**.** Alternatively, a pipette tip was used for the maceration. Milli-Q water (250 µL) was added and washed twice for 15 min. Gel pieces were then washed twice with 50% ACN (250 µL) for 15 min, 25 mM AMBIC (250 µL) was added and shaken for 15 min. 100% ACN (250 µL) was added and washed for another 15 min. The supernatant was discarded. If the gel pieces were still colored

with Coomassie stain, the last 2 wash steps were repeated. Samples could be left in 500 µL of 25 mM AMBIC/ACN (1:1 v/v) overnight if necessary.

2.2.10.2 Dehydration of gel pieces

The supernatant was replaced with 100% ACN (100 µL) and left for 5 min. When dehydrated, the gel pieces appeared white. The supernatant was removed and the gel pieces dried in a Speedvac for 15 min.

2.2.10.3 In-gel protein digestion

Ten µL of trypsin solution (0.02 µg/µL of modified trypsin in Milli-Q water) were added to an 8 mm^3 dried gel volume (i.e. a cube which measures approximately 2 × 2 × 2 mm) and the gel slices allowed to re-swell (left until the pieces became clear). Enough 20 mM AMBIC to cover the gel piece (approximately 10 µL per 8 mm^3 of dry gel) was added. Tube caps were securely depressed to avoid drying out of the sample and incubated at 37 ^oC overnight (8 – 16 h).

2.2.10.4 Extraction

100% ACN (50 µL) was added to the gel piece from the digestion step and shaken for 30 min. The supernatant was transferred to a microfuge tube and dried in a Speedvac (10 – 20 min). The dried sample was resuspended in 20 µL of 5% ACN/0.1%TFA, vortexed, centrifuged, sonicated and centrifuged again. The sample was left for 2 min to ensure it was fully dissolved.

2.2.10.5 Zip tipping

0.1% TFA (20 µL) was added to the sample. Using a C_{18} Zip Tip on a 10 µL pipette, 50% ACN (10 µL) was aspirated and ejected onto a Kimwipe. This step was repeated and the tip wiped. The Zip Tip was washed twice with 10 µL of 0.1% TFA/5% ACN, which was ejected onto a Kimwipe. The sample was aspirated up and down 8 times, being very careful not to introduce air bubbles. The Zip Tip was again washed twice with 10 µL of 0.1% TFA/5% ACN, which was ejected onto a Kimwipe. 0.1% TFA/50% ACN (4 µL) was aspirated and emptied into a pre-washed Eppendorf tube.

2.2.11 N-terminal sequencing by Edman degradation

Fig. 7 depicts the chemistry underlying Edman degradation. Coupling of *N*-terminal amino groups of a protein or peptide (1) with phenylisothiocyanate (PITC, Edman reagent) (2) forms an open chain thiourea derivative (3). The *N*-terminal amino acid is split off as the anilinothiazolinone (ATZ) derivative (5) with trifluoroacetic acid. This unstable ATZ-derivative is converted into a more stable phenylthiohydantoin (PTH) derivative (6), which is separated by reversed phase HPLC and identified by comparison with a standard.

Peptides for sequence analysis were subjected to SDS-PAGE (7.5 - 20% acrylamide gradient gel) and transferred to Immobilon-P Membrane (one of the PVDF membranes from Millipore) for 3 h at 80 V and 4 °C in 25 mM Tris, 192 mM glycine and 20% (v/v) methanol using a Bio-Rad Trans Blot Cell. The membranes were stained with Ponceau S (Sigma) to visualize the peptides, which were cut out of the membrane for Edman degradation at the University of Dundee.

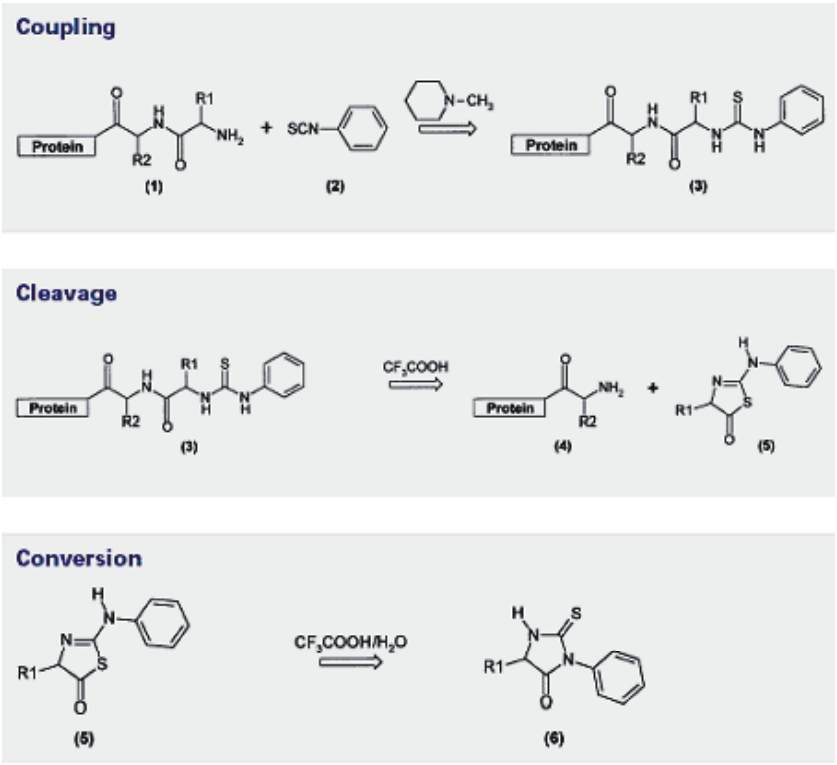

Figure 7. Edman degradation reaction.

2.2.12 Other methods

2.2.12.1 Measurement of protein concentration (BCA assay and amino acid analysis)

The BCA Protein Assay Reagent Kit (Pierce) combines the well-known reduction of Cu^{2+} to Cu^{+} by protein in an alkaline medium (the biuret reaction) with the highly sensitive and selective colorimetric detection of the cuprous cation (Cu^{+}) using a unique reagent containing bicinchoninic acid. The purple-colored reaction product of this assay is formed by the chelation of 2 molecules of BCA with one cuprous ion. This water-soluble complex exhibits a strong absorbance at 562 nm, which is linear with increasing protein concentrations over a broad working range of 20 μg/mL to 2000 μg/mL. The BCA method is not a true end point method; the final color continues to develop, but following incubation the rate of color development is slowed sufficiently to allow large numbers of samples to be analysed in a single assay. The macromolecular structure of protein, the number of peptide bonds and the presence of four amino acids (cysteine, cystine, tryptophan and tyrosine) are reported to be responsible for color formation with BCA.

The concentration of S100A11 was determined by quantitative amino acid analysis at the Alberta Peptide Institute, University of Alberta.

2.2.12.2 Sodium dodecyl sulfate-polyacrylamide gel electrophoresis (SDS-PAGE)

Under denaturing conditions, proteins can be separated on the basis of mass by electrophoresis in a polyacrylamide gel. SDS is an anionic detergent that disrupts nearly all non-covalent interactions in native proteins. β-mercaptoethanol is also included in the sample buffer to reduce disulfide bonds. The SDS complexes with the denatured proteins are then separated by electrophoresis on a polyacrylamide gel. The gels were composed

of two layers: a 7.5 - 20% acrylamide separating gel (pH 8.8) that separates the proteins according to size, and a lower percentage (5%) stacking gel (pH 6.8) that ensures the proteins' simultaneous entry into the separating gel at the same height.

The separating gel was poured between two glass plates, separated by 0.75 - 1.5 mm. Isopropanol was added to the surface of the gel to exclude air and ensure flatness of the surface. After polymerization of the separating gel, it was rinsed twice with H_2O to remove the isopropanol. The stacking gel was poured on top of the separating gel, the comb was inserted, and gels were allowed to polymerize (~30 min at room temperature). Samples were loaded into the wells of the gel and running buffer was added to the upper and lower chambers. A cover was then placed over the gel chamber and various voltages applied. The negatively charged SDS-protein complexes migrate toward the anode at the bottom of the gel. Small proteins move more rapidly through the gel, whereas large ones migrate more slowly. Proteins that differ in mass by ~ 2% are separated and can be distinguished. The electrophoretic mobility of many proteins in SDS-polyacrylamide gels is proportional to the logarithm of their mass. Gels were stained overnight in 45% (v/v) ethanol, 10% (v/v) acetic acid containing 0.1% (w/v) Coomassie Brilliant Blue R250 (Bio-Rad) and destained in 10% (v/v) acetic acid.

2.3 Materials

2.3.1 Chemical reagents and general materials

1 kb DNA ladder (Sigma), 1,2-diolein (Doosan Serdary Research Labs.), glacial acetic acid (EMD Chemicals Inc.), acetonitrile (ACN) (EMD Chemicals Inc.), ammonium bicarbonate (AMBIC) (BDH Inc.), ammonium sulphate (BDH Inc.), aprotinin (Sigma),

[γ-^{32}P]ATP (NP Biomedicals), acrylamide (30%)/bisacrylamide (0.8%) (Bio-Rad), Becto™ Agarose (BD), Becto™ Tryptone (BD), Becto™ yeast extract (BD), ammonium acetate (Sigma), ammonium persulphate (APS) (Bio-Rad), ampicillin (Sigma), bovine serum albumin (BSA) (Sigma), bromphenol blue (Sigma), β-mercaptoethanol (Promega), calcium chloride ($CaCl_2$) (Sigma), chloroform (Sigma), citric acid (BDH Inc.), CNBr-activated Sepharose 4 Fast flow beads (Pharmacia Biotech), Coomassie Brilliant Blue R250 (Bio-Rad), diisopropylfluorophosphate (DFP) (Calbiochem), dimethylsuberimidate (DMS) (Pierce), dithiothreitol (DTT) (ICN Biomedicals Inc.), DEAE-Sephacel™ (Amersham Biosciences), deoxynucleoside triphosphates (dNTP) (Promega), ethanolamine (Fisher Scientific), ethylenediamine tetraacetic acid, disodium salt (EDTA) (Sigma), ethyleneglycol-*bis*(β-aminoethylether)-N, N, N', N'-tetraacetic acid (EGTA) (Sigma), ethanol (Roche), ethidium bromide (Life Technologies, Inc.), formaldehyde (Promega), glutathione-Sepharose (Pharmacia Biotech.), glycerol (Sigma), glycine (Bio-Rad), HiTrap™ Protein A HP (Amersham Pharmacia Biotech.), isopropyl-β-D-thiogalactopyranoside (IPTG) (Sigma), I-BLOCK™ (Tropix), imidazole (BDH Inc.), isopropanol (Sigma), leupeptin (Sigma), magnesium chloride (Sigma), methanol (EMD Chemicals Inc.), microcystin-LR (Axxora) (phosphatase inhibitor), Immobilon-P Membrane (Millipore), nitrocellulose membrane (Bio-Rad), pepstatin A (Sigma), phenyl-Sepharose CL-4B (Pharmacia Biotech.), phosphatidylserine (Avanti Polar Lipids Inc.), Ponceau S (Sigma), potassium chloride (KCl) (Sigma), potassium dihydrogen phosphate (KH_2PO_4) (BDH Inc.), potassium hydrogen phosphate (K_2HPO_4) (BDH Inc.), protein A-Sepharose™ CL-4B (Amersham Biotech.), pre-stained protein markers (Promega), phenylmethylsulfonyl fluoride (PMSF) (Sigma), Sequencing Grade Modified TPCK-

Trypsin (Promega), sodium azide (BDH Inc.), SDS (sodium dodecyl sulfate) (Bio-Rad), sodium fluoride (Sigma), sodium HEPES (Sigma), sodium dihydrogen phosphate (NaH_2PO_4) (BDH Inc.), sodium hydrogen phosphate (Na_2HPO_4) (BDH Inc.), sodium bicarbonate (BDH Inc.), sodium hydroxide (Sigma), sodium orthovanadate ($NaVO_4$) (Sigma), Soybean Trypsin Inhibitor (STI) (US Biochemical Coporation), Superose 12, prep grade (Pharmacia Biotech), TEMED (N,N,N',N'-tetramethylethylenediamine) (Bio-Rad), triethanolamine (Fisher), trifluoroacetic acid (TFA) (EM Science), Tris-(hydroxymethyl)-aminomethane (Tris) (EMD Chemicals Inc.), Triton X-100 (Bio-Rad), Tween (Bio-Rad), X-ray film (Kodak), xylene cyanol (Roche Applied Science).

2.3.2 Enzymes

Calf intestinal phosphatase (CIP) (New England Biolabs), Taq polymerase (New England Biolabs), T4 ligase (Roche), restriction endonucleases (New England Biolabs), PreScission® protease (Pharmacia Biotech.), cPKC (purified from rat brain in our laboratory), RNAase out (New England Biolabs), RT-superscript III (New England Biolabs).

2.3.3 Kits

SuperSignal® West Femto Maximum Sensitivity Substrate (Pierce), SuperSignal® West Pico Chemiluminescent Substrate (Pierce), QIAEX II gel extraction kit (Qiagen), QIAGEN plasmid kit (Mini) (Qiagen), BCA Protein Assay Reagent Kit (Pierce).

2.3.4 Plasmid DNA

pGEX-2TK (Pharmacia Biotech.), pGEX-6P-1 (from Dr. Justin MacDonald, University of Calgary).

2.3.5 Bacterial strains

BL21 (Stratagene), optimized for DNA transformation and protein translation.

2.3.6 Solutions and buffers

2.3.6.1 Bacterial medium and DNA isolation buffers

LB (Luria-Bertani) medium: 10 g/L Bacto tryptone, 10 g/L NaCl, 5 g/L yeast extract, pH adjusted to 7.5 with NaOH. For plates, 5 g Bacto-agar was added.

2 × YT medium: 10 g/L yeast extract, 16 g/L Bacto tryptone, 5 g/L NaCl, pH adjusted to 7.5 with NaOH.

SOC medium: 20 g/L Bacto tryptone, 5 g/L Bacto yeast extract, 10 mL of 1 N NaCl, 2.5 mL of 1 M KCl, 5 mL 1 M $MgCl_2$, 5 mL 1 M $MgSO_4$, 10 mL of 2 M glucose, 800 mL of distilled de-ionized water, pH adjusted to 7.0, volume made up to 1 L and filter sterilized.

Buffer P1 (resuspension buffer): 50 mM Tris-HCl, 10 mM EDTA, 10 mg/mL RNAase A, pH 8.0.

Buffer P2 (Lysis buffer): 10% SDS, 200 mM NaOH.

Buffer P3 (Neutralization buffer): 3 M potassium acetate, pH 5.5.

2.3.6.2 DNA buffers

10 × DNA Gel Loading Buffer: 40% (w/v) saccharose, 0.25% bromphenol blue,

0.25% xylene cyanol, used as a 1 × solution.

1 × Tris-Acetate-EDTA (TAE): 40 mM Tris-HCl, 40 mM acetic acid, 2 mM EDTA, pH 7.8.

2.3.6.3 Protein methods buffers

1 M Potassium phosphate buffer, pH 7: 1 M potassium dihydrogen phosphate (KH_2PO_4) was added to 1 M potassium hydrogen phosphate (K_2HPO_4) until a pH of 7 was achieved.

PBS, pH 7.4: 136 mM NaCl, 2.7 mM KCl, 10 mM Na_2HPO_4, 1.5 mM NaH_2PO_4.

Running Buffer (for SDS-PAGE): 25 mM Tris, 250 mM glycine, 0.1 % (w/v) SDS, pH 8.8.

5 × SDS-loading Buffer (for SDS-PAGE): 1 mM Tris HCl, pH 6.8, 1% (w/v) SDS, 5 % (w/v) glycerol, 2.5 % (v/v) β-mercaptoethanol, 0.05 % (w/v), bromphenol blue, 1 × solution.

Sodium dodecyl sulfate-polyacrylamide gel electrophoresis (SDS-PAGE):

All the gels were prepared by mixing the 7.5% and 20% sodium dodecyl sulfate polyacrylamide gel stocks.

7.5% separating gel solution (32 mL): 8 mL lower gel stock (pH 8.8), 8 mL acrylamide (30%)/bisacrylamide (0.8%), 15.8 mL ddH_2O, 0.2 mL glycerol, 160 µL 10% APS, 16 µL TEMED.

20% separating gel solution (32 mL): 8 mL lower gel stock (pH 8.8), 21.3 mL acrylamide (30%)/bisacrylamide (0.8%), 2.3 mL ddH_2O, 0.4 mL glycerol, 160 µL 10% APS, 16 µL TEMED.

5% stacking gel solution (20 mL): 5 mL upper gel stock (pH 6.8), 3 mL acrylamide (30%)/bisacrylamide (0.8%), 12 mL ddH_2O, 120 µL 10% APS, 16 µL TEMED.

Lower gel stock solution, pH 8.8: 1.5 M Tris-HCl, pH 8.8, 0.4% SDS.

Upper gel stock solution, pH 6.8: 0.5 M Tris-HCl, pH 6.8, 0.4% SDS.

CHAPTER 3:

RESULTS

3.1 Identification of a novel S100A11-binding protein

An extract of chicken gizzard smooth muscle, prepared in the absence of Ca^{2+}, was applied to an S100A11 affinity column in the presence of Ca^{2+}. Unbound proteins were washed through the column and non-specifically-bound proteins were eluted with NaCl. Proteins bound in a Ca^{2+}-dependent manner were then eluted by chelation of Ca^{2+} with EGTA (Fig. 8). Three proteins (of 70, 44 and 37 kDa) were detected in the EGTA eluate by Coomassie Blue staining following SDS-PAGE of column fractions.

Control experiments demonstrated that the 70 kDa protein did not bind to a blank Sepharose column (without S100A11) or if loaded on an S100A11 affinity column in the presence of EGTA. On the other hand, the 44 and 37 kDa proteins bound to both control columns (Fig. 9).

The 70 kDa protein, therefore, interacts specifically with S100A11 in a Ca^{2+}-dependent manner. This protein was cut out of the gel, digested with trypsin and subjected to matrix-assisted laser desorption ionization/time-of-flight (MALDI-TOF) mass spectrometry (Fig. 10). The S100A11-binding protein was thus identified as annexin A6.

3.2 Purification of GST fusion proteins

S100A11 (WT and site-directed mutants), annexin A6 (full-length and deletion mutants) and their GST-fusion counterparts, subcloned into pGEX-6P-1, were expressed in *E. coli* and purified to electrophoretic homogeneity. Both GST-fusion proteins and the proteins after removal of the GST moiety were purified (Fig. 11).

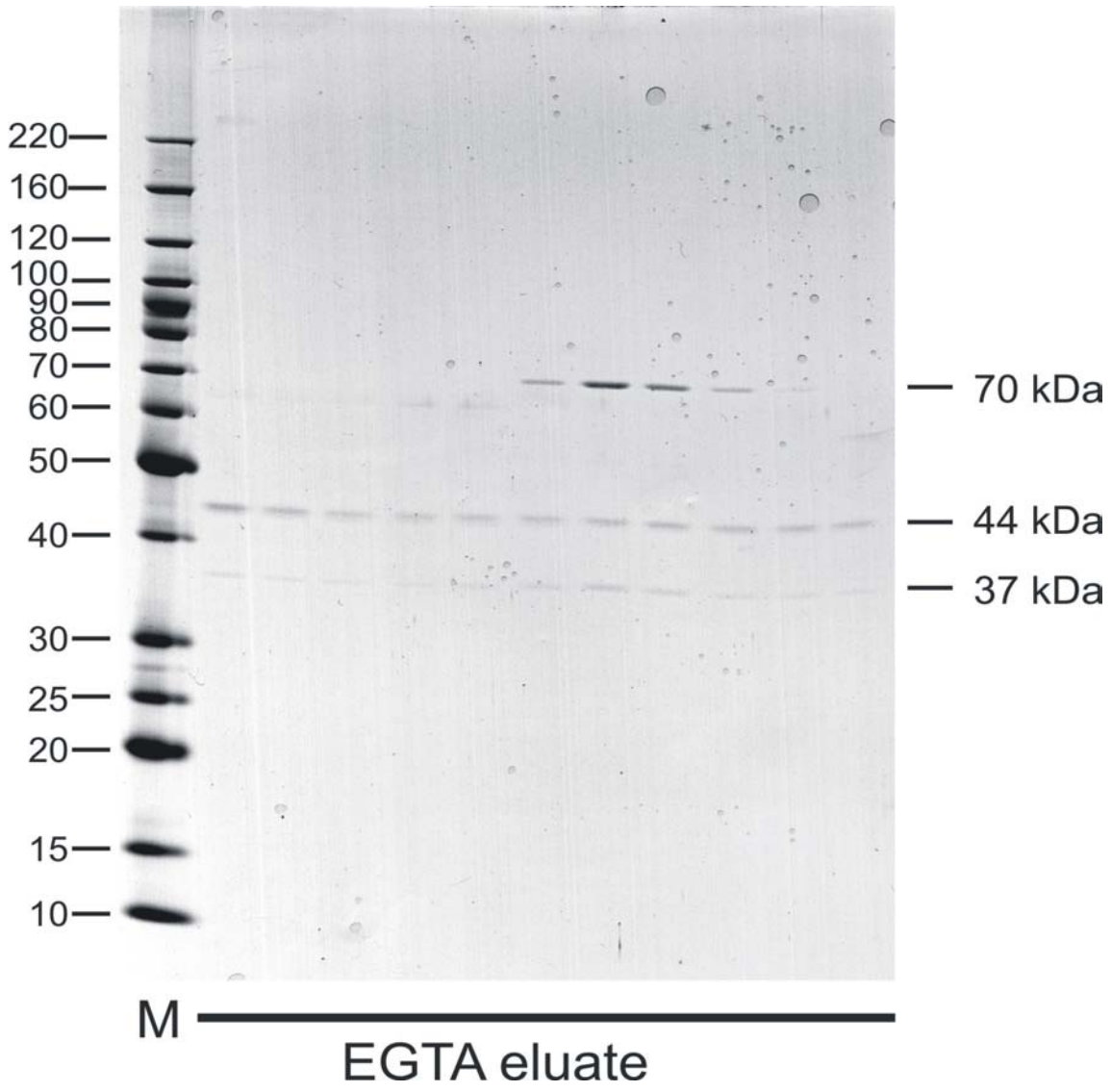

Fig. 8: SDS-PAGE of fractions eluted from an S100A11 affinity column with EGTA. S100A11-Sepharose was produced as described in section 2.2.2.1. Affinity chromatography of a chicken gizzard extract was carried out as described in section 2.2.2.2. (Carried out by Cindy Sutherland and Ning Chang, n = 4). M = molecular weight markers.

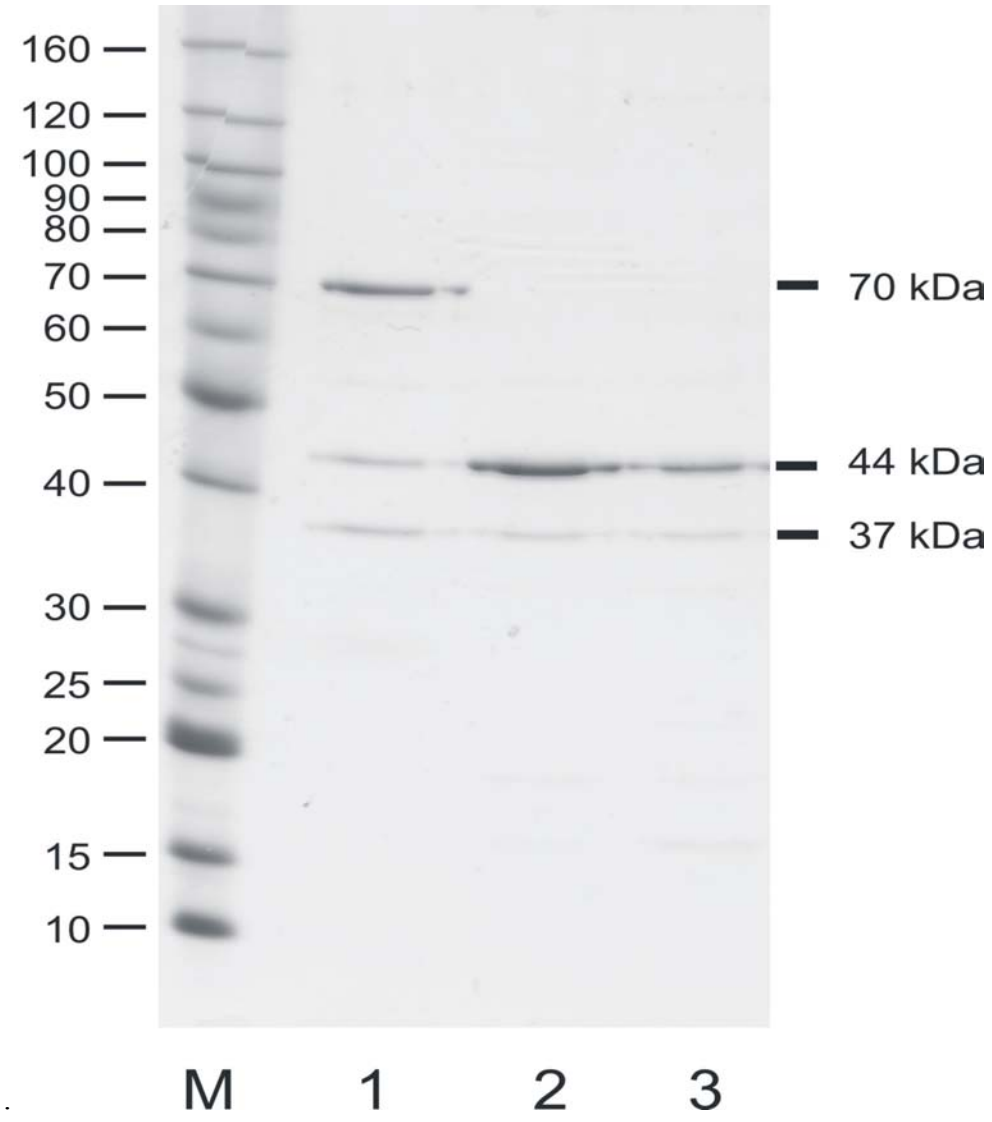

Fig. 9: Specific and Ca^{2+}-dependent interaction of the 70 kDa protein with S100A11. M = molecular weight markers; 1 = proteins bound to S100A11-Sepharose in the presence of Ca^{2+} and eluted with EGTA; 2 = proteins bound to control Sepharose in the presence of Ca^{2+} and eluted with EGTA; 3 = proteins bound to S100A11-Sepharose in the presence of EGTA and eluted with EGTA. (Carried out by Cindy Sutherland, n = 3).

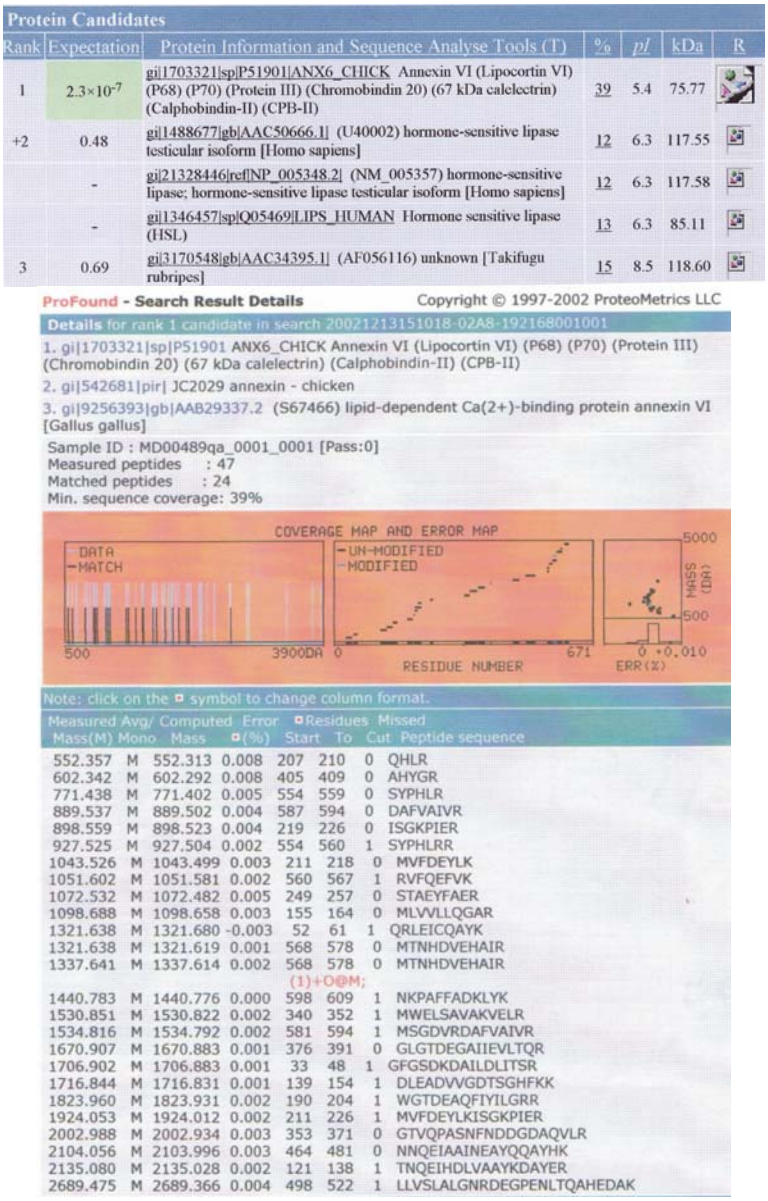

Protein Candidates

Rank	Expectation	Protein Information and Sequence Analyse Tools (T)	%	pI	kDa	R
1	2.3×10^{-7}	gi|1703321|sp|P51901|ANX6_CHICK Annexin VI (Lipocortin VI) (P68) (P70) (Protein III) (Chromobindin 20) (67 kDa calelectrin) (Calphobindin-II) (CPB-II)	39	5.4	75.77	
+2	0.48	gi|1488677|gb|AAC50666.1| (U40002) hormone-sensitive lipase testicular isoform [Homo sapiens]	12	6.3	117.55	
	-	gi|21328446|ref|NP_005348.2| (NM_005357) hormone-sensitive lipase; hormone-sensitive lipase testicular isoform [Homo sapiens]	12	6.3	117.58	
	-	gi|1346457|sp|Q05469|LIPS_HUMAN Hormone sensitive lipase (HSL)	13	6.3	85.11	
3	0.69	gi|3170548|gb|AAC34395.1| (AF056116) unknown [Takifugu rubripes]	15	8.5	118.60	

ProFound - Search Result Details Copyright © 1997-2002 ProteoMetrics LLC

Details for rank 1 candidate in search 20021213151018-02A8-192168001001

1. gi|1703321|sp|P51901 ANX6_CHICK Annexin VI (Lipocortin VI) (P68) (P70) (Protein III) (Chromobindin 20) (67 kDa calelectrin) (Calphobindin-II) (CPB-II)
2. gi|542681|pir| JC2029 annexin - chicken
3. gi|9256393|gb|AAB29337.2 (S67466) lipid-dependent Ca(2+)-binding protein annexin VI [Gallus gallus]

Sample ID : MD00489qa_0001_0001 [Pass:0]
Measured peptides : 47
Matched peptides : 24
Min. sequence coverage: 39%

COVERAGE MAP AND ERROR MAP
DATA
MATCH
UN-MODIFIED
MODIFIED
MASS (DA)
5000
500
500
3900DA
0
671
RESIDUE NUMBER
0 +0.010
ERR(%)

Note: click on the ▫ symbol to change column format.

Measured Mass(M)	Avg/ Mono	Computed Mass	Error ▫(%)	Residues Start	To	Missed Cut	Peptide sequence
552.357	M	552.313	0.008	207	210	0	QHLR
602.342	M	602.292	0.008	405	409	0	AHYGR
771.438	M	771.402	0.005	554	559	0	SYPHLR
889.537	M	889.502	0.004	587	594	0	DAFVAIVR
898.559	M	898.523	0.004	219	226	0	ISGKPIER
927.525	M	927.504	0.002	554	560	1	SYPHLRR
1043.526	M	1043.499	0.003	211	218	0	MVFDEYLK
1051.602	M	1051.581	0.002	560	567	1	RVFQEFVK
1072.532	M	1072.482	0.005	249	257	0	STAEYFAER
1098.688	M	1098.658	0.003	155	164	0	MLVVLLQGAR
1321.638	M	1321.680	-0.003	52	61	1	QRLEICQAYK
1321.638	M	1321.619	0.001	568	578	0	MTNHDVEHAIR
1337.641	M	1337.614	0.002	568	578	0	MTNHDVEHAIR
				(1)+O@M;			
1440.783	M	1440.776	0.000	598	609	1	NKPAFFADKLYK
1530.851	M	1530.822	0.002	340	352	1	MWELSAVAKVELR
1534.816	M	1534.792	0.002	581	594	1	MSGDVRDAFVAIVR
1670.907	M	1670.883	0.001	376	391	0	GLGTDEGAIIEVLTQR
1706.902	M	1706.883	0.001	33	48	1	GFGSDKDAILDLITSR
1716.844	M	1716.831	0.001	139	154	1	DLEADVVGDTSGHFKK
1823.960	M	1823.931	0.002	190	204	1	WGTDEAQFIYILGRR
1924.053	M	1924.012	0.002	211	226	1	MVFDEYLKISGKPIER
2002.988	M	2002.934	0.003	353	371	0	GTVQPASNFNDDGDAQVLR
2104.056	M	2103.996	0.003	464	481	0	NNQEIAAINEAYQQAYHK
2135.080	M	2135.028	0.002	121	138	1	TNQEIHDLVAAYKDAYER
2689.475	M	2689.366	0.004	498	522	1	LLVSLALGNRDEGPENLTQAHEDAK

Fig. 10: Mass spectrometric identification of the 70 kDa protein that interacts with S100A11 in a Ca^{2+}-dependent manner. The 70 kDa protein was subjected to tryptic digestion and MALDI-TOF MS analysis as described in section 2.2.10. The profile of tryptic peptide masses was compared with the predicted tryptic peptide mass profiles in the protein sequence data banks and the protein identified as annexin A6 with an expectation value of 2.3 x 10^{-7} and 24 matched peptides covering 39% of the sequence. (Carried out by Cindy Sutherland and the Southern Alberta Mass Spectrometry Centre).

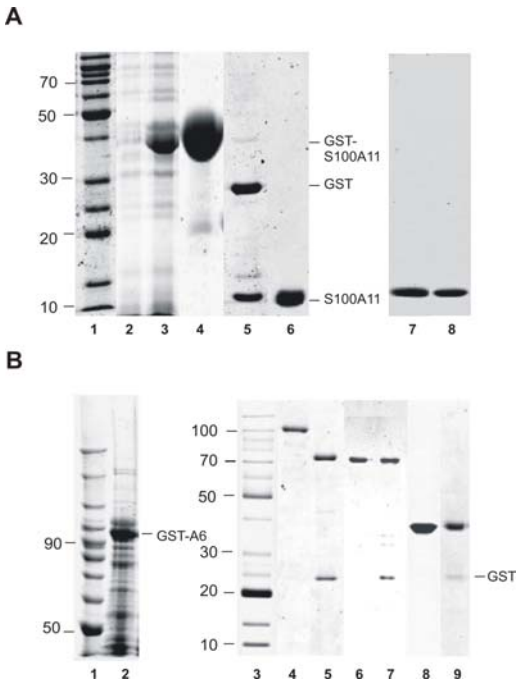

Fig. 11: Purification to electrophoretic homogeneity of S100A11, annexin A6 and their GST-fusion counterparts. ***A.*** Purification of recombinant S100A11 and site-directed mutants. Recombinant chicken S100A11 was expressed in *E. coli* as a GST-fusion protein, purified, cleaved and S100A11 purified as described in section 2.2.1.2.1. 1 = marker proteins; 2 = control *E. coli* lysate; 3 = *E. coli* lysate expressing GST-S100A11; 4 = purified GST-S100A11; 5 = GST-S100A11 cleaved with PreScission™ protease; 6 = purified S100A11; 7 = purified S100A11 mutant (T9A); 8 = purified S100A11 mutant (T9D). ***B.*** Purification of annexin A6 and deletion mutants. Recombinant wild-type chicken annexin A6 and various deletion mutants were expressed in *E. coli* as GST-fusion proteins, purified, cleaved, and further purified as described in section 2.2.1.2.2. 1 = marker proteins; 2 = lysate of *E. coli* expressing GST-annexin A6; 3 = marker proteins; 4 = purified GST-annexin A6; 5 = GST-annexin A6 cleaved with PreScission™ protease; 6 = purified annexin A6; 7 = Δ(1-20)annexin A6; 8 = *C*-terminal half of annexin A6 (M340-D672); 9 = *N*-terminal half of annexin A6 (G5-R339).

3.3 Smooth muscle cells express both S100A11 and annexin A6

RT-PCR was performed on mRNA from isolated vascular smooth muscle cells of the rat basilar artery using primers specific for S100A11 and annexin A6. Messages of the predicted sizes were detected, which were confirmed by sequencing, indicating the expression of both S100A11 and annexin A6 at the message level in vascular smooth muscle cells (Fig. 12). Purity of the isolated cells was confirmed by the absence of message encoding endothelin-1 (an endothelial cell marker) or ERG-3 (a neuronal marker) (data not shown).

3.4 Confirmation of the Ca^{2+}-dependent interaction between S100A11 and annexin A6

3.4.1 Ca^{2+}-dependent binding of purified recombinant annexin A6 to immobilized S100A11

Bacterially-expressed purified annexin A6 interacted with S100A11 in a Ca^{2+}- dependent manner (Fig. 13).

3.4.2 Ca^{2+}-dependent binding of purified recombinant S100A11 to immobilized annexin A6

The Ca^{2+}-dependent interaction between S100A11 and annexin A6 was confirmed in a reciprocal experiment. S100A11 bound to an annexin A6-Sepharose affinity column in a Ca^{2+}-dependent manner (Fig. 14A). S100A11 did not bind to a control column lacking annexin A6 (Fig. 14B).

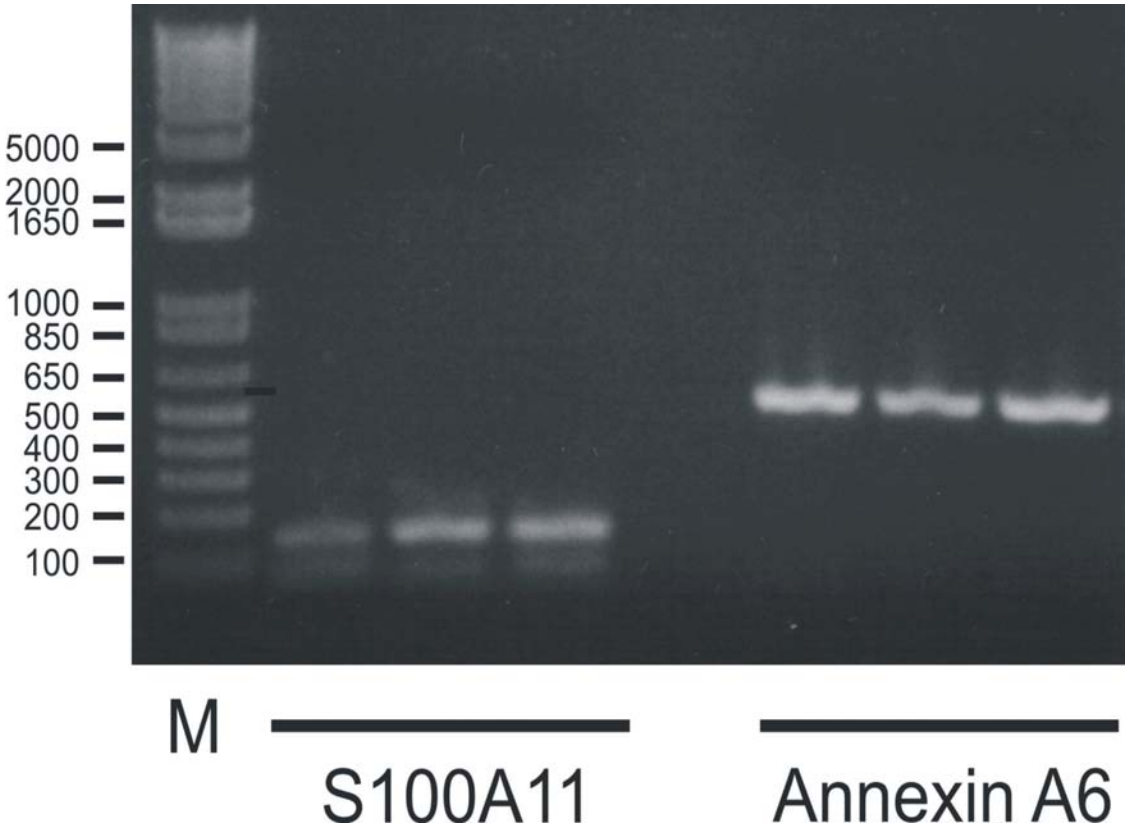

Fig. 12: S100A11 and annexin A6 are expressed at the mRNA level in rat basilar arterial smooth muscle cells. M = DNA ladder. Three separate mRNA preparations from isolated rat basilar arterial smooth muscle cells were analysed by RT-PCR for S100A11 and annexin A6 messages. (Carried out by William Wiehler).

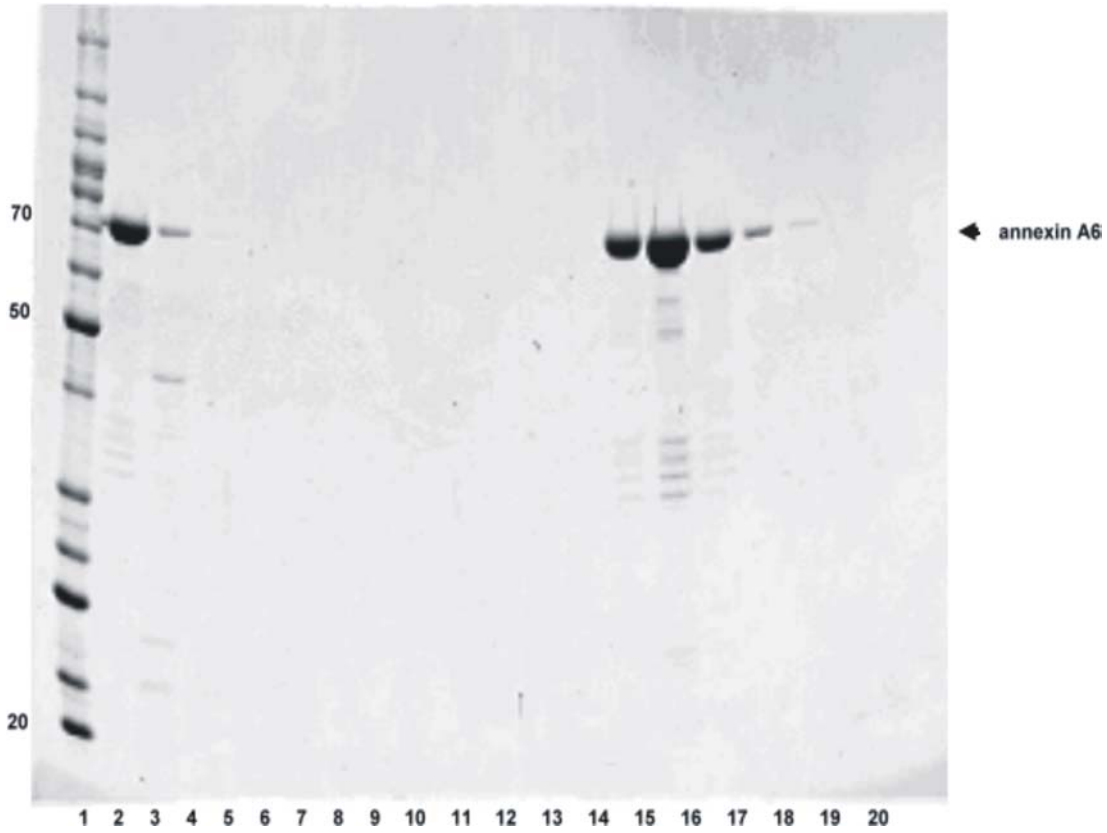

Fig. 13: Ca^{2+}-dependent interaction of purified annexin A6 with immobilized S100A11. Purified recombinant annexin A6 was applied to an S100A11-Sepharose affinity column in the presence of Ca^{2+} and bound protein was eluted with EGTA. 1 = marker proteins; 2 = purified annexin A6; 3 = flow through; 4 – 10 = fractions eluted in the presence of Ca^{2+}; 11 – 20 = fractions eluted in the presence of EGTA. Identical results were obtained in 3 independent experiments.

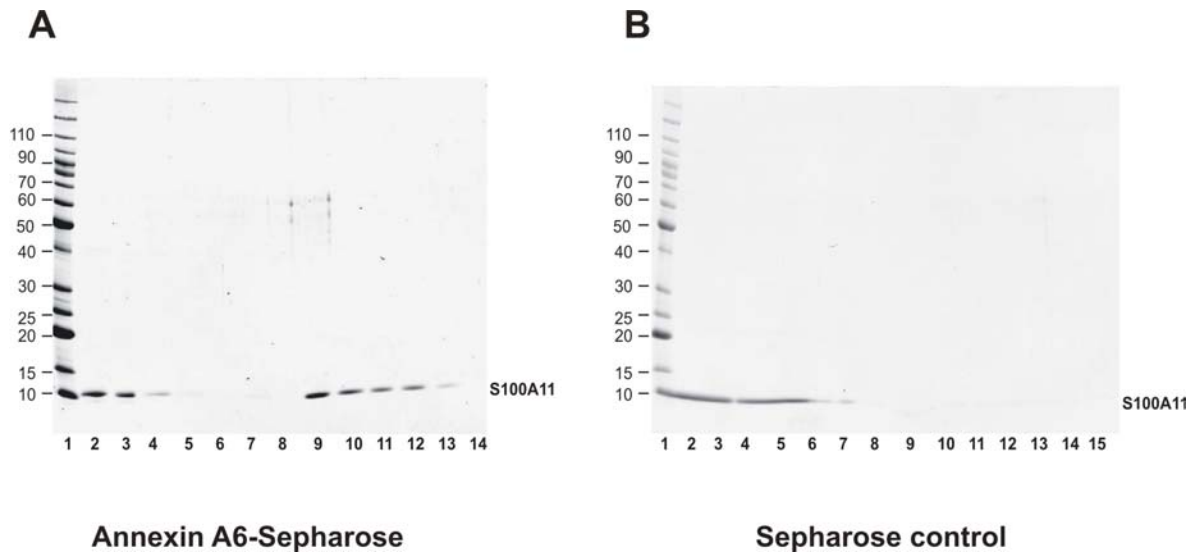

Fig. 14: Ca^{2+}-dependent interaction of purified S100A11 with immobilized annexin A6. ***A.*** Purified recombinant S100A11 was applied to an annexin A6-Sepharose affinity column in the presence of Ca^{2+} and bound protein was eluted with EGTA as described in section 2.2.3. 1 = marker proteins; 2 = purified S100A11 (load); 3 = flow through; 4 – 8 = fractions eluted in the presence of Ca^{2+}; 9 – 14 = fractions eluted in the presence of EGTA. Identical results were obtained in 3 independent experiments. ***B.*** The same procedure was carried out with a control column without annexin A6.

3.4.3 Liposome co-pelleting assay

Liposomes are known to bind annexin A6 in a Ca^{2+}-dependent manner. We reasoned, therefore, that it should be possible to confirm Ca^{2+}-dependent binding of S100A11 to annexin A6 in the presence of liposomes using a co-pelleting assay. It was first necessary, however, to investigate whether or not S100A11 itself binds to liposomes.

3.4.3.1 S100A11 interacts with liposome-bound annexin A6 in a Ca^{2+}-dependent manner

Therefore, liposomes were isolated from rat tail artery, incubated with purified S100A11 and/or annexin A6 in the absence or presence of Ca^{2+} and centrifuged at high speed to pellet liposomes and bound proteins. Pellets and supernatants were analyzed by SDS-PAGE with Coomassie Blue staining (Fig. 15). As expected, annexin A6 bound to liposomes only in the presence of Ca^{2+} (compare lanes 8 and 9 of Fig. 15, which shows that all the annexin A6 is recovered in the supernatant in the presence of EGTA but in the pellet in the presence of Ca^{2+}). In the case of S100A11, however, the results were unexpected (compare lanes 11 and 12 in Fig 15). Some of the S100A11 bound to liposomes in the presence but not absence of Ca^{2+}. Nevertheless, there appeared to be more S100A11 in the pellet fraction in the presence of Ca^{2+} when annexin A6 was also present (compare lanes 12 and 15 in Fig. 15), consistent with Ca^{2+}-dependent interaction between S100A11 and annexin A6. This was confirmed in several experiments in which bound and free S100A11 and annexin A6 were quantified by scanning densitometry. After subtracting the amount of S100A11 that bound to liposomes in the absence of annexin A6, 0.38 ± 0.07 μg S100A11 bound to 2.5 μg of liposome-bound annexin A6 (n

= 4). This corresponds to a stoichiometry of 1 S100A11 monomer : 1 annexin A6 or 1 S100A11 dimer : 2 annexin A6 monomers.

3.4.3.2 Ca^{2+}-dependent binding of S100A11 to phosphatidylserine liposomes

The co-pelleting assay was repeated with liposomes prepared from pure phosphatidylserine. Phosphatidylserine liposomes from porcine brain were incubated with different amounts of purified recombinant chicken S100A11 in the presence of Ca^{2+} or EGTA, centrifuged and the liposomal pellets were resuspended in EGTA or Ca^{2+} buffer. Both the supernatants and pellets were subjected to SDS-PAGE with Coomassie Blue staining (Fig. 16). These results confirm the Ca^{2+}-dependent interaction of S100A11 with phosphatidylserine liposomes.

3.4.4 Characterization of polyclonal rabbit anti-(chicken S100A11)

Polyclonal rabbit anti-(chicken S100A11) was generated by our laboratory (Allen *et al.*, 1996) and characterized by Western blotting in this study (Fig. 17). The antibody was capable of clearly detecting 40 ng of chicken S100A11, but did not recognize rat S100A11 (data not shown). The non-crossreactivity of this antibody between chicken and rat S100A11 indicates that the slight differences in the *N*- and/or *C*-terminal sequences might be responsible for the epitope(s) generation (Fig. 3).

3.4.5 Characterization of monoclonal mouse anti-(rat S100A11)

The monoclonal antibody raised against full-length rat S100A11 clearly detected 0.1 μg of rat S100A11 (Fig. 18). This antibody clearly detected S100A11 in an extract of rat tail

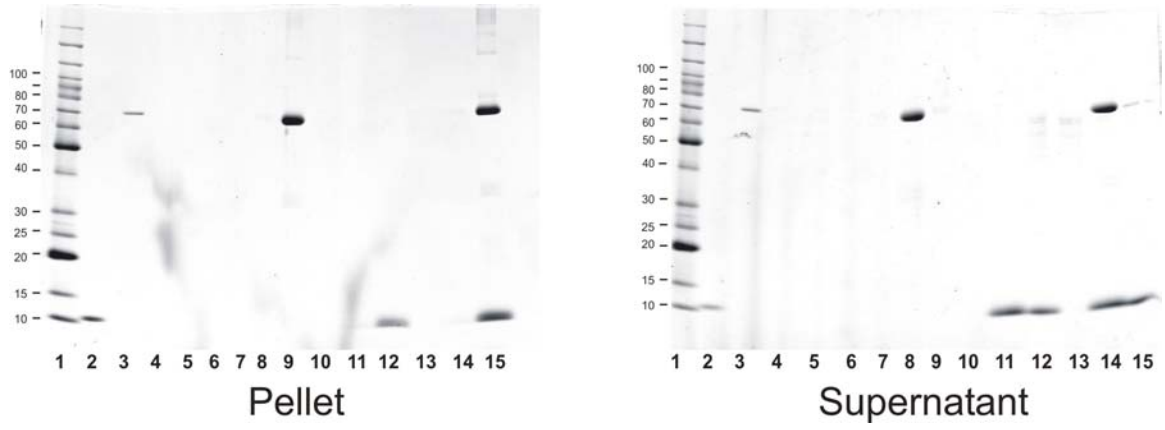

Fig. 15: Ca^{2+}-dependent interaction of S100A11 with liposomes and liposome-bound annexin A6. Rat tail arterial liposomes were isolated and the binding of S100A11 and annexin A6 analyzed as described in section 2.2.9.2. The resultant Coomassie Blue-stained gels are shown. 1 = marker proteins; 2 = S100A11; 3 = annexin A6; 4 = blank; 5 = liposomes in the presence of EGTA; 6 = liposomes in the presence of Ca^{2+}; 7 = blank; 8 = liposomes with annexin A6 in the presence of EGTA; 9 = liposomes with annexin A6 in the presence of Ca^{2+}; 10 = blank; 11 = liposomes with S100A11 in the presence of EGTA; 12 = liposomes with S100A11 in the presence of Ca^{2+}; 13 = blank; 14 = liposomes with annexin A6 and S100A11 in the presence of EGTA; 15 = liposomes with annexin A6 and S100A11 in the presence of Ca^{2+}.

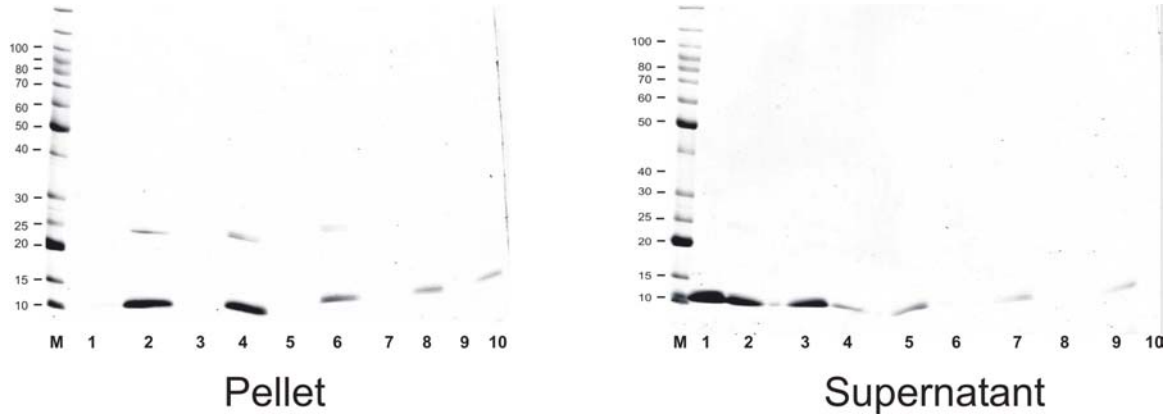

Fig. 16: S100A11 binds to phosphatidylserine liposomes in a Ca^{2+}-dependent manner. Phosphatidylserine liposomes were prepared and the binding of S100A11 examined as described in section 2.2.9.1. The resultant Coomassie Blue-stained gels are shown. M = marker proteins; 1, 3, 5, 7, 9 = liposomes incubated with 10, 5, 2.5, 1, 0.5 µg of S100A11, respectively, in the presence of EGTA; 2, 4, 6, 8, 10 = liposomes incubated with 10, 5, 2.5, 1, 0.5 µg of S100A11, respectively, in the presence of Ca^{2+}. Identical results were obtained in 3 independent experiments.

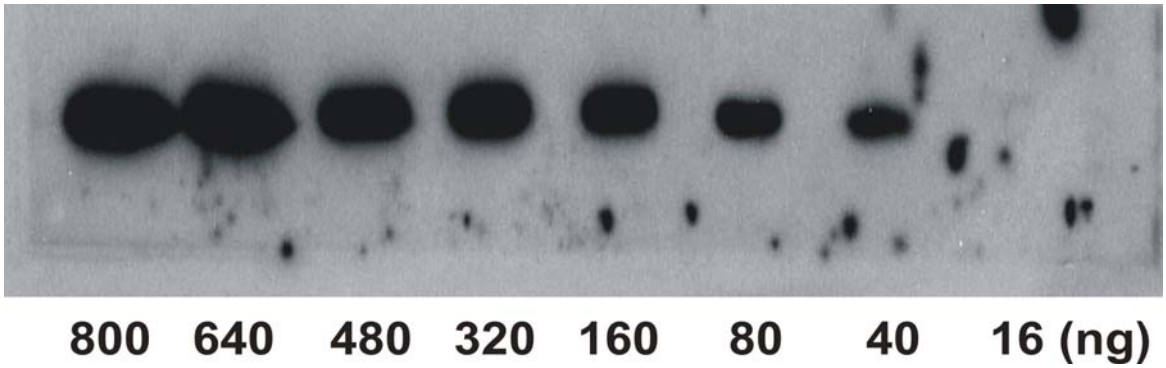

Fig. 17: Characterization of polyclonal rabbit anti-(chicken S100A11). The indicated amounts of purified chicken S100A11 were subjected to SDS-PAGE and Western blotting with polyclonal rabbit anti-(chicken S100A11) as described in section 2.2.5.3 (n = 6).

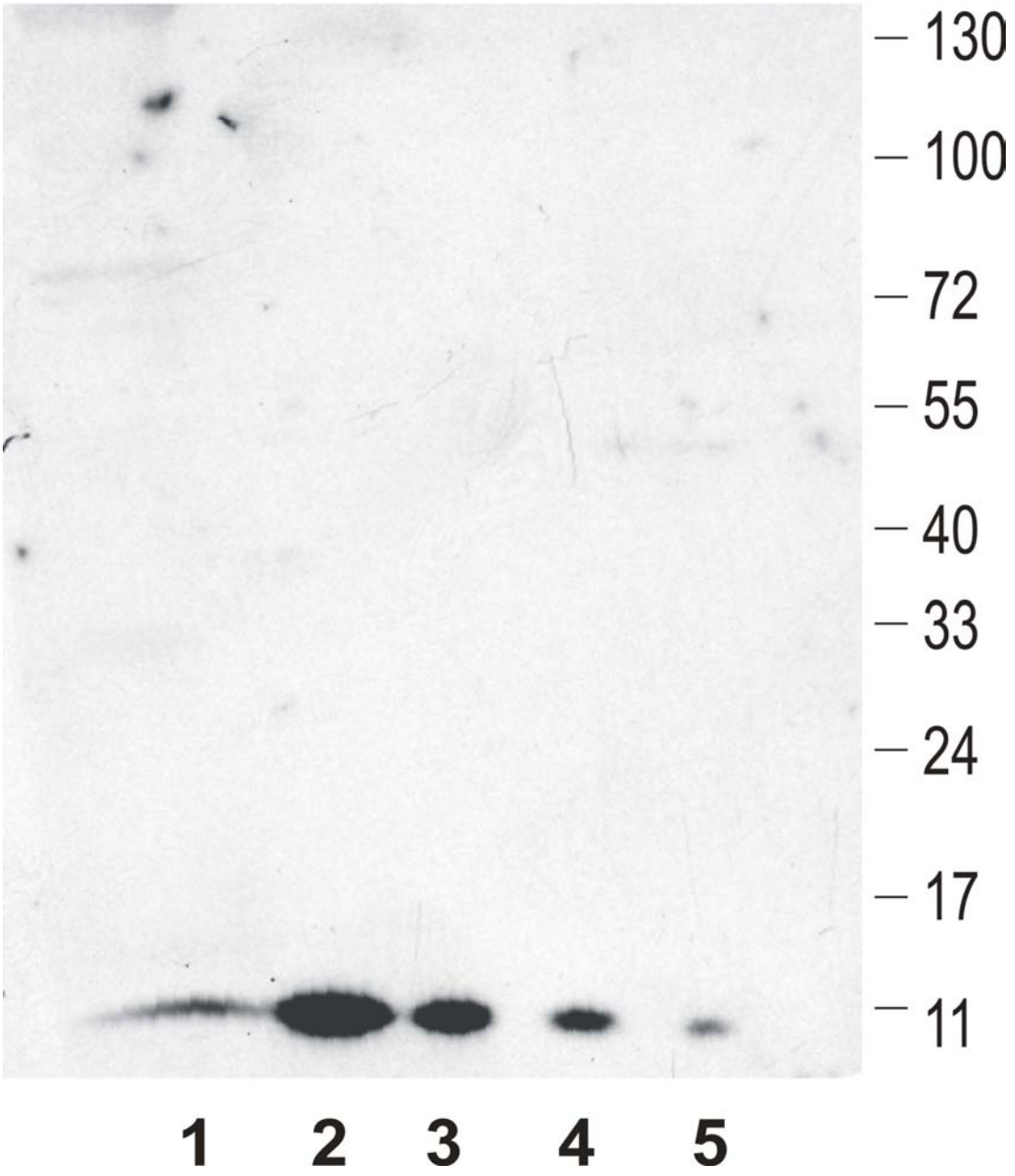

Fig. 18: Characterization of monoclonal anti-(rat S100A11). 1 = 2 strips of rat tail artery; 2 – 5 = 1.5, 0.5, 0.25 and 0.1 µg, respectively, of purified rat S100A11 were subjected to SDS-PAGE and Western blotting with monoclonal anti-(rat S100A11) as described in section 2.2.5.2 (n = 3).

arterial smooth muscle (Fig. 18, lane 1).

3.4.6 Characterization of rabbit anti-(rat annexin A6)

A polyclonal antibody to rat annexin A6 was generated against the *N*-terminal peptide of 12 amino acids (AKIAQGAMYRGS). The IgG fractions of rat annexin A6 antisera were purified by protein A-Sepharose column chromatography. The polyclonal antibody to rat annexin A6 could clearly detect the protein in 1/10 of a strip of rat tail artery (Fig. 19A). Antibody specificity was confirmed by pre-absorption of the antibody with the peptide antigen (Fig. 19B).

3.4.7 Confirmation of the Ca^{2+}-dependent interaction between S100A11 and annexin A6 by chemical cross-linking

S100A11 and annexin A6 were treated, alone and together, with the cross-linking agent dimethylsuberimidate in the presence of EGTA or Ca^{2+} (Fig. 20).

Comparing the EGTA blot with the Ca^{2+} blot, 2 specific bands (indicated by * in Fig. 20B) were seen only in the presence of both S100A11 and annexin A6 in Ca^{2+}: one of ~81 kDa corresponding to a 1:1 complex of S100A11 and annexin A6, and one of ~93 kDa corresponding to a 1:2 complex of annexin A6 and S100A11. The other bands, based on the control, are the homo-dimer, trimer and tetramer, respectively, of S100A11.

3.5 Identification of the binding site of annexin A6 for S100A11

3.5.1 Ca^{2+}-dependent binding of recombinant Δ(1-20)annexin A6 to immobilized S100A11

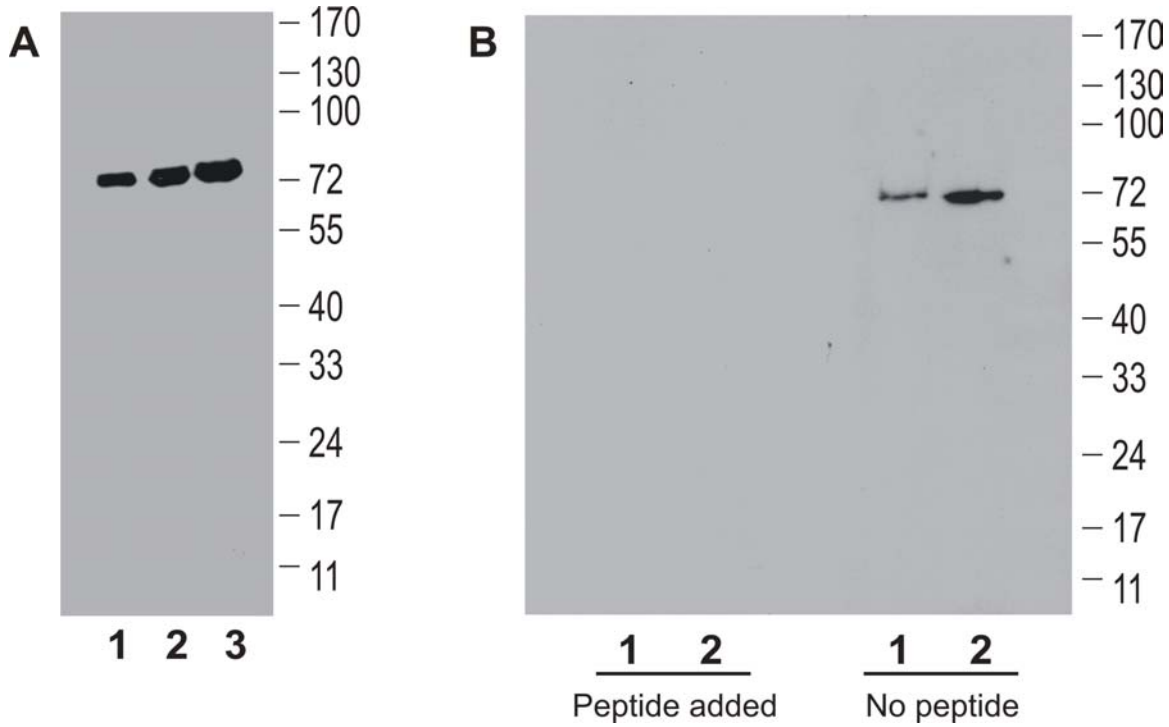

Fig. 19: Characterization of polyclonal rabbit anti-(rat annexin A6). ***A.*** 1 – 3 = 1/10, 1/4 and 1/2 strip of rat tail artery (RTA), respectively. ***B.*** Peptide blockage experiment: 1 and 2 = 1/10 and 1/4 strip of RTA, respectively with or without pre-absorption of the antibody with the antigenic peptide, as indicated. Tissue proteins were separated by SDS-PAGE prior to Western blotting with polyclonal rabbit anti-(rat annexin A6) as described in section 2.2.5.1. Identical results were obtained in 3 independent experiments.

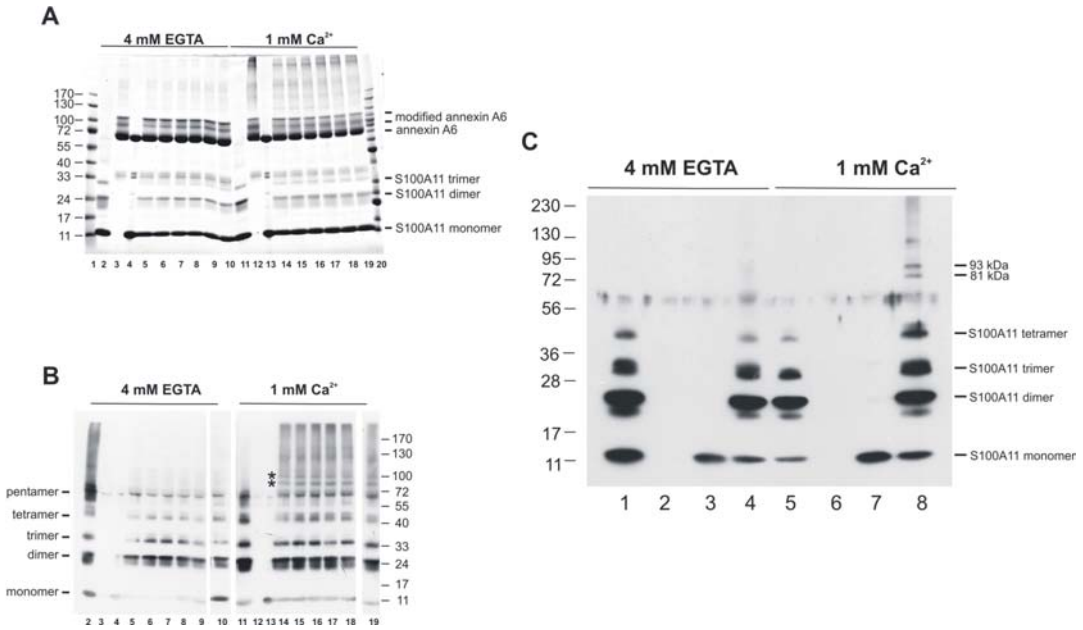

Fig. 20: Cross-linking of S100A11 and annexin A6. Cross-linking of recombinant chicken S100A11 and annexin A6 was carried out as described in section 2.2.8. ***A.*** Coomassie stained gel. ***B.*** Western blotting with anti-S100A11. 1 = protein marker ladder; 2 = S100A11 cross-linked in the presence of EGTA for 5 h; 3 = annexin A6 cross-linked in the presence of EGTA for 5 h; 4 – 10 = S100A11 and annexin A6 cross-linked in the presence of EGTA for 0, 0.5, 1, 2, 3, 4 and 5 h, respectively; 11 = S100A11 cross-linked in the presence of Ca^{2+} for 5 h; 12 = annexin A6 cross-linked in the presence of Ca^{2+} for 5 h; 13 – 19 = S100A11 and annexin A6 cross-linked in the presence of Ca^{2+} for 0, 0.5, 1, 2, 3, 4 and 5 h, respectively (***A, B***) (n = 3). ***C.*** Western blot with anti-S100A11 confirming the Ca^{2+}-dependent cross-linking of annexin A6 and S100A11. 1, 2 = S100A11 and annexin A6, respectively, cross-linked in the presence of EGTA for 5 h; 3, 4 = S100A11 and annexin A6 cross-linked in the presence of EGTA for 0 and 5 h, respectively; 5, 6 = S100A11 and annexin A6, respectively, cross-linked in the presence of Ca^{2+} for 5 h; 7, 8 = S100A11 and annexin A6 cross-linked in the presence of Ca^{2+} for 0 and 5 h, respectively.

Recombinant Δ(1-20)annexin A6, which lacks the *N*-terminal head region, was applied to an S100A11-Sepharose affinity column in the presence of Ca^{2+} and bound protein was eluted with EGTA (Fig. 21).

Δ(1-20)annexin A6 interacted with immobilized S100A11 in a Ca^{2+}-dependent manner, indicating that the *N*-terminal head region is not required for the interaction

3.5.2 Confirmation of the Ca^{2+}-dependent interaction of S100A11 and Δ(1-20)annexin A6 by gel overlay

Purified recombinant annexin A6 and Δ(1-20)annexin A6 were subjected to SDS-PAGE and transferred to nitrocellulose. The blot was incubated in purified S100A11 and, following washout of unbound S100A11, bound S100A11 was detected with anti-S100A11 (Fig. 22).

Therefore, gel overlay assay confirmed that both full-length annexin A6 and Δ(1-20)annexin A6 interact with S100A11 in a Ca^{2+}-dependent manner.

3.5.3 Ca^{2+}-dependent binding of tryptic fragments of annexin A6 to immobilized S100A11

Preliminary experiments were carried out to determine a suitable trypsin : annexin A6 ratio and incubation time to achieve site-specific digestion and thereby generate large fragments of annexin A6. The resultant digest is shown in Fig. 23 (lane 4). Two major fragments were detected of M_r ~68 kDa (slightly smaller than full-length annexin A6)

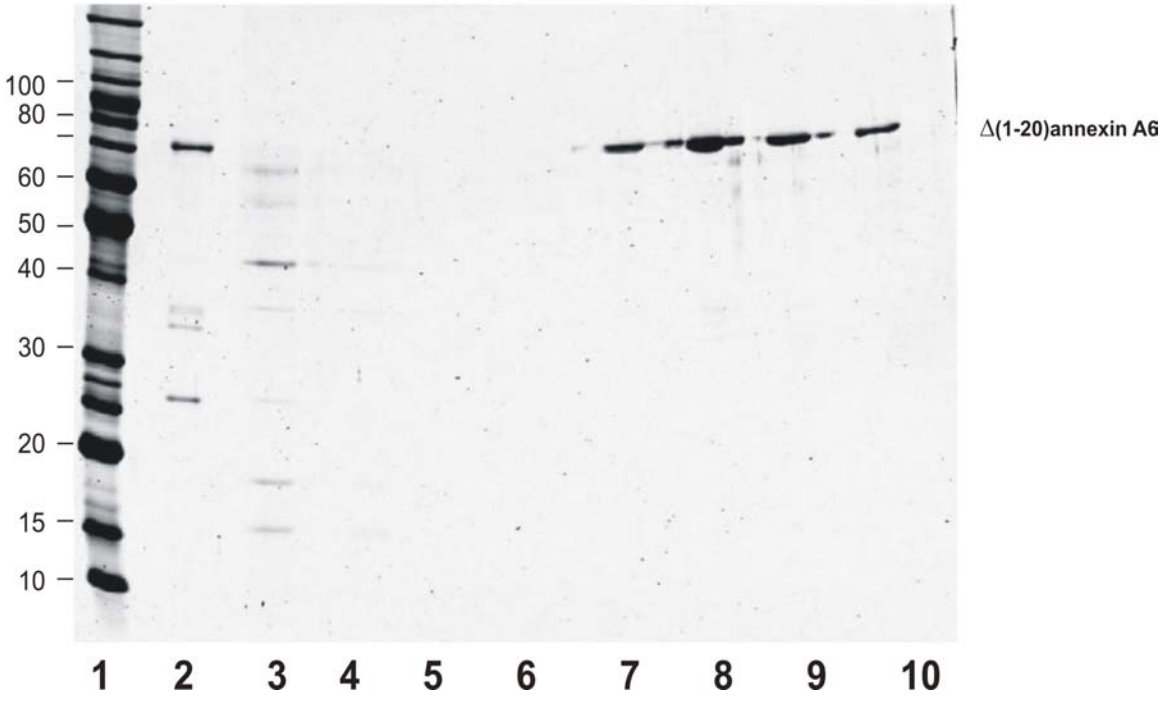

Fig. 21: Affinity chromatography of Δ(1-20)annexin A6 on S100A11-Sepharose. Δ(1-20)annexin A6 was expressed and purified as described in section 2.2.1.2.2. Its ability to bind to immobilized S100A11 in a Ca^{2+}-dependent manner was determined by affinity chromatography as described in section 2.2.2.3. The resultant Coomassie Blue-stained gel is shown. 1 = marker proteins; 2 = Δ(1-20)annexin A6; 3 = flow through; 4 – 6 = fractions eluted in the presence of Ca^{2+}; 7 – 10 = fractions eluted in the presence of EGTA. (n = 2).

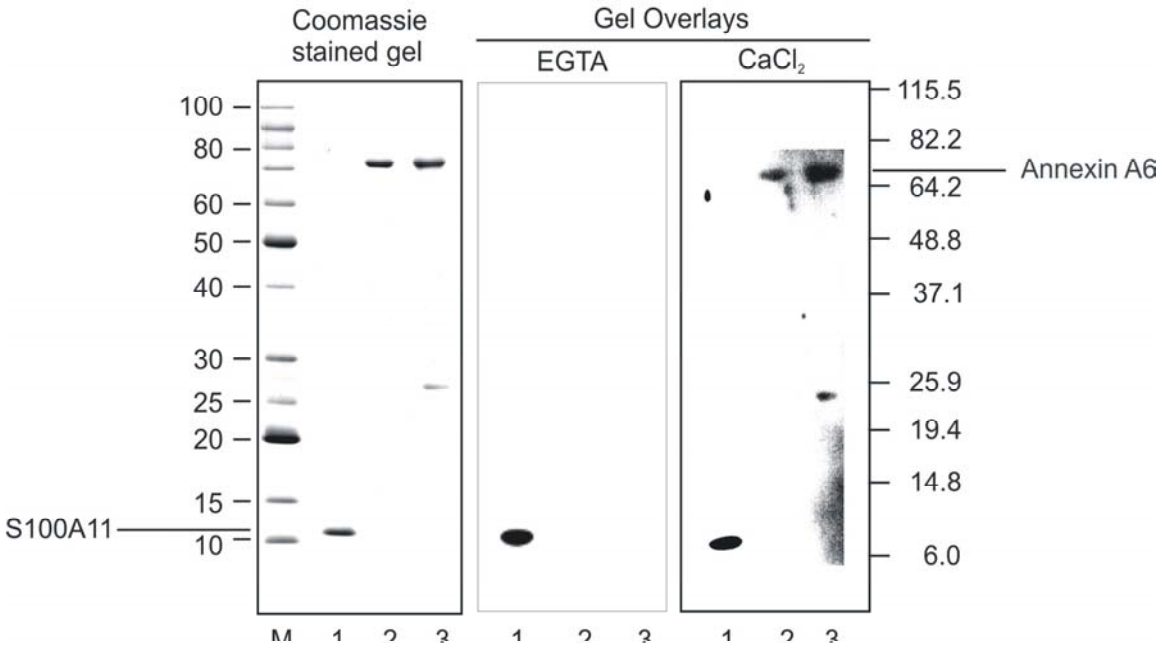

Fig. 22: Gel overlay assay for the binding of S100A11 to full-length annexin A6 and Δ(1-20)annexin A6. S100A11, annexin A6 and Δ(1-20)annexin A6 were subjected to SDS-PAGE, transblotted to nitrocellulose and incubated with S100A11 in the presence of EGTA or Ca^{2+} as described in section 2.2.6. Bound S100A11 was detected with anti-S100A11 (Gel Overlays). M = marker proteins; 1 = S100A11; 2 = annexin A6; 3 = Δ(1-20)annexin A6. (n = 3).

and ~ 34 kDa, indicating the presence of major tryptic cleavage sites near one end of the annexin A6 molecule and in the centre of the molecule. The partial digest of purified recombinant annexin A6 was then applied to an S100A11-Sepharose affinity column in the presence of Ca^{2+} and bound peptides were eluted with EGTA (Fig. 23).

These peptide fragments of annexin A6 of ~ 68 kDa and ~34 kDa (lanes 13 - 17) bound to immobilized S100A11 in a Ca^{2+}-dependent manner.

3.5.4 MS analysis of tryptic peptides of annexin A6 bound to S100A11-Sepharose

Fraction 16 (Fig. 23) from the S100A11-Sepharose affinity column and intact recombinant annexin A6 (lane 3, Fig. 23) were analyzed by MALDI-TOF MS (Fig. 24).

Four tryptic fragments (as well as soybean trypsin inhibitor used to stop the trypsin digestion) were identified by MS and the molecular weight of each fragment was measured (Table 1).

Based on the available cleavage sites in full-length annexin A6 (trypsin cleaves after Lys or Arg when the next residue is not Pro) and comparison of the molecular weights measured by MS with those of tryptic fragments predicted from the annexin A6 sequence (Fig. 26), the identities of the peptides were deduced. These results indicate that: (i) cleavage at K4 – G5 generates the ~ 68 kDa tryptic fragment, and (ii) subsequent cleavage at R339 – M340 and K348 – V349 generates 3 tryptic fragments corresponding to G5 – R339, M340 – D672 and V349 – D672, all of which bind to S100A11 in a Ca^{2+}-dependent manner.

The three ~34 kDa tryptic fragments (Fig. 24B) were cut out of the gel, completely digested with trypsin and subjected to MS analysis (Fig. 25).

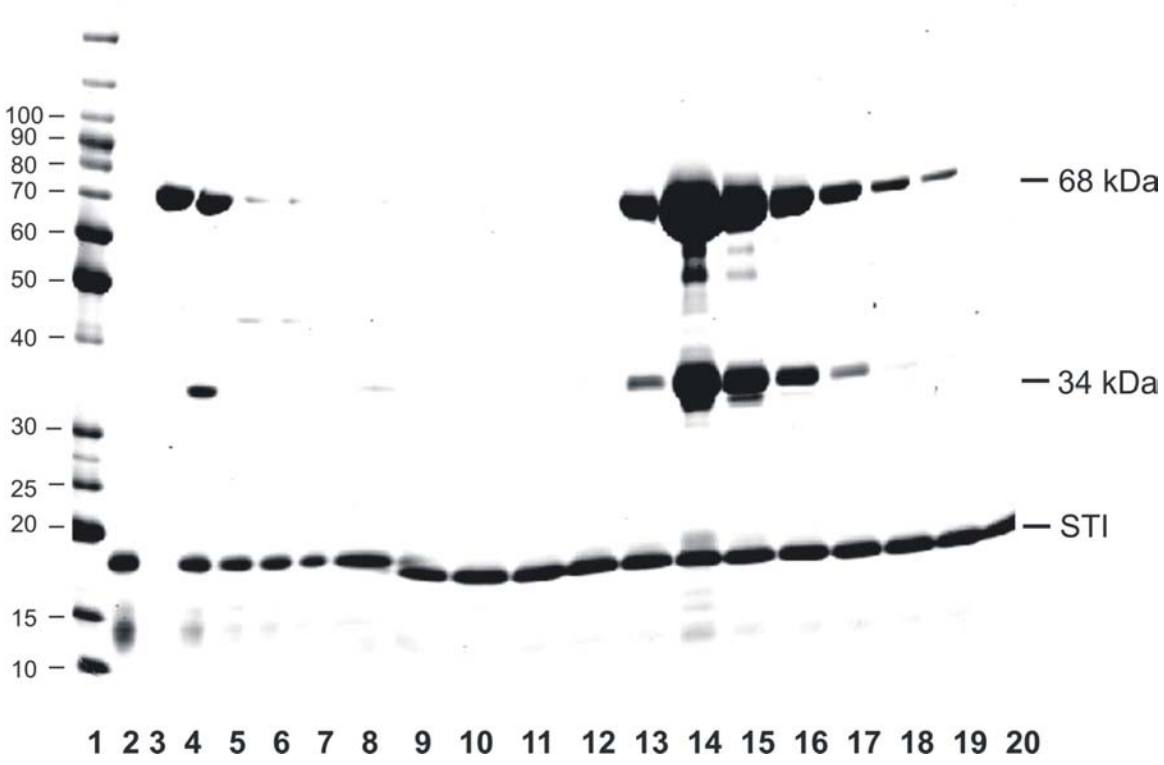

Fig. 23: S100A11-Sepharose affinity chromatography of a partial tryptic digest of annexin A6. Annexin A6 was partially digested with trypsin, applied to S100A11-Sepharose in the presence of Ca^{2+} and bound proteins eluted with EGTA as described in section 2.2.7. Coomassie Blue-stained SDS gel of: 1 = marker proteins; 2 = soybean trypsin inhibitor (STI); 3 = recombinant annexin A6; 4 = partially digested annexin A6 (affinity column load); 5 = flow through; 6 – 9 = fractions eluted in the presence of Ca^{2+}; 10 – 20 = fractions eluted in the presence of EGTA. (n = 2).

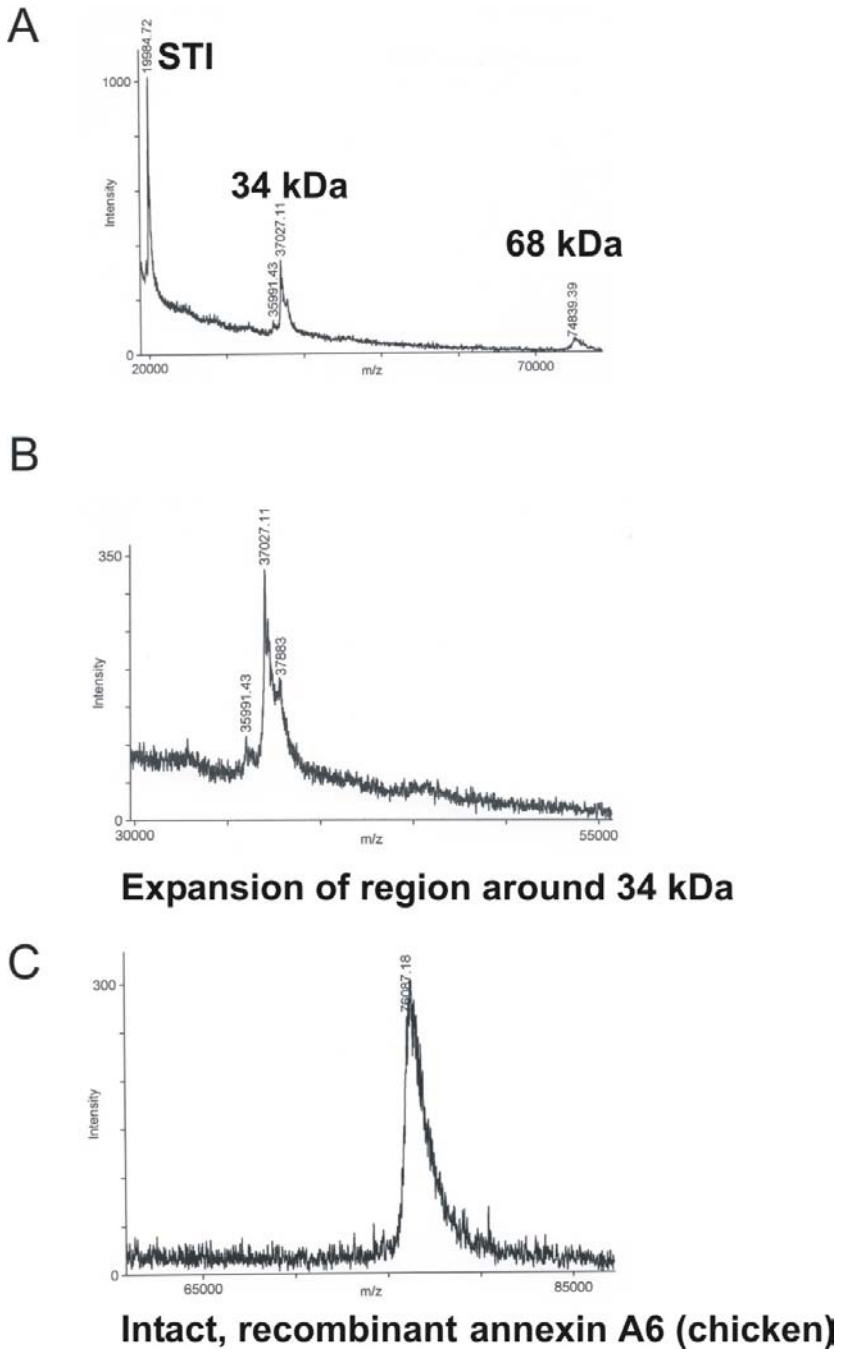

Fig. 24: MALDI-TOF MS analysis of tryptic fragments of annexin A6 bound to immobilized S100A11 in a Ca^{2+}-dependent manner. Samples were prepared for and subjected to MALDI-TOF MS as described in section 2.2.7. ***A.*** MS profile of fraction 16 from the S100A11-Sepharose column (Fig. 23); ***B.*** Expansion of the region of ~34 kDa; ***C.*** MS of intact recombinant annexin A6 (Fig. 23, lane 3).

Table 1 MALDI-TOF MS analysis of tryptic fragments of annexin A6 bound to S100A11-Sepharose

Protein	Measured Mass (Da)	Computed Mass (Da)	Sequence[a]
Full-length	**76,087.18**	**76,003.40**	**M1-D672 + *N*-terminal extension (GPLGSPEF)**
~68 kDa fragment	**74,839.39**	**74,790.97**	**G5-D672**
~34 kDa fragment 1	**37,883**	**37,884**	**G5-R339**
~34 kDa fragment 2	**37,027.11**	**36,924.83**	**M340-D672**
~34 kDa fragment 3	**35,991.43**	**35,908.61**	**V349-D672**

[a]Residue numbers refer to the amino acid sequence of annexin A6 (Fig. 26).

MATRIX SCIENCE Mascot Search Results

Protein View

Match to: gi|50982399 Score: 128 Expect: 1.7e-07
annexin A6 [Gallus gallus]

Nominal mass (M_r): 75179; Calculated pI value: 5.57
NCBI BLAST search of gi|50982399 against nr
Unformatted sequence string for pasting into other applications

Taxonomy: Gallus gallus

Variable modifications: Oxidation (M)
Cleavage by Trypsin: cuts C-term side of KR unless next residue is P
Number of mass values searched: 40
Number of mass values matched: 19
Sequence Coverage: 30%

Matched peptides shown in Bold Red

```
  1 MAPKGKVYRG SVKDFPGFNA SQDADALYNA MKGFGSDKDA ILDLITSRSN
 51 KQRVEICQAY KSQYGKDLIA DLKYELTGKF ERLIVSLMRP PAYSDAKEIK
101 DAIAGIGTDE KCLIEILASR TNQEIHDLVA AYKDAYERDL EADVVGDTSG
151 HFKKMLVVLL QGAREEDDVV SEDLVEQDAK DLLEAGELKW GTDEAQFIYI
201 LGRRSKQHLR MVFDEYLKIS GKPIERSIRA ELSGDFEKLM LAVVKCVRST
251 AEYFAERLYK AMKGLGTRDN TLIRIMVSRS EIDMLDIREV FRTKYDKSLH
301 NMIKEDTSGE YKKALLKLCG GDDDAAGEFF PEAAQVAYRM WELSAVAKVE
351 LRGTVQPASN FNDDGDAQVL RKAMKGLGTD EGAIIEVLTQ RSNAQRQQIL
401 KAYKAHYGRD LLADLKSELS GSLAKLILGL MLTPAQYDAK QLRKAVEGAG
451 TDESTLIEIM ATRNNQEIAA INEAYQQAYH KSLEDDLSSD TSGHFKRILV
501 SLALGNRDEG PENLTQAHED AKVVAETLKL ADVASNDSSD SLETRFLSIL
551 CTRSYPHLRR VFQEEVKMTN HDVEHAIRKR MSGDVRDAFV AIVRSVKNKP
601 AFFADKLYKS MKGAGTDERT LTRIMISRSE IDLLNIRGEF IDLFDKSLYH
651 MIEKDTSGDY CKALLALCGG DD
```

Fig. 25: MS analysis of the ~34 kDa tryptic fragments of annexin A6. The peptides in red are those that matched sequences in the NCBI databank.

The matched peptides come from both *N*- and *C*-terminal halves of annexin A6, confirming that partial trypsin digestion had indeed cleaved in the centre of the molecule to generate similarly-sized peptides corresponding to the *N*-terminal and *C*-terminal halves of the protein.

3.5.5 N-terminal sequencing of tryptic peptides of annexin A6

Fig. 26 shows the amino acid sequence of chicken annexin A6. To confirm the sites of cleavage by trypsin, deduced from MS analysis (Figs. 24, 25 and Table 1), fraction 16 (Fig. 23, page 79) was subjected to SDS-PAGE, transferred to PVDF membrane, and stained with Ponceau S to visualize the proteins. The Ponceau S-stained 68 kDa band was cut out of the gel and the ~34 kDa bands were cut in half (upper and lower bands) for Edman sequencing (Table 2). The 68 kDa band began at Gly5, as did the upper 34 kDa peptide. Three peptides were detected in the lower 34 kDa band: one began at Gly5 (like the upper 34 kDa peptide), one at Met340 and one at Val349. These results confirm that there are three major tryptic cleavage sites in chicken annexin A6: Lys4 – Gly5, Arg339 – Met340 and Lys348 – Val349. One of the cleavage sites is located in the *N*-terminal head region and the other two in the linker region between annexin repeats 4 and 5 (Fig. 26), consistent with the accessibility of these regions apparent from the crystal structure (Fig. 6B). Taken together with the MS data (Table 1 and Figs. 24 and 25), we can conclude that 4 tryptic fragments bound to the S100A11 affinity column in a Ca^{2+}-dependent manner (Fig. 23) and correspond to: G5 – D672, G5 – R339, M340 – D672 and V349 – D672 of annexin A6.

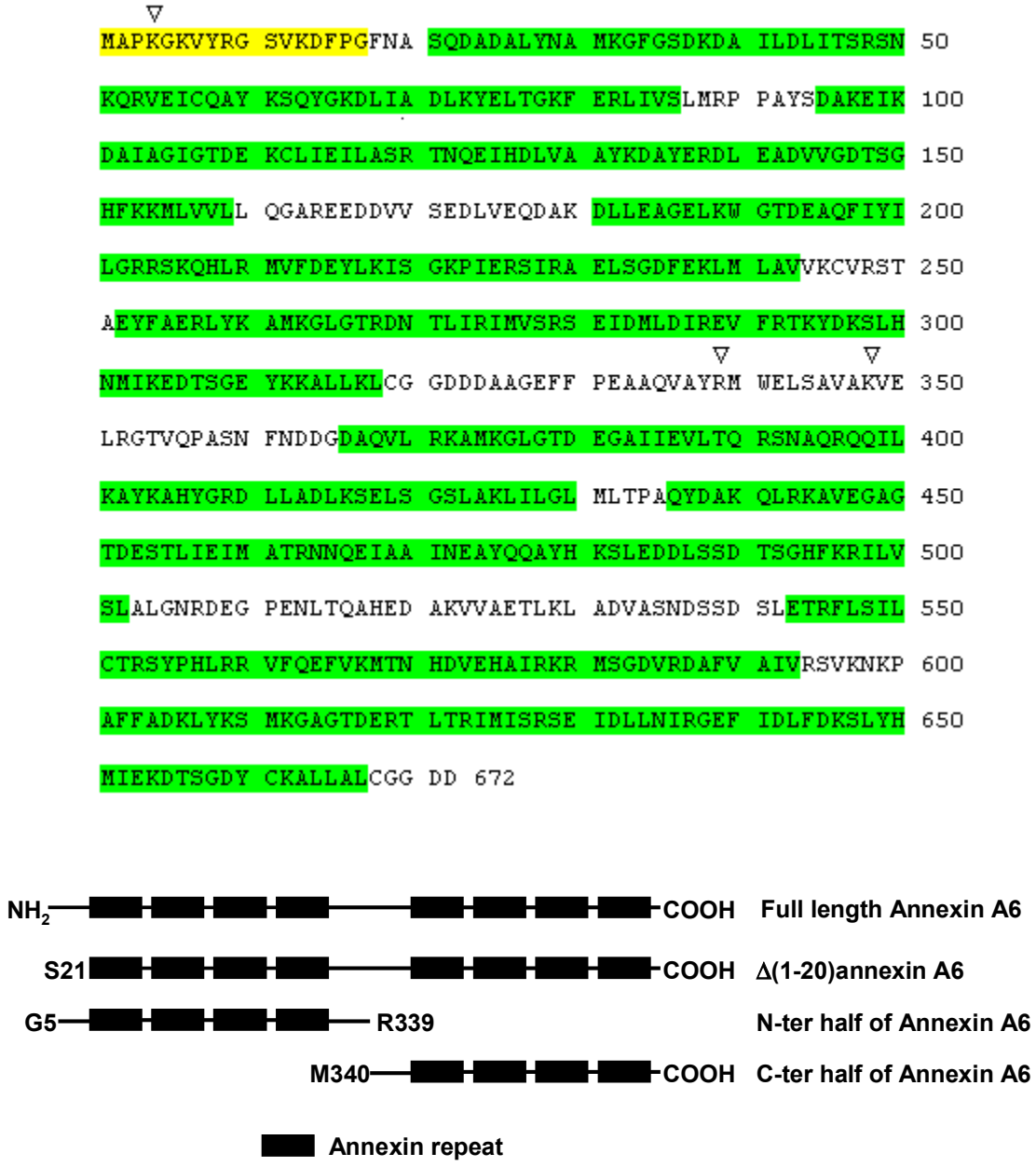

Fig. 26: Chicken annexin A6 amino acid sequence and different constructs. The *N*-terminal tail, which is different in all annexins, is highlighted in yellow. The 8 annexin repeats are highlighted in green. The identified tryptic cleavage sites (see text) are indicated with triangles. NCBI accession number: Q6B344. Different recombinant constructs for annexin A6 generated are shown in the diagram below the sequence.

Table 2 *N*-terminal sequencing of tryptic fragments of annexin A6 bound to S100A11-Sepharose

Peptide	*N*-terminal sequence	Residues
68 kDa	GKVYRGSVKD	5-14
34 kDa upper	GKVYRGSVKD	5-14
34 kDa lower	GKVYRGSVKD	5-14
	MWELSAVA	340-347
	VELRGTVQ	349-356

To gain further insight into the S100A11-binding sites on annexin A6, fragments of annexin A6 were expressed in *E. coli,* purified and their ability to bind S100A11 in a Ca^{2+}-dependent manner assessed.

3.5.6 Ca^{2+}-dependent binding of purified recombinant C-terminal annexin A6 (M340-D672) to immobilized S100A11

The *C*-terminal half of annexin A6 (M340-D672) was cloned, expressed in *E. coli* and purified. The purified recombinant *C*-terminal annexin A6 was applied to an S100A11-Sepharose affinity column in the presence of Ca^{2+} and bound protein was eluted with EGTA (Fig. 27).

This experiment confirmed the Ca^{2+}-dependent interaction of the *C*-terminal domain of annexin A6 with S100A11.

3.5.7 Confirmation of Ca^{2+}-dependent binding of purified recombinant S100A11 to the C-terminal half of annexin A6 by gel overlay

The purified recombinant *C*-terminal half of annexin A6 was subjected to SDS-PAGE and transferred to nitrocellulose. The blot was incubated with purified S100A11. Unbound S100A11 was washed out, and bound S100A11 detected with anti-S100A11 (Fig. 28).

It was, therefore, confirmed independently by gel overlay that the *C*-terminal half of annexin A6 contains an S100A11-binding site.

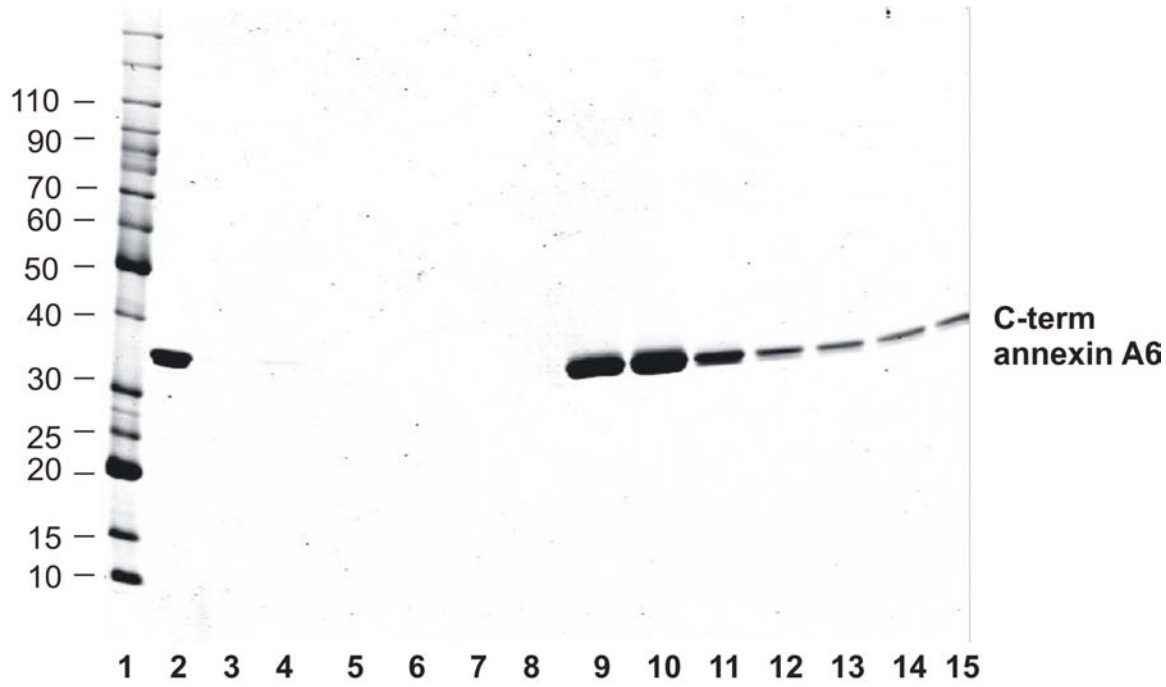

Fig. 27: Ca^{2+}-dependent interaction of the *C*-terminal half of annexin A6 with immobilized S100A11. Annexin A6 (M340-D672) was expressed and purified as described in section 2.2.1.2.2. Its ability to bind to immobilized S100A11 in a Ca^{2+}-dependent manner was determined by affinity chromatography as described in section 2.2.2.3. Coomassie Blue-stained SDS gel of: 1 = marker proteins; 2 = purified *C*-terminal annexin A6; 3 = flow through; 4 – 8 = fractions eluted in the presence of Ca^{2+}; 9 – 15 = fractions eluted in the presence of EGTA (n = 3).

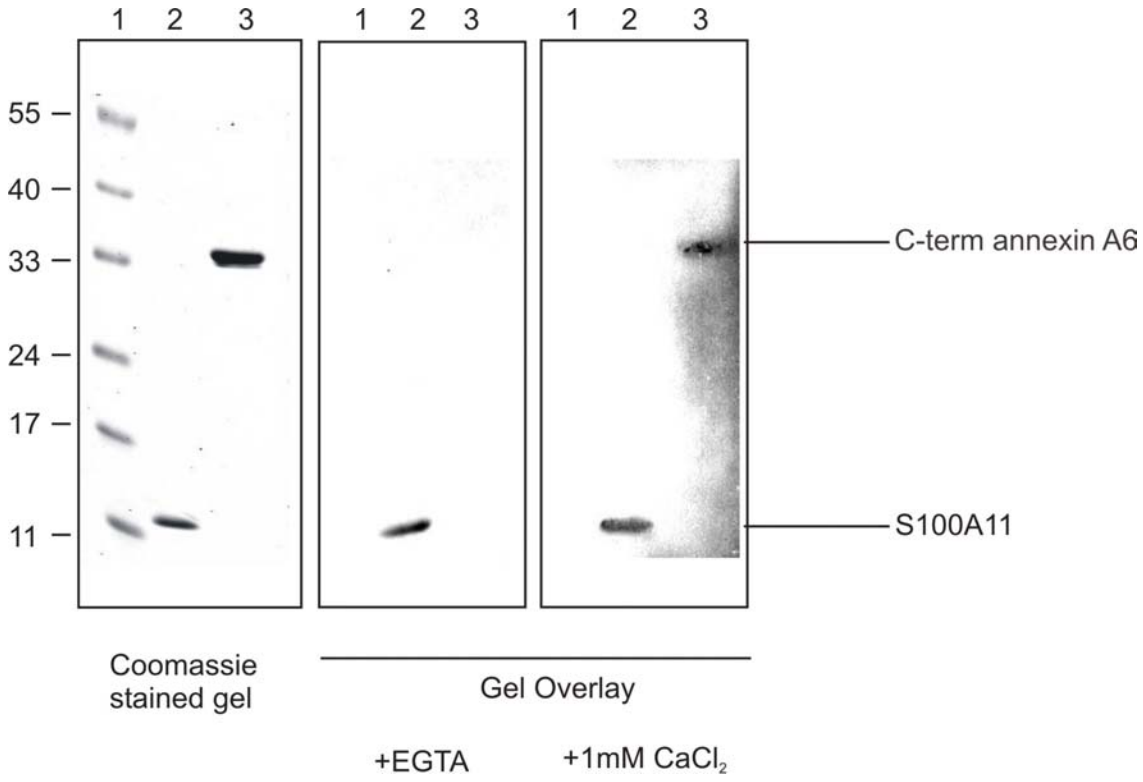

Fig. 28: Ca^{2+}-dependent interaction of S100A11 with the *C*-terminal half of annexin A6 demonstrated by gel overlay. S100A11 and annexin A6 (M340-D672) were subjected to SDS-PAGE, transblotted to nitrocellulose and incubated with S100A11 in the presence of EGTA or Ca^{2+} as described in section 2.2.6. Bound S100A11 was detected with anti-S100A11 (Gel Overlay). 1 = prestained markers; 2 = S100A11; 3 = *C*-terminal annexin A6 (n = 3).

3.5.8 Ca^{2+}-dependent binding of purified recombinant N-terminal half of annexin A6 (G5-R339) to immobilized S100A11

The purified recombinant *N*-terminal half of annexin A6 (G5-R339) was applied to an S100A11-Sepharose affinity column in the presence of Ca^{2+} and bound protein was eluted with EGTA (Fig. 29).

Therefore, like the *C*-terminal half, the *N*-terminal half of annexin A6 binds to S100A11 in a Ca^{2+}-dependent manner.

3.5.9 Confirmation of Ca^{2+}-dependent binding of purified recombinant S100A11 to the N-terminal half of annexin A6 by gel overlay

The purified recombinant *N*-terminal half of annexin A6 was subjected to SDS-PAGE and transferred to nitrocellulose. The blot was incubated with purified S100A11, unbound S100A11 was washed out, and bound S100A11 detected with anti-S100A11 (Fig. 30).

It was, therefore, confirmed independently by gel overlay that the *N*-terminal half of annexin A6 contains an S100A11-binding site.

3.6 Phosphorylation of S100A11 *in vitro*

3.6.1 Phosphorylation of S100A11 by cPKC

S100A11 has been shown to be phosphorylated by PKCα at Thr10 (human numbering) (Sakaguchi *et al*., 2004), which corresponds to Thr9 of chicken S100A11 (see Fig. 3 on page 10). Wild-type (WT) and 2 site-directed mutants (T9A, T9D) of chicken S100A11 were incubated with cPKC (a mixture of Ca^{2+}-dependent PKC isoenzymes α, β and γ

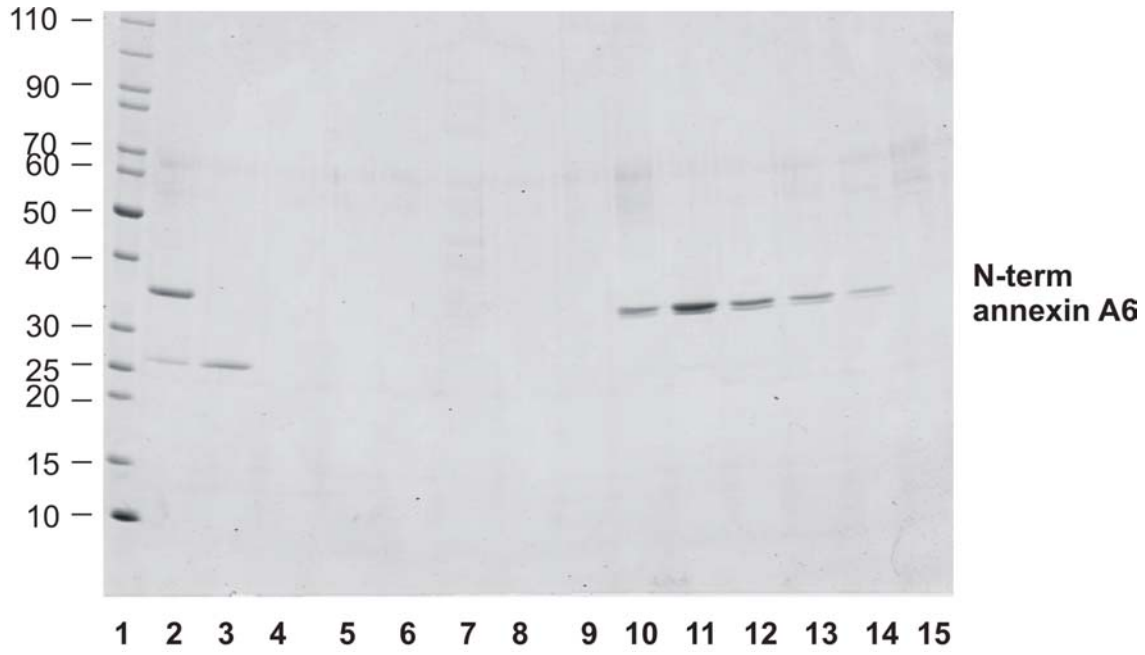

Fig. 29: Ca^{2+}-dependent interaction of the *N*-terminal half of annexin A6 with immobilized S100A11. Annexin A6 (G5-R339) was expressed and purified as described in section 2.2.1.2.2. Its ability to bind to immobilized S100A11 in a Ca^{2+}-dependent manner was determined by affinity chromatography as described in section 2.2.2.3. Coomassie Blue-stained SDS gel of: 1 = marker proteins; 2 = purified *N*-terminal annexin A6; 3 = flow through; 4 – 8 = fractions eluted in the presence of Ca^{2+}; 9 – 15 = fractions eluted in the presence of EGTA (n = 2).

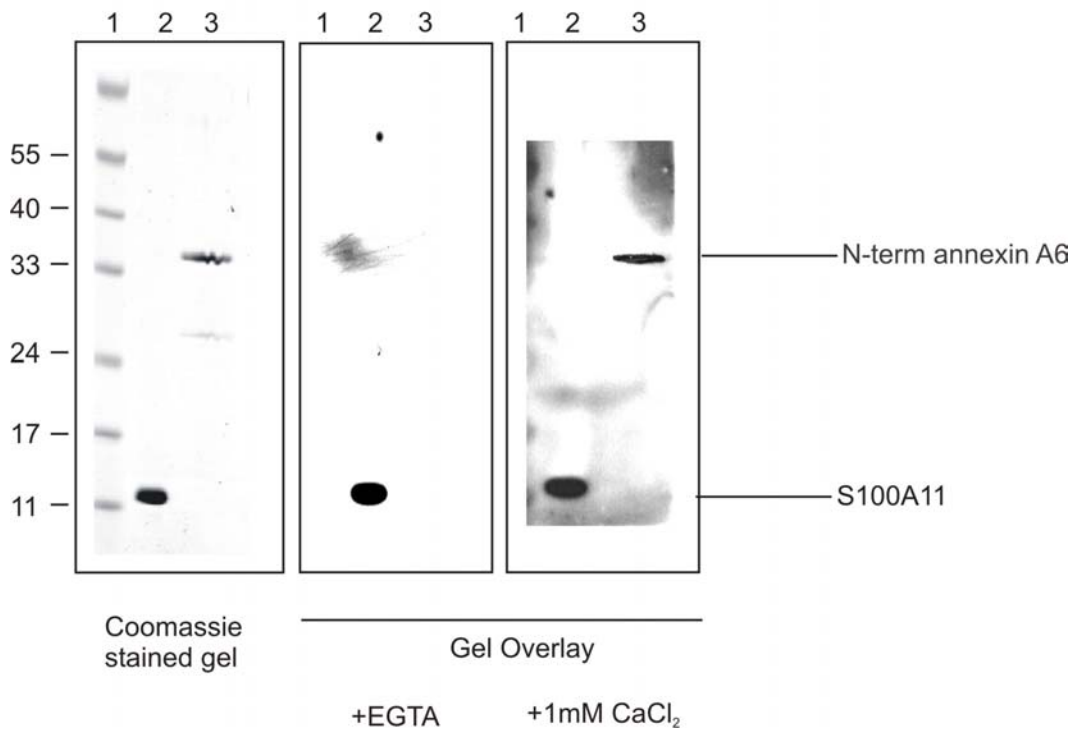

Fig. 30: Ca^{2+}-dependent interaction of S100A11 with the *N*-terminal half of annexin A6 demonstrated by gel overlay. S100A11 and annexin A6 (G5-R339) were subjected to SDS-PAGE, transblotted to nitrocellulose and incubated with S100A11 in the presence of EGTA or Ca^{2+} as described in section 2.2.6. Bound S100A11 was detected with anti-S100A11 (Gel Overlays). 1 = prestained markers; 2 = S100A11; 3 = *C*-terminal annexin A6 (n = 3).

isolated from rat brain) in the presence of Ca^{2+} and Mg[γ-^{32}P]ATP. Samples were withdrawn at selected times for quantification of ^{32}P incorporation into S100A11 (Fig. 31A). At the end of the reaction, samples (1 μg S100A11) were subjected to SDS-PAGE, stained with Coomassie Blue and exposed to X-ray film for 16 h (Fig. 31B).

WT S100A11 was phosphorylated to ~ 0.3 mol P_i/mol S100A11, whereas T9A and T9D S100A11 reached very low phosphorylation stoichiometry. These results confirm that Thr9 is the principal site of phosphorylation in S100A11 by Ca^{2+}-dependent PKC.

3.6.2 Phosphorylation of S100A11 disrupts its interaction with annexin A6

Purified recombinant S100A11 was phosphorylated by cPKC, applied to an annexin A6-Sepharose affinity column in the presence of Ca^{2+} and bound protein was eluted with EGTA (Fig. 32A).

In control experiments, unphosphorylated S100A11 bound to immobilized annexin A6 in a Ca^{2+}-dependent manner (Fig. 32B). On the other hand, very little phosphorylated S100A11 bound to immobilized annexin A6 in the presence of Ca^{2+} (Fig. 32A), indicating that phosphorylation by cPKC at Thr9 of S100A11 disrupts its interaction with annexin A6. Unbound S100A11 in the flow through was due to the excess of S100A11 applied to the column to ensure maximal binding.

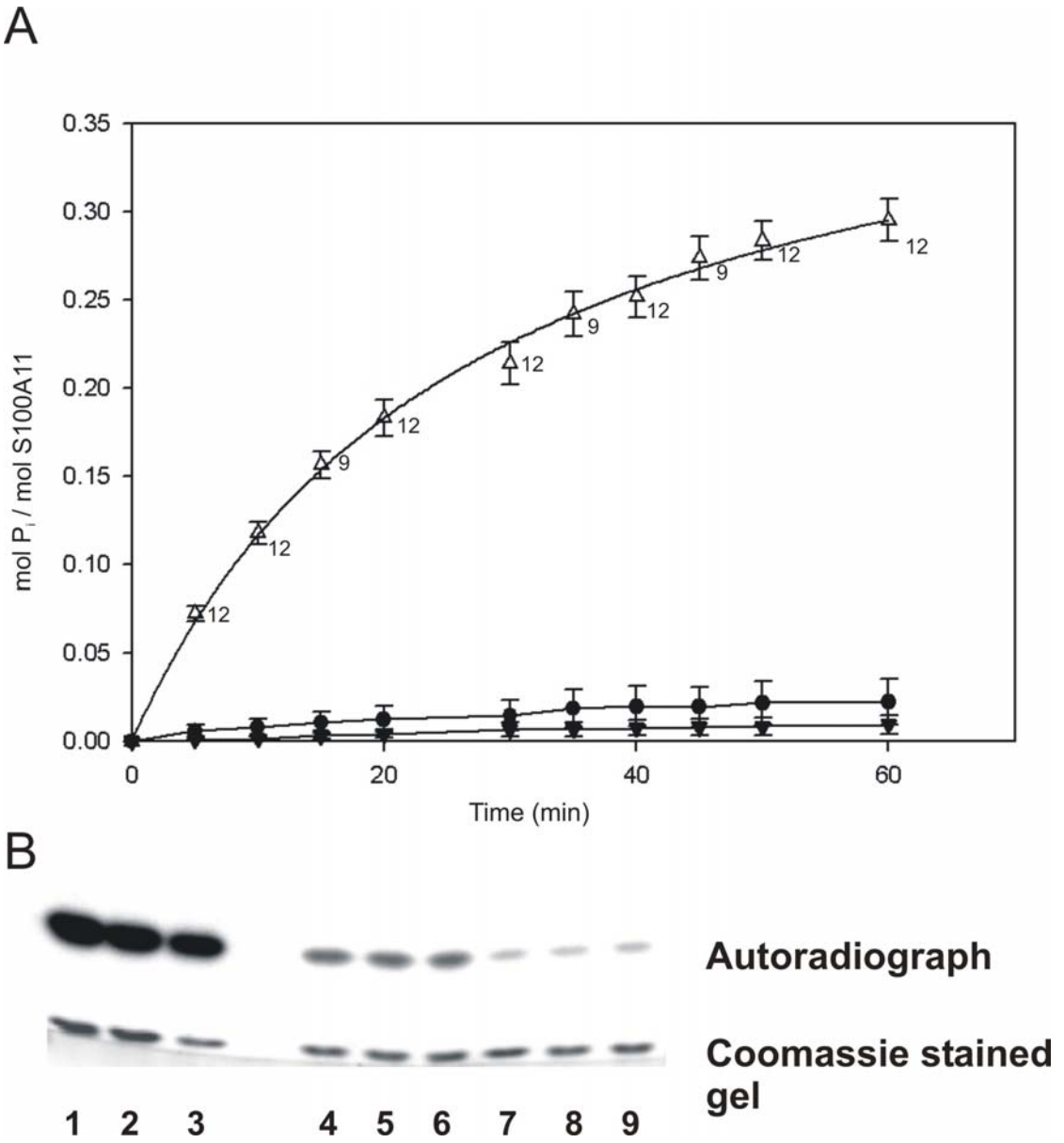

Fig. 31: Phosphorylation of S100A11 by Ca^{2+}-dependent PKC. ***A.*** Time course of phosphorylation of WT S100A11 (Δ), T9A-S100A11 (●) and T9D-S100A11 (▼), quantified as described in section 2.2.4.1. Numbers indicate n values at each time point for all 3 reactions. ***B.*** At the end of the reaction, triplicate samples were analysed by SDS-PAGE and autoradiography to verify S100A11 phosphorylation. 1 – 3 = 1 µg WT chicken S100A11; 4 – 6 = 1 µg T9A chicken S100A11; 7 – 9 = 1 µg T9D chicken S100A11.

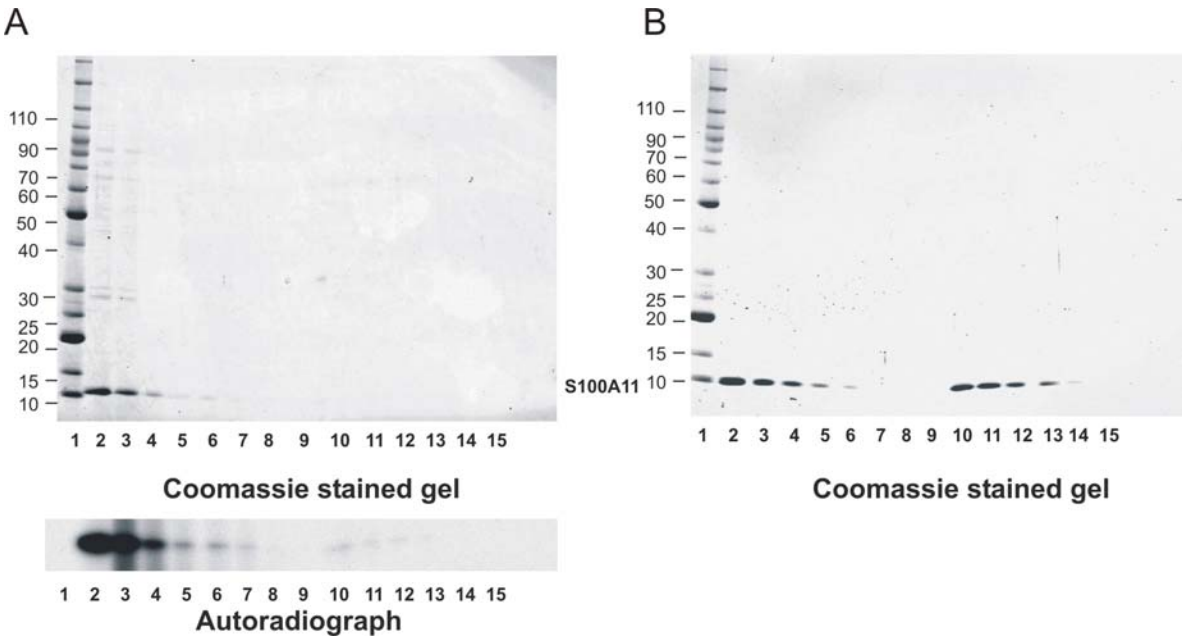

Fig. 32: Phosphorylation of S100A11 disrupts its interaction with annexin A6. ***A.*** Affinity chromatography of phosphorylated S100A11 as described in section 2.2.4.2. Upper panel: Coomassie Blue-stained gel of column fractions; lower panel: corresponding autoradiogram. ***B.*** Control showing affinity chromatography of unphosphorylated S100A11. 1 = marker proteins; 2 = column load; 3 = flow through; 4 – 8 = fractions eluted in the presence of Ca^{2+}; 9 – 15 = fractions eluted in the presence of EGTA. (n = 3).

CHAPTER 4:

DISCUSSION

4.1 The discovery of a novel S100A11-binding protein

Functional characterization of protein-protein interactions is of great importance since the identification of an interacting partner of a protein of unknown function can help to clarify its function, mechanism of action and regulation. Although S100A11 was identified in smooth muscle 17 years ago, the actual role it plays is still unknown. Based on its biochemical and structural properties, we conclude that S100A11 acts as a "Ca^{2+} sensor": in response to an appropriate stimulus, it undergoes a conformational change with exposure of a hydrophobic surface that interacts with a target protein(s) and thereby regulates its function. The identification of the target(s) of S100A11 in smooth muscle is, therefore, important in elucidating the function of this Ca^{2+}-binding protein. Using S100A11 affinity chromatography, we showed for the first time that the Ca^{2+}- and phospholipid-binding protein annexin A6 is a Ca^{2+}-dependent binding partner of S100A11 in smooth muscle (Figs. 8 – 10). No annexin A1 was identified in the EGTA-eluted fractions, likely due to the absence or trace amount of expression in chicken smooth muscle. Smooth muscle cells expressed mainly annexin A6 and annexin A2 (Carmors *et al.,* 2005).

4.2 Co-expression of S100A11 and annexin A6 in the same smooth muscle cell

It has already been demonstrated that annexin A6 (Babiychuk *et al*., 1999; Babiychuk & Draeger, 2000) and S100A11 (Allen *et al*., 1996) are both expressed in smooth muscle tissue. In this study, co-expression of S100A11 and annexin A6 in smooth muscle cells was confirmed at the message level by RT-PCR on small numbers of isolated smooth muscle cells from rat basilar arterial smooth muscle (Fig. 12). Co-expression of S100A11

and annexin A6 in an extract of rat tail arterial smooth muscle was confirmed at the protein level with a monoclonal antibody raised against full-length rat S100A11 (Fig. 18) and a polyclonal peptide-directed anti-(rat annexin A6) (Fig. 19).

4.3 Verification of the interaction between S100A11 and annexin A6

Direct Ca^{2+}-dependent interaction between S100A11 and annexin A6 was confirmed by chromatography of purified bacterially-expressed annexin A6 on an affinity column of S100A11 coupled to Sepharose-4B (Fig. 13) and by the reciprocal procedure (Fig. 14). Gel overlay (Fig. 22), liposome co-pelleting assay (Fig. 15) and cross-linking experiments (Fig. 20) confirmed the direct Ca^{2+}-dependent interaction between the two proteins. In this study, we report for the first time a Ca^{2+}-dependent interaction of S100A11 with phosphatidylserine liposomes (Fig. 16), which explains the unexpected binding of S100A11 to liposomes isolated from rat tail artery in the presence but not absence of Ca^{2+} (compare lanes 11 and 12 in Fig. 15). Nevertheless, in 4 independent experiments, we observed more S100A11 in the pellet fraction in the presence of Ca^{2+} when annexin A6 was also present (compare lanes 12 and 15 in Fig. 15), which was consistent with the Ca^{2+}-dependent interaction between them. After subtracting the amount of S100A11 that bound to liposomes in the absence of annexin A6, a 1:1 stoichiometry was obtained between S100A11 and annexin A6, which corresponds to a stoichiometry of 1 S100A11 monomer : 1 annexin A6 or 1 S100A11 dimer : 2 annexin A6 monomers. This stoichiometry is consistent with that obtained in chemical cross-linking experiments in which the ~81 kDa band corresponds to a 1:1 complex of S100A11 and annexin A6 (Fig. 20). A ~93 kDa band was also observed in cross-linking

experiments, corresponding to a stoichiometry of 1 annexin A6 monomer : 1 S100A11 dimer (Fig. 20). Fig. 33 shows the theoretical interaction between annexin A6 and S100A11 in the liposome co-pelleting assay (***A***) and cross-linking experiments (***B***).

4.4 Identification of two binding sites on annexin A6 for S100A11

Both annexin A1 and annexin A6 interact with S100A11 in a Ca^{2+}-dependent manner. The *N*-terminal domain of annexin A1 is responsible for the binding to S100A11 (Mailliard *et al*., 1996; Osterloh *et al*., 2000). We had anticipated that the *N*-terminal domain of annexin A6 might also be the binding site for S100A11. However, Δ(1-20)annexin A6, which lacks this domain of annexin A6, bound to S100A11 in a Ca^{2+}-dependent manner (Fig. 21), indicating that the *N*-terminal head region of annexin A6 is not required for the interaction. This conclusion was supported by gel overlay (Fig. 22). To identify the binding site on annexin A6, S100A11-Sepharose affinity chromatography of a partial tryptic digest of annexin A6 was performed and two major fragments were detected of M_r ~68 kDa (slightly smaller than full-length annexin A6) and ~ 34 kDa, indicating the presence of major tryptic cleavage sites near one end of the annexin A6 molecule and in the centre of the molecule (Fig. 23). Based on the available cleavage sites in full-length annexin A6 (trypsin cleaves after Lys or Arg when the next residue is not Pro) and comparison of the molecular weights measured by MS with those of tryptic fragments predicted from the annexin A6 sequence (Figs. 24 – 26 and Table 1), the identities of the peptides were deduced, indicating that: (i) cleavage at K4 – G5 generates the ~ 68 kDa tryptic fragment, and (ii) subsequent cleavage at R339 – M340 and K348 – V349 generates 3 tryptic fragments corresponding to G5 – R339, M340 – D672 and

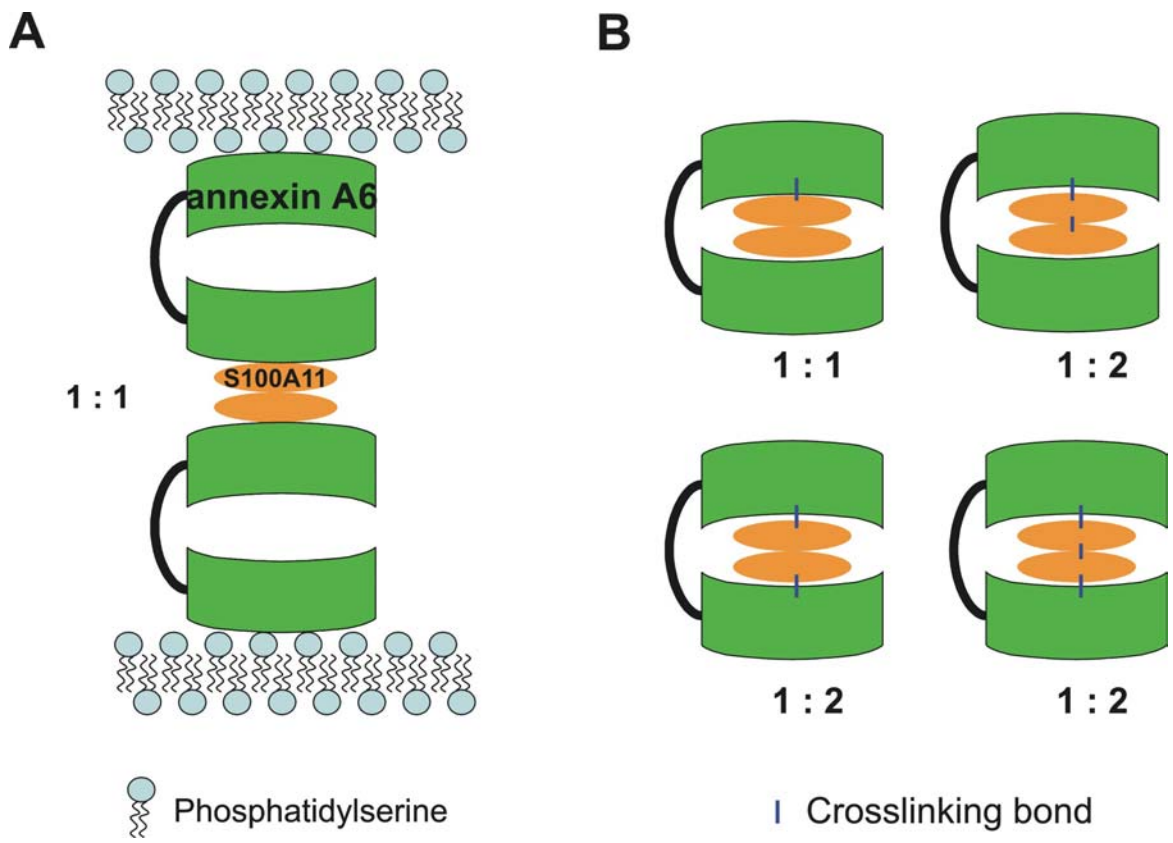

Fig. 33: Stoichiometry between annexin A6 and S100A11 in liposome co-pelleting assay (*A*) and chemical cross-linking (*B*).

V349 – D672, all of which bind to S100A11 in a Ca^{2+}-dependent manner (Fig. 23). These conclusions were confirmed by MS analysis of the ~34 kDa tryptic fragments of annexin A6 and *N*-terminal sequencing of tryptic peptides of annexin A6 (Fig. 25 and Table 2). Therefore, one of the tryptic cleavage sites is located in the *N*-terminal head region and the other two in the linker region between annexin repeats 4 and 5 (Fig. 26), consistent with the accessibility of these regions apparent from the crystal structure (Fig. 6B). Taken together, therefore, we can conclude that 4 tryptic fragments bound to the S100A11 affinity column in a Ca^{2+}-dependent manner (Fig. 23) and correspond to: G5 – D672, G5 – R339, M340 – D672 and V349 – D672 of annexin A6.

We confirmed that the *N*-terminal head region is not required for the interaction. Furthermore, both the *N*-terminal half (G5 – R339) (Figs. 29 and 30) and the *C*-terminal half (M340 – D672) of annexin A6 (Figs. 27 and 28) interact with S100A11 in a Ca^{2+}-dependent manner. It was reported that the central linker region of annexin A6 is responsible for the interaction with the key Ras regulatory protein p120-GTPase activating protein ($p120^{GAP}$) (Chow & Gawler, 1999) and mu subunit of the clathrin assembly proteins (Creutz & Snyder, 2005). Therefore, the exposed hydrophobic central linker of annexin A6 might be responsible for the interaction with S100A11. Alternatively, the data would be consistent with a binding site within the *N*-terminal 4-annexin repeat domain and a binding site within the *C*-terminal 4-annexin repeat domain. These possibilities could be distinguished by characterizing the S100A11-binding capabilities of the following 3 expressed domains (cf. Fig. 26): (i) S21 - L318, (ii) C319 - G365 and (iii) D366 – L667.

4.5 The effect of phosphorylation on the interaction between S100A11 and annexin A6

In this study, it is reported for the first time that chicken S100A11 can be phosphorylated *in vitro* by cPKC (Fig. 31). Wild-type S100A11 was phosphorylated to ~ 0.3 mol P_i/mol S100A11, whereas T9A and T9D S100A11 reached very low phosphorylation stoichiometry (Fig. 31), suggesting that Thr9 is the site of phosphorylation by Ca^{2+}-dependent PKC. It had previously been shown that the corresponding site in human S100A11 (Thr10) is phosphorylated by PKCα (Sakaguchi *et a*l., 2004). One question that arises concerns why the phosphorylation stoichiometry of WT S100A11 is low (~0.3 mol P_i/mol S100A11). Since S100A11 can bind to phosphatidylserine in a Ca^{2+}-dependent manner (Fig. 16), the phosphatidylserine-containing mixed micelles used to activate cPKC may partially mask the phosphorylation site. Alternatively, perhaps only one S100A11 molecule in the dimer can be phosphorylated by cPKC.

Recently, it was reported that, upon exposure of human keratinocytes to high [Ca^{2+}], S100A11 was specifically phosphorylated at Thr10 by PKCα and the phosphorylation facilitated the binding of S100A11 to nucleolin, resulting in nuclear translocation of S100A11. In the nuclei, S100A11 liberated Sp1/3 from nucleolin. The resulting free Sp1/3 transcriptionally activated $p21^{CIP1/WAF1}$, a negative regulator of cell growth (Sakaguchi *et al.*, 2003; *ibid*, 2004).

As shown in Fig. 32, phosphorylated S100A11 lost the binding capacity for immobilized annexin A6, although a very small amount of bound S100A11 was detected by autoradiography. PKC-catalysed phosphorylation of S100A11 may, therefore, be very important in regulating the localization of S100A11 and, consequently, its physiological

function. How the association and dissociation of the Ca^{2+}-dependent interaction between S100A11 and annexin A6 is regulated by Ca^{2+} remains to be elucidated. On the one hand, Ca^{2+} induces the binding of S100A11 to annexin A6. On the other hand, Ca^{2+} activates cPKC, which phosphorylates S100A11 and inhibits its binding to annexin A6. An agonist-induced increase in cytosolic free [Ca^{2+}] may lead to formation of the S100A11-annexin A6 complex, which forms a physical connection between the plasma membrane and cytoskeleton that is essential for transmission of mechanical signals leading to contraction. Activation of cPKC requires diacylglycerol production in addition to an increase in [Ca^{2+}], so S100A11 phosphorylation and dissociation from annexin A6 would require diacylglycerol production. There may also be differences in the time courses of the Ca^{2+} signal and diacylglycerol production, and in their localization.

As mentioned earlier, the phosphorylation stoichiometry of WT S100A11 is low (~0.3 mol P_i/mol S100A11). The Ca^{2+}-dependent binding of S100A11 to phosphatidylserine-containing liposomes might interfere with the affinity chromatography. These data must, therefore, be considered preliminary and the limitations referred to require emphasis. A constitutively-active PKC (Ca^{2+}- and lipid-independent) would be very useful to further address this question.

Evidence from other cell types has implicated annexin A6 in Ca^{2+}-dependent formation of signaling complexes. For example, annexin A6 has been shown to associate in a Ca^{2+}-dependent manner with lipid rafts along with PKCα and neurocalcin-α (Orito *et al.*, 2001) and direct interaction between annexin A6 and skeletal muscle PKCα has been demonstrated (Schmitz-Peiffer *et al.*, 1998). Annexin A6 has also been identified in a complex with the GTPase activating protein p120 Ras-GAP and the tyrosine kinases Fyn

and Pyk2, annexin A6 interacting directly with p120 Ras-GAP and Fyn, but not Pyk2 (Chow *et al*., 2000). Taken together, these results suggest that annexin A6 might regulate the localization of Ca^{2+}-dependent PKC upon activation, thereby ensuring phosphorylation of specific substrate pools such as annexin A6-bound S100A11, by acting as an adaptor protein. By virtue of its preference for acidic phospholipids, annexin A6 may help create high density phosphatidylserine domains in cell membranes that are required for PKC activity. S100A11 may confer the high sensitivity to Ca^{2+} that is observed for association of annexin A6 with the sarcolemma (Babiychuk & Draeger, 2000).

4.6 Conclusions and future directions

In summary, the following principal conclusions can be drawn from this study: (i) the EF-hand Ca^{2+}-binding protein S100A11 interacts with the Ca^{2+}- and phospholipid-binding protein annexin A6 in a Ca^{2+}-dependent manner; (ii) S100A11 and annexin A6 are both expressed in vascular smooth muscle cells; (iii) the *N*-terminal head region of annexin A6 is not required for the interaction; (iv) both *N*- and *C*-terminal halves of annexin A6 contain S100A11-binding sites; (v) the interaction between S100A11 and annexin A6 is disrupted by phosphorylation of S100A11 at Thr9 by Ca^{2+}-dependent protein kinase C.

Members of the annexin protein family, including annexin A6, have been implicated in smooth muscle membrane organization, constituting a reversible, Ca^{2+}-dependent link between the sarcolemma and the cytoskeleton. Since the S100A11-annexin A6

interaction is Ca^{2+}-dependent, the possibility arises that Ca^{2+}-dependent formation of a complex of annexin A6 and S100A11 links the plasma membrane to the cytoskeleton.

To evaluate the physiological relevance of the Ca^{2+}-dependent interaction between S100A11 and annexin A6, co-immunoprecipitation of the complex from a rat tail arterial smooth muscle extract will be performed in the presence of Ca^{2+} using our monoclonal mouse anti-(rat S100A11) and polyclonal rabbit anti-(rat annexin A6). Furthermore, the co-localization of S100A11 and annexin A6 in vascular smooth muscle cells will be verified at the protein level by double-labeling immunocytochemistry with isolated smooth muscle cells from the rat tail artery.

Whether S100A11 and annexin A6 could form a Ca^{2+}-dependent membrane-cytoskeleton complex in vascular smooth muscle will be investigated, predicting that S100A11 and annexin A6 interact in response to a Ca^{2+} transient and translocate from a cytosolic location to the sarcolemma. Confocal immunocytochemistry and co-immunoprecipitation with isolated vascular smooth muscle cells at rest and stimulated with an α_1-adrenergic agonist (cirazoline), angiotensin II, the thromboxane A_2 mimetic U46619, or Ca^{2+} ionophore (A23187) will be performed. Immunocytochemistry will also be performed in the presence of ML-9 (myosin light chain kinase inhibitor) or butanedione monoxime (actomyosin ATPase inhibitor) to prevent Ca^{2+}-induced contraction, which would likely affect the fluorescent signal and render translocation difficult to visualize. Annexin A6 has been implicated in the Ca^{2+}-dependent formation of a membrane-cytoskeleton complex in gastrointestinal smooth muscle. Using a combination of subcellular fractionation and immunocytochemistry, as described by Babiychuk *et al* (1999), we will determine if the same is true for vascular smooth muscle

and will test the hypothesis that the Ca^{2+}-dependent interaction of S100A11 with annexin A6 results in the association of S100A11 with this complex using our antibodies to S100A11 in Western blotting experiments. These experiments with intact tissue preparations will be complemented by similar experiments with α-toxin-permeabilized vascular smooth muscle, in which $[Ca^{2+}]_i$ can be set at any desired level using an EGTA buffering system to determine the Ca^{2+} dependence of translocation.

In addition, we will investigate the translocation of annexin A6 and S100A11 specifically to caveolae in response to a Ca^{2+} transient elicited by the same agonists listed above since Babiychuk *et al* (1999) concluded that annexin A6 associated specifically with this sarcolemmal structure in response to stimulation. Our antibodies to S100A11 and annexin A6 should enable us to address the important question of whether S100A11 and annexin A6 co-translocate to caveolae in response to an increase in cytosolic $[Ca^{2+}]$, thereby providing an association between this region of the plasma membrane and the cytoskeleton.

The binding sites on annexin A6 for S100A11 remain to be localized precisely. Three deletion mutants of annexin A6 (G5-L318, C319-G365 and D366-L667), which correspond to the *N*-terminal lobe, central linker and *C*-terminal lobe, respectively, will be generated, expressed and purified. Gel overlay with S100A11 and S100A11-affinity chromatography will be performed. If the *N*-terminal lobe and *C*-terminal lobe of annexin A6 lose the binding capability but the central linker does not, we would conclude that the binding sites are located within the central linker. The peptide corresponding to the central linker could then be used to disrupt the S100A11-annexin A6 interaction in intact cells or freshly-isolated vascular smooth muscle strips. The peptide will be made

membrane permeant so that it can be effectively introduced into intact smooth muscle cells or freshly-isolated vascular smooth muscle strips and the effects on contractility will be evaluated. The prediction would be that the peptide will induce relaxation due to disruption of the membrane-cytoskeleton interaction mediated by the S100A11-annexin A6 complex, or inhibit the contractile response if the tissue is incubated with peptide prior to stimulation.

Determination of the three-dimensional structure of $(Ca^{2+})_4$-S100A11$_2$ bound to the annexin A6 peptide will represent a major advance in understanding of the protein-protein interactions between S100 and annexin family members. Given the fact that the binding site on S100 proteins for annexins, e.g., the binding site on S100A11 for annexin A1 (Fig. 6B), involves regions of the protein quite far apart in the linear sequence, the deletion mutagenesis approach would not be feasible for S100A11. Direct structure determination by, e.g., NMR spectroscopy is therefore the method of choice to define the S100A11 amino acid residues that are involved in binding to annexin A6. In the future, NMR spectroscopy might also help to investigate the Ca^{2+}-dependent binding site on S100A11 for phosphatidylserine.

Another approach that could be used to address the functional role of the S100A11-annexin A6 interaction involves down-regulation of S100A11 and annexin A6 by small interfering RNA (siRNA). The prediction would be that the down-regulation of either protein would attenuate the contractile response to stimuli. The functional significance of the Ca^{2+}-dependent interaction between S100A11 and annexin A6 that we have demonstrated *in vitro* could also be investigated by generating knockout mouse models of S100A11 and annexin A6. The fact that blood pressure in annexin A6 null mice appears

normal (Hawkins et al., 1999) suggests that there may be compensation for the absence of annexin A6, perhaps by overexpression of another annexin. The generation of a double knockout of S100A11 and annexin A6 would then be necessary.

To assess the functional significance of the phosphorylation of S100A11 by cPKC and the phosphorylation-dependent disruption of the interaction between S100A11 and annexin A6 that we have demonstrated *in vitro*, it would first be necessary to verify, using phosphospecific antibodies, that S100A11 phosphorylation indeed occurs in intact smooth muscle tissues in response to PKC activation by, e.g. phorbol 12, 13-dibutyrate and physiological stimuli such as α_1-adrenergic agonists. The effects of such treatments on the localization of S100A11 in real-time could be investigated using GFP-S100A11 in conjunction with confocal fluorescence microscopy.

In conclusion, we have reported a novel Ca^{2+}-dependent interaction between the Ca^{2+}–binding protein S100A11 and the Ca^{2+}- and phospholipid-binding protein annexin A6 of smooth muscle, which is disrupted by phosphorylation of S100A11 at Thr9 by Ca^{2+}-dependent PKC. This regulated protein-protein interaction may play a role in control of membrane-cytoskeleton connections, which are necessary for force development, and/or control of formation of signaling complexes at the sarcolemma. In the course of this work, several tools were developed, including S100A11- and annexin A6-specific antibodies, which will be useful in elucidating the physiological role of the Ca^{2+}-dependent S100A11-annexin A6 interaction.

REFERENCES

ALLEN, B., DURUSSEL, I., WALSH, M. & COX, J. (1996). Characterization of the Ca^{2+}-binding properties of calgizzarin (S100C) isolated from chicken gizzard smooth muscle. *Biochemistry and Cell Biology* **74,** 687-694.

AVILA-SAKAR, A., CREUTZ, C. & KRETSINGER, R. (1998). Crystal structure of bovine annexin VI in a calcium bound state. *Biochimica et Biophysica Acta* **1387,** 103-116.

AVILA-SAKAR, A., CREUTZ, C. & KRETSINGER, R. (2000). Membrane-bound 3D structures reveal the intrinsic flexibility of annexin VI. *Journal of Structural Biology* **130,** 54–62.

BABIYCHUK, E., PALSTRA, R. J., SCHALLER, J., KAMPFER, U. & DRAEGER, A. (1999). Annexin VI participates in the formation of a reversible, membrane-cytoskeleton complex in smooth muscle cells. *Journal of Biological Chemistry* **274,** 35191-35195.

BABIYCHUK, E. & DRAEGER, A. (2000). Annexins in cell membrane dynamics: Ca^{2+}-regulated association of lipid microdomains. *Journal of Cell Biology* **150,** 1113-1123.

BENZ, J., BERGNER, A., HOFMANN, A., DEMANGE, P., GÖTTIG, P., LIEMANN, S., HUBER, R. & VOGES, D. (1996). The structure of recombinant human annexin VI in crystals and membrane-bound. *Journal of Molecular Biology* **260,** 638-643.

BERRIDGE, M., BOOTMAN, M. & LIPP, P. (1998). Calcium - a life and death signal. *Nature* **395,** 645-648.

BERRIDGE, M., LIPP, P. & BOOTMAN, M. (2000). The versatility and universality of calcium signaling. *Nature Reviews Molecular and Cell Biology* **1,** 11-21.

BIANCHI, R., PULA, G., CECCARELLI, P., GIAMBANCO, I. & DONATO, R. (1992). S100 protein binds to annexin II and p11, the heavy and light chains of calpactin I. *Biochimica et Biophysica Acta* **1160,** 67-75.

BIANCHI, R., GIAMBANCO, I., ARCURI, C. & DONATO, R. (2003). Subcellular localization of S100A11 (S100C) in LLC-PK1 renal cells: Calcium- and protein kinase C-dependent association of S100A11 with S100B and vimentin intermediate filaments. *Microscopy Research and Technique* **60,** 639-651.

CAMORS, E., MONCEAU, V. & CHARLEMAGNE, D. (2005). Annexins and Ca^{2+} handling in the heart. *Cardiovasular Research* **65**, 793-802

CHOW, A. & GAWLER, D. (1999). Mapping the site of interaction between annexin VI and the $p120^{GAP}$ C2 domain. *FEBS Letters* **460**, 166-172.

CHOW, A., DAVIS, A. & GAWLER, D. (2000). Identification of a novel protein complex containing annexin VI, Fyn, Pyk2, and the p120GAP C2 domain. *FEBS Letters* **469,** 88-92.

CREUTZ, C. (1992). The annexins and exocytosis. *Science* **258,** 924-931.

CREUTZ, C. & SNYDER, S. (2005). Interactions of annexin with the mu subunits of the clathrin assembly proteins. *Biochemistry* **44**, 13975-13806.

CUSCHIERI, J., BULGER, E., GARCIA, I. & MAIER, R. (2005). Oxidative-induced calcium mobilization is dependent on annexin A6 release from lipid rafts. *Surgery* **138,** 158-164.

DELOULME, J., ASSARD, N., MBELE, G., MANGIN, C., KUWANO, R. & BAUDIER, J. (2000). S100A6 and S100A11 are specific targets of the calcium- and zinc-binding S100B protein *in vivo*. *Journal of Biological Chemistry* **275,** 35302-35310.

DEMPSEY, A., WALSH, M. & SHAW, G. (2003). Unmasking the annexin I interaction from the structure of apo-S100A11. *Structure* **11,** 887-897.

DE VRIES, G., MCDONALD, J. & WALSH, M. (1989). Calmodulin-like Ca^{2+}-binding proteins of smooth muscle. In *Cell Calcium Metabolism*. (Fiskum, G., *ed*.), Plenum Publishing Corp., New York. pp. 427-437.

DIAKONOVA M., GERKE, V., ERNST, J., LIAUTARD, J., VAN DER VUSSE, G. & GRIFFITHS, G. (1997). Localization of five annexins in J774 macrophages and on isolated phagosomes. *Journal of Cell Science* **110,** 1199-1213.

DONATO, R. (1999). Functional roles of S100 proteins, calcium-binding proteins of the EF-hand type. *Biochimica et Biophysica Acta* **1450,** 191-231.

DONATO, R. (2001). S100: a multigenic family of calcium-modulated proteins of the EF-hand type with intracellular and extracellular functional roles. *International Journal of Biochemistry & Cell Biology* **33,** 637-668.

DONATO, R. (2003). Intracellular and extracellular roles of S100 proteins. *Microscopy Research and Technique* **60,** 540-551.

ECKERT, R., BROOM, A., RUSE, M., ROBINSON, N., RYAN, D. & LEE, K. (2004). S100 proteins in the epidermis. *Journal of Investigative Dermatology* **123,** 23-33.

FILIPEK, A., WOJDA, U. & LESNIAK, W. (1995). Interaction of calcyclin and its cyanogen bromide fragments with annexin II and glyceraldehyde-3-phosphate dehydrogenase. *International Journal of Biochemistry and Cell Biology* **27,** 1123-1131.

FREYE-MINKS, C., KRETSINGER, R. & CREUTZ, C. (2003). Structural and dynamic changes in human annexin VI induced by a phosphorylation-mimicking mutation, T356D. *Biochemistry* **42,** 620-630.

GARBUGLIA, M., VERZINI, R. & DONATO, R. (1998). Annexin VI binds to S100A1 and S100B and blocks the ability of S100A1 and S100B to inhibit desmin and GFAP assemblies into intermediate filaments. *Cell Calcium* **4,** 177-191.

GERKE, V. & MOSS, S. (1997). Annexins and membrane dynamics. *Biochimica et Biophysica Acta* **1357,** 129-154.

GERKE, V. & MOSS, S. (2002). Annexins: from structure to function. *Physiological Reviews* **82,** 331-371.

GERKE, V. & MOSS, S. (2005). Annexins: linking Ca^{2+} signaling to membrane dynamics. *Nature Reviews | Molecular Cell Biology* **6,** 449-461.

GERKE, V. & WEBER, K. (1984). Identity of p36K phosphorylated upon Rous sarcoma virus transformation with a protein purified from brush borders; calcium-dependent binding to non-erythroid spectrin and F-actin. *EMBO Journal* **3,** 227-233.

GLENNEY, J. (1986). Two related but distinct forms of the Mr 36,000 tyrosine kinase substrate (calpactin) that interact with phospholipid and actin in a Ca^{2+}-dependent manner. *Proceedings of the National Academy of Sciences USA* **83,** 4258-4262.

GLENNEY, J., TACK, B. & POWELL, M. (1987). Calpactins: Two distinct Ca^{++}-regulated phospholipid- and actin-binding proteins isolated from lung and placenta. *Journal of Cell Biology* **104,** 501-511.

HAESELEER, F., IMANISHI, Y., SOKAL, I., FILIPEK S. & PALCZEWSKI, K. (2002). Calcium-binding proteins: Intracellular sensors from the calmodulin superfamily. *Biochemical and Biophysical Research Communications* **290,** 615-623.

HAWKINS, T., ROES, J., REES, D., MONKHOUSE, J. & MOSS, S. (1999). Immunological development and cardiovascular function are normal in annexin VI null mutant mice. *Molecular and Cellular Biology* **19,** 8028-8032.

HEIZMANN, C. & COX, J. (1998). New perspectives on S100 proteins: a multi-functional Ca^{2+}-, Zn^{2+}- and Cu^{2+}-binding protein family. *BioMetals* **11,** 383-397.

HEIZMANN, C. W., FRITZ, G. & SCHAFER, B. W. (2002). S100 proteins: Structure, functions and pathology. *Frontiers in Bioscience* **7**, D1356-D1368.

HO, S. N., HUNT, H. D., HORTON, R. M., PULLEN, J. K. & PEASE, L. R. (1989). Site-directed mutagenesis by overlap extension using the polymerase chain reaction. Gene**. 77**:51–59.

HOSOYA, H., KOBAYASHI, R., TSUKITA, S. & MATSUMURA, F. (1992). *Cell Motility and the Cytoskeleton* **22,** 200-210.

IKEBUCHI, N. & WAISMAN, D. (1990). Calcium-dependent regulation of actin filament bundling by lipocortin-85. *Journal of Biological Chemistry* **265,** 3392-3400.

KAETZEL, M. & DEDMAN, J. (2004). Annexin A6 regulation of cardiac function. *Biochemical and Biophysical Research Communications* **322,** 1171-1177.

KAMM, K. & STULL, J. (2001). Dedicated myosin light chain kinases with diverse cellular functions. *Journal of Biological Chemistry* **276,** 4527-4530.

KANAMORI, T., KENJI, T., MASAKI, M., MASATOSHI, K., KEN, F., MASAKIYO, S., NAM-HO, H., KAORU, S., TOSHIHARU, S., JUN, F. and SHINGO, F. (2004). Increased expression of calcium-binding protein S100 in human uterine smooth muscle tumours. *Molecular Human Reproduction* **10**, 735-742.

KARAKI, H., OZAKI, H., HORI, M., MITSUI-SAITO, M., AMANO, K.-I., HRADA, K.-I., MIYAMOTO, S., NAKAZAWA, H., WON, K.-J. & SATO, K. (1997). Calcium movements, distribution, and functions in smooth muscle. *Pharmacological Reviews* **49,** 157-230.

KAWASAKI, H., AVILA-SAKAR, A., CREUTZ, C. & KRETSINGER, R. (1996). The crystal structure of annexin VI indicates relative rotation of the two lobes upon membrane binding. *Biochimica et Biophysica Acta* **1313,** 277-282.

KAWASAKI, H., NAKAYAMA, S. & KRETSINGER, R. (1998). Classification and evolution of EF-hand proteins. *BioMetals* **11,** 277-295.

MAILLIARD, W., HAIGLER, H. & SCHLAEPFER, D. (1996). Calcium-dependent binding of S100C to the N-terminal domain of annexin I. *Journal of Biological Chemistry* **271,** 719-725.

MAKINO, E., SAKAGUCHI, M., IWATSUKI, K. & HUH, N. (2004). Introduction of an N-terminal peptide of S100C/A11 into human cells induces apoptotic cell death. *Journal of Molecular Medicine* **82**, 612-620.

MANN, M., HENDRICKSON, R. & PANDEY, A. (2001). Analysis of proteins and proteomes by mass spectrometry. *Annual Review of Biochemistry* **70,** 437-473.

MARSDEN, B., SHAW, G. & SYKES, B. (1990). Calcium binding proteins. Elucidating the contributions to calcium affinity from an analysis of species variants and peptide fragments. *Biochemistry and Cell Biology* **68,** 587-601.

MEMON, A., BOE, S., PETER, M., LARS, F., THOMAS, T. & EBBA, N. (2005). Down-regulation of S100C is associated with bladder cancer progression and poor survival. *Clinical Cancer Research* **11,** 606-611.

NGAI, P., CARRUTHERS, C. & WALSH, M. (1984). Isolation of the native form of chicken gizzard myosin light-chain kinase. *Biochemical Journal* **218,** 863-870.

NIKI, I., YOKOKURA, H., SUDO, T., KATO, M. & HIDAKA, H. (1996). Ca^{2+} signaling and intracellular Ca^{2+} binding proteins. *Journal of Biochemistry (Tokyo)* **120,** 685-698.

ODINK, K., CERLETTI, N., BRUGGEN, J., CLERC, R., TARCSAY, L., ZWADLO, G., GERHARDS, G., SCHLEGEL, R. & SORG, C. (1987). Two calcium-binding proteins in infiltrate macrophages of rheumatoid arthritis. *Nature* **330,** 80-82.

OHTA, H., SASAKI, T., NAKA, M., HIRAOKA, O., MIYAMOTO, C., FURUICHI, Y. & TANAKA, T. (1991). Molecular cloning and expression of the cDNA coding for a new member of the S100 protein family from porcine cardiac muscle. *FEBS Letters* **295,** 93-96.

ORITO, A., KUMANOGOH, H., YASAKA, K., SOKAWA, J., HIDAKA, H., SOKAWA, Y. & MAEKAWA, S. (2001). Calcium-dependent association of annexin VI, protein kinase C α , and neurocalcin α on the raft fraction derived from the synaptic plasma membrane of rat brain. *Journal of Neuroscience Research* **64,** 235-241.

OSTERLOH, D., ARIE, J.-P., TABARIES, S., SEEMANN, J., RUSSO-MARIE, F., GERKE, V. & LEWIT-BENTLEY, A. (2000). Structural basis of the Ca^{2+}-dependent association between S100C (S100A11) and its target, the N-terminal part of annexin I. *Structure* **8,** 175-184.

RAYNAL, P., POLLARD, H. & SRIVASTAVA, M. (1997). Cell cycle and post-transcriptional regulation of annexin expression in IMR-90 human fibroblasts. *Biochemical Journal* **322,** 365-371.

RAYNAL, P. & POLLARD, H. (1994). Annexins: the problem of assessing the biological role for a gene family of multifunctional calcium- and phospholipid-binding proteins. *Biochimica et Biophysica Acta* **1197,** 63-93.

RESCHER, U. & GERKE, V. (2004). Annexins – unique membrane binding proteins with diverse functions. *Journal of Cell Science* **117**, 2631-2639.

RETY, S., OSTERLOH, D., ARIE, J.-P., TABARIES, S., SEEMANN, J., RUSSO-MARIE, F., GERKE, V. & LEWIT-BENTLEY, A. (2000). Structural basis of the Ca^{2+}-dependent association between S100C (S100A11) and its target, the *N*-terminal part of annexin I. *Structure* **8**, 175-184.

RINTALA, A., SCHONEKESS, B., WALSH, M. & SHAW, G. (2002). ^{1}H, ^{15}N and ^{13}C resonance assignments of rabbit apo-S100A11. *Journal of Biomolecular NMR* **22,** 191-192.

ROBINSON, N. & ECKERT, R. (1998). Identification of transglutaminase-reactive residues in S100A11. *Journal of Biological Chemistry* **273,** 2721-2728.

SAKAGUCHI, M., MIYAZAKI, M., INOUE, Y., TSUJI, T., KOUCHI, H., TANAKA, T., YAMADA, H. & NAMBA, M. (2000). Relationship between contact inhibition and intranuclear S100C of normal human fibroblasts. *Journal of Cell Biology* **149**, 1193-1206.

SAKAGUCHI, M.**,** YAMADA, H., TSUJI, T., INOUE, Y., MIYAZAKI, M., TANAKA, T. & NAMBA, M. (2001). Loss of nuclear localization of the S100C protein in immortalized human fibroblasts. *Radiation Research* **155**, 208-214.

SAKAGUCHI, M., MIYAZAKI, M., TAKAISHI, M., SAKAGUCHI , S., MAKINO, E., KATAOKA, N., YAMADA, M., NAMBA, M. & HUH, N. (2003). S100C/A11 is a key mediator of Ca^{2+}-induced growth inhibition of human epidermal keratinocytes**.**

Journal of Cell Biology **163**, 825-835.

SAKAGUCHI, M., MIYAZAKI, M., SONEGAWA, H., KASHIWAGI, M., OHBA, M., KUROKI, T., NAMBA, M. & HUH, N. (2004). PKCα mediates TGFß-induced growth inhibition of human keratinocytes via phosphorylation of S100C/A11**.** *Journal of Cell Biology* **164**, 979-984.

SANTAMARIA-KISIEL, L., RINTALA-DEMPSEY, A & SHAW, G. (2006). Calcium-dependent and –independent interaction of the S100 protein family. *Biochemical Journal* **396**, 201-214.

SCHÄFER, B., WICKI, R., ENGELKAMP, D., MATTEI, M. & HEIZMANN, C. (1995). Isolation of a YAC clone covering a cluster of nine S100 genes on human chromosome 1q21: rationale for a new nomenclature of the S100 calcium-binding protein family. *Genomics* **25,** 638-643.

SCHÄFER, B. & HEIZMANN, C. (1996). The S100 family of EF-hand calcium-binding proteins: functions and pathology. *Trends in Biochemical Sciences* **21,** 134-140.

SCHMITZ-PEIFFER, C., BROWNE, C., WALKER, J. & BIDEN, T. (1998). Activated protein kinase C α associates with annexin VI from skeletal muscle. *Biochemical Journal* **330,** 675-681.

SCHÖNEKESS, B. & WALSH, M. (1997). Molecular cloning and expression of avian smooth muscle S100A11 (calgizzarin, S100C). *Biochemistry and Cell Biology* **75,** 771-775.

SEATON, B. & DEDMAN, J. (1998). Annexins. *BioMetals* **11,** 399-404.

SEEMANN, J., WEBER, K. & GERKE, V. (1996). Structural requirements for annexin 1-S100C complex-formation. *Biochemical Journal* **319,** 123-129.

SMALL, J. & GIMONA, M. (1998). The cytoskeleton of the vertebrate smooth muscle cell. *Acta Physiologica Scandinavica* **164,** 341-348.

SMITH, S. & SHAW, G. (1998). A change-in-hand mechanism for S100 signalling. *Biochemistry and Cell Biology* **76,** 324-333.

SUDO, T. & HIDAKA, H. (1999). Characterization of the calcyclin (S100A6) binding site of annexin XI-A by site-directed mutagenesis. *FEBS Letters* **444,** 11-14.

TANAKA, M., ADZUMA, K., IWAMI, M., YOSHIMOTO, K., MONDEN, Y. & ITAKURA, M. (1995). Human calgizzarin; one colorectal cancer-related gene selected by a large scale random cDNA sequencing and northern blot analysis. *Cancer Letters* **89**,195–200.

TAYLOR, W. R. and GEISOW, M. J. (1987). Predicted structure for the calcium-dependent membrane-binding proteins p35, p36, and p32. *Protein Engineering.* **1**, 183-187.

TODOROKI, H., KOBAYASHI, R., WATANABE, M., MINAMI, H. & HIDAKA, H. (1991). Purification, characterization, and partial sequence analysis of a newly identified EF-hand type 13-kDa Ca^{2+}-binding protein from smooth muscle and non-muscle tissues. *Journal of Biological Chemistry* **266,** 18668-18673.

VAN ELDIK, L. & GRIFFIN, W. (1994). S100b expression in Alzheimer's disease: relation to neuropathology in brain regions. *Biochimica et Biophysica Acta* **1223,** 398-403.

VAN LIEROP, J., WILSON, D., DAVIS, J., TIKUNOVA, S., SUTHERLAND, C., WALSH, M. & JOHNSON, J. (2002). Activation of smooth muscle myosin light chain

kinase by calmodulin: The role of Lys30 and Gly40. *Journal of Biological Chemistry* **277,** 6550-6558.

WALSH, M., HINKINS, S., FLINK, I. & HARTSHORNE, D. (1982). Bovine stomach myosin light chain kinase: Purification, characterization and comparison with the turkey gizzard enzyme. *Biochemistry* **21,** 6890-6896.

WALSH, M., HINKINS, S., DABROWSKA, R. & HARTSHORNE, D. (1983). Purification of smooth muscle myosin light chain kinase. *Methods in Enzymology* **99,** 279-288.

WICKI, R., SCHAFER, B., ERNE, P. & HEIZMANN, C. (1996a). Characterization of the human and mouse cDNAs coding for S100A13, a new member of the S100 protein family. *Biochemical and Biophysical Research Communications* **227,** 594-599.

WICKI, R., MARENHOLZ, I., MISCHKE, D., SCHAFER, B. & HEIZMANN, C. (1996b). Characterization of the human *S100A12* (*calgranulin C*, *p6*, *CAAF1*, *CGRP*) gene, a new member of the S100 gene cluster on chromosome 1q21. *Cell Calcium* **20,** 243-254.

WILDER, P. T., BALDISSERI, D. M., UDAN, R., VALLELY, K. M. & WEBER, D. J. (2003). Location of the Zn^{2+}-binding site on S100B as determined by NMR spectroscopy and site-directed mutagenesis. *Biochemistry* **42**, 13410-13421.

WILSON, D., SUTHERLAND, C. & WALSH, M. (2002). Ca^{2+} activation of smooth muscle contraction. Evidence for the involvement of calmodulin that is bound to the Triton-insoluble fraction even in the absence of Ca^{2+}. *Journal of Biological Chemistry* **277,** 2186-2192.

ZHAO, X., NAKA, M., MUNEYUKI, M. & TANAKA, T. (2000). Ca^{2+}-dependent inhibition of actin-activated myosin ATPase activity by S100C (S100A11), a novel member of the S100 protein family. *Biochemical and Biophysical Research Communications* **267**, 77-79.

ZIMMER, D. B., CORNWALL, E. H., LANDER, A. & SONG, W. (1995). The S100 protein family - History, function, and expression. *Brain Research Bulletin* **37**, 417-429.

ZIMMER, D. B., CHESSHER, J. & SONG, W. (1996). Nucleotide homologies in genes encoding members of the S100 protein family. *Biochimica et Biophysica Acta* **1313,** 229-238.